Research Square

Preprints are preliminary reports that have not undergone peer review.
They should not be considered conclusive, used to inform clinical practice,
or referenced by the media as validated information.

Geochemistry in relation to soil colour, physicochemical properties, weathering pattern and metal contamination of laterite-associated soils of Kerala, India

B. P. Bhaskar
ICAR–National Bureau of Soil Survey and Land Use Planning
R. P. Sharma
rpsharma64@gmail.com

ICAR–National Bureau of Soil Survey and Land Use Planning
P. N. Dubey
ICAR–National Bureau of Soil Survey and Land Use Planning
P. S. Butte
ICAR–National Bureau of Soil Survey and Land Use Planning

Research Article

Keywords: CIE Lab* colour system, elemental geochemistry, Harker diagrams, metal contamination, pollution load index, soil series, ternary diagrams, weathering indices, weathering intensity, regression analysis

Posted Date: November 3rd, 2026

DOI: https://doi.org/10.21203/rs.3.rs-11162088/v1

License: This work is licensed under a Creative Commons Attribution 4.0 International License.
Read Full License

Additional Declarations: No competing interests reported.

Geochemistry in relation to soil colour, physicochemical properties, weathering pattern and metal contamination of laterite-associated soils of Kerala, India

B. P. Bhaskar, R. P. Sharma[1*], P. N. Dubey and P. S. Butte

ICAR–National Bureau of Soil Survey and Land Use Planning, Amravati Road, Nagpur 440033, Maharashtra, India

[1]ICAR–National Bureau of Soil Survey and Land Use Planning, Regional Centre, Udaipur 313001, Rajasthan, India

*Corresponding Author (email): rpsharma64@gmail.com

Abstract

Geochemical indicators provide valuable insights into the degree of weathering/laterization and help to elucidate the relationships between pedogenic processes with the physicochemical properties of rubified soils of Malabar region. This study investigated five representative laterite-associated soil series—Madgaon, Darbandora, Kinalur, Kanjirapalli and Athirampuzha—from the southern midland zone of Kerala, India, to assess their morphological, physical, chemical and elemental characteristics in relation to weathering intensity and metal contamination. The soils were characterized by high organic carbon (>1.5%) and very dark reddish-brown to dark reddish-brown Ap horizons, whereas the subsurface horizons exhibited dark red to red with a 2.5YR hue and clay enrichment. These soils have argillic/kandic horizons and classified in the subgroup of the Ultisols and Alfisols orders. Significant relationships were observed between CIE L*a*b* colour parameters and selected soil properties, with regression models providing reasonable estimates of organic carbon (R^2 = 0.78, $P < 0.01$) and Al_2O_3 (R^2 = 0.67, $P < 0.01$). The Kanjirapalli and Athirampuzha series contained >20% Al_2O_3 and exhibited a high degree of weathering based on the Chemical Index of Alteration, Index of Laterization, Mafic Index of Alteration and other diagnostic weathering indices. Harker and ternary diagrams indicated intense *in situ* weathering, preferential enrichment of Al-bearing minerals and relatively weak laterization, as reflected by the SiO_2–Al_2O_3–Fe_2O_3 (SAF). The A–CN–K diagram indicated progressive loss of base cations and development of a kaolinitic to kaolinite–smectite mineral assemblage, while the ALF and AF–CNK–M diagrams further supported extensive desilication and base depletion during pedogenesis. Assessment of metal contamination

indicated moderate enrichment of Fe and Al, whereas Cd showed high to extremely high contamination based on the geo-accumulation index (Igeo) and enrichment factor. In contrast, Cu, Zn, Cr and Ni remained within baseline levels and exhibited low potential ecological risk, with a pollution load index (PLI) < 1. The results demonstrate the value of series-level geochemical datasets for characterizing spatial variability in weathering intensity, identifying pedogenic thresholds and interpreting the influence of parent material and climatic conditions on soil development. Such information provides a useful basis for understanding soil evolution and supporting sustainable land-use and soil management in the rubber-growing regions of Kerala.

Keywords: CIE L*a*b* colour system; elemental geochemistry; Harker diagrams; metal contamination; pollution load index; soil series; ternary diagrams; weathering indices; weathering intensity; regression analysis.

1. Introduction

Lateritic soils occupy extensive areas of tropical and subtropical regions of India, with an estimated extent of about 24.8 Mha across Karnataka, Kerala, Madhya Pradesh, the Eastern Ghats of Odisha, Maharashtra and parts of Assam (Raychaudhuri, 1980). Following soil resource mapping of India at 1:250,000 scale, lateritic soils were estimated to occupy about 18.09 Mha (5.5%), whereas red soils covered approximately 87.98 Mha (26.8%) (Bhattacharyya et al., 2009). In Kerala, lateritic soils classified as Ultisols occupy approximately 2.29 Mha, with Inceptisols covering 0.91 Mha (Bhattacharyya et al., 2009). These soils are morphologically characterized by strong chroma and redder hues, together with clay-enriched subsurface horizons containing abundant Fe and Al sesquioxides. Such characteristics reflect the prolonged weathering, leaching and redistribution of elements that accompany lateritic soil formation.

Soil colour is an important morphological indicator of pedogenesis and can provide indirect information on mineralogical composition and the degree of weathering. The conversion of conventional Munsell colour notation into the quantitative CIE L*a*b* colour system and the derivation of colour indices, including redness and I_{Lab}, have provided an objective approach for characterizing variations in soil colour and Fe oxide composition. These indices have been used to infer the relative contribution of hematite and goethite to Fe oxide assemblages and to support interpretations of soil genesis and classification (Torrent and Barrón, 1993;

Vodyanitskii and Kirillova, 2016; Vodyanitskii, 2019). Recent studies of lateritic soils of Nellore demonstrated a strong positive relationship between redness rating and the a^* *parameter of the CIE Lab* system, together with a moderate positive relationship with clay (Bhaskar, 2026). The approach was subsequently applied to highly weathered soils of the Meghalaya Plateau (Bhaskar et al., 2026). These findings suggest that quantitative soil-colour parameters can be useful for establishing relationships between soil morphology and selected physicochemical and geochemical properties.

The Malabar region of Kerala is characterized by extensive occurrence of ferruginous soils with considerable genetic variability. These soils commonly exhibit nodular structures, saprolitic materials and distinct patterns of elemental mobility associated with tropical weathering environments. Variations in their development have been related to the duration of dry periods and the length of soil-moisture deficits (Nair et al., 2010). The widespread occurrence of lateritic materials in the region and their potential for agricultural use have attracted scientific attention since the early description of laterite by Buchanan (1807), followed by extensive investigations of their morphology, genesis, mineralogy and geochemistry (Sahasrabudhe and Deshmukh, 1981; Bruckner, 1989; Bruhn, 1990; Achyuthan, 1996; Valeton, 1994; Widdowson and Cox, 1996; Widdowson and Gunnell, 1999; Karathanasis et al., 2005).

Laterite and lateritic profiles develop under humid to seasonally humid tropical conditions through prolonged chemical weathering, intense leaching and progressive redistribution of silica, bases, Fe and Al. The concept of laterite has been defined both qualitatively on the basis of morphological and pedogenic characteristics (Sivaranjasingham et al., 1962) and quantitatively using chemical criteria (Schellmann, 1986a). Geochemical studies of lateritic profiles in Kerala have demonstrated depletion of silica accompanied by relative enrichment of Fe and Al sesquioxides during weathering (Narayanaswamy, 1992). The intensity of chemical weathering can be quantified using several geochemical indices, including the Chemical Index of Alteration (CIA; Nesbitt and Young, 1982), Chemical Index of Weathering (CIW; Harnois, 1988) and Plagioclase Index of Alteration (PIA; Fedo et al., 1995). These indices have been widely applied to evaluate weathering intensity in soil profiles and weathering sequences (Price and Velbel, 2003; Souri et al., 2006; Abbaslou et al., 2013; Yousefifard et al., 2014).

The application of geochemical indices has provided important insights into the evolution of lateritic and highly weathered soils in different climatic and geological settings. For example, chemical weathering indices have been used to characterize lateritic profiles developed over chlorite schists in South Cameroon (Beyala et al., 2009). An assessment of 126 soils from North America established relationships between precipitation and chemical weathering, including the chemical index of weathering and molar ratios of bases to alumina and K or Na to alumina (Sheldon et al., 2002). In lateritic soils of the east coast of India, high Si–Al–Fe relationships and ternary diagrams based on IOL and CIA indicated extensive kaolinitization and an advanced stage of laterization. Significant relationships between the Kornberg-A index and Plagioclase Index ($r = 0.92$, $P < 0.01$), and between CIA and Weathering Index ($r = 0.86$, $P < 0.01$), further demonstrated the usefulness of multiple weathering indices for evaluating the intensity of chemical alteration (Bhaskar, 2026; Bhaskar and Gopal Tiwari, 2017).

Several mineralogical and geochemical investigations have already been conducted on laterite-associated soils of Kerala (Satyanarayana and Thomas, 1962; Varghese and Byju, 1993; Omana and Santosh, 1995; Sehgal, 1998; Chandran et al., 2005; Dubey et al., 2016, 2018) and the east coast of India (Bhaskar and Tiwari, 2017). Silica has been used as an invariant element to establish geochemical mass balances in laterite-associated soils of the Somasila project area (Bhaskar et al., 1999). The dark-red subsurface horizons has been associated with Fe oxide minerals such as lepidocrocite, hematite and goethite, together with a high proportion of dithionite-soluble Fe relative to oxalate-soluble Fe (Basavaraj and Sarma, 1993). Geochemical and morphological investigations of lateritic soils in North Kerala have indicated intense lateritization and kaolinization of quartzo-felspathic mica-gneiss, with contrasting reducing and oxidizing conditions associated with grey carbonaceous and hematite-rich ferruginous horizons, respectively (Manju et al., 2001). The occurrence of halloysite in association with kaolinite, goethite, gibbsite and quartz was reported, with these mineral assemblages contributing to the characteristic physical and chemical properties of these soils (Ramahashay et al., 1987). Mineralogical investigations of Alfisols and Ultisols of Kerala have reported a predominance of kaolinite (Bhattacharyya et al., 2009), whereas gibbsite–goethite assemblages have been identified in strongly weathered profiles of the high-rainfall zones of the Western Ghats (Deepthy and Balakrishnan, 2005).

The behaviour and redistribution of trace and potentially toxic elements during intense tropical weathering are also important for understanding the environmental quality of lateritic soils. Studies in Kerala have reported spatial variations in metal concentrations and contamination levels. Investigations in the Periyar River basin identified elevated Zn and Ni concentrations in riverbank soils, indicating potential environmental and health concerns (Chandni et al., 2026). In Kollam district, the reported intensity of heavy-metal contamination followed the order Fe > Pb > Cd > As > Cr > Zn > Cu > Ni > Mn (George et al., 2023). Similarly, assessment of the degree of contamination, enrichment factor and geo-accumulation index in the Koratty region identified Cd, Ni and Pb as important contaminants (Prasanth et al., 2012). Elevated concentrations of Cr and Pb have also been reported in soils of the Edayar region of Ernakulam, with potential implications for human health and ecosystem quality (Syamlal and Sayantan, 2024a). These studies highlight the need to distinguish between the natural geochemical signatures associated with parent material and weathering and anthropogenic metal enrichment.

Although extensive information is available on the morphology, mineralogy and general geochemistry of lateritic soils of Kerala, comparatively limited attention has been given to integrating soil colour, particle-size distribution, chemical properties, elemental composition, weathering intensity and metal contamination at the soil-series level, particularly in the Southern Midland Zone (SMZ). This region is characterized by humid to perhumid climatic conditions, strongly weathered hill-land systems and extensive cultivation of rubber (*Hevea brasiliensis*) on terraced slopes extending across the parts of southern and central Kerala. The combination of intense monsoonal weathering, steep slopes, land-use intensification, quarrying, sand mining and repeated application of agrochemicals creates a complex soil–landscape environment in which the mobility and accumulation of elements may vary substantially. Such environmental pressures are further associated with land degradation and slope instability, emphasizing the need for improved understanding of the geochemical characteristics and evolutionary pathways of these soils.

A soil-series-level geochemical database can therefore provide a useful framework for linking morphological properties, particularly colour and texture, with elemental composition and quantitative indicators of weathering. It may also help distinguish pedogenic enrichment of Fe and Al from the accumulation of potentially toxic metals and establish baseline information for environmentally sustainable soil management. The present study was

therefore designed to investigate whether differences in weathering intensity among laterite-associated soil profiles are reflected in soil colour, physicochemical properties, elemental composition and metal contamination. Specifically, the study aimed to: (i) characterize and classify the selected laterite-associated soils; (ii) quantify the degree of chemical weathering using elemental geochemistry, weathering indices and ternary diagrams; (iii) examine relationships between CIE L*a*b* colour parameters and selected soil properties; and (iv) assess the degree of metal enrichment and contamination using appropriate pollution indices. The integrated assessment was intended to improve understanding of the pedogenic development and geochemical variability of laterite-associated soils in the Southern Midland Zone of Kerala and to provide a baseline for sustainable management of soils under rubber cultivation.

2. Materials and Methods

2.1. Environmental settings

The study was conducted in the Southern Midland Zone (SMZ) of Kerala, India, covering selected areas of Kottayam, Ernakulam and Kozhikode districts where laterite-associated soils are extensively developed. The region is underlain predominantly by Precambrian crystalline rocks, including charnockites, with narrow bands of pyroxene granulites and magnetite–quartz rocks (Damodaran, 1954). In the Nilambur Valley of Kozhikode district, the dominant lithologies include magnetite quartzite, pyroxene and hornblende granulites, and charnockitic gneiss (Sawarkar, 1980). The contrasting lithological composition provides an important geological framework for interpreting the elemental composition and weathering characteristics of the soils investigated in the present study.

The soils of the region were initially described as red sandy and sandy clay loams (Kamath, 1985), but subsequent investigations classified them as ferrallitic soils according to the French soil classification system (Bourgeon, 1989). During detailed soil surveys of rubber-growing areas of Kerala, these soils were further classified into the subgroups of Ultisols, Alfisols and Inceptisols (Soil Survey Staff, 2022). Lateritic formations occupy a substantial proportion of the Kerala landscape, with approximately 60% of the land area reported to be covered by lateritic materials (Krishnan et al., 1996; Harindranath et al., 1999). The landscape exhibits a distinct geomorphic sequence comprising undulating and steep slopes, lateritic uplands and coastal plains, with a general decrease in elevation towards the west (Nair, 1987; Ramasamy et al., 2020). Highly weathered and leached red soils commonly

occur on the elevated lateritic surfaces developed over crystalline rocks, including charnockites (Bhattacharya et al., 1979).

The lateritic landscapes of western peninsular India have also been interpreted in relation to the regional tectonic and geomorphic evolution associated with the separation of Madagascar and the Seychelles during the Mesozoic. Major rifting events around 88 and 65 Ma were associated with the evolution of the western margin of peninsular India and the Deccan continental flood basalt province (Mahoney, 1988; Saunders et al., 2007; Collier et al., 2008). Remnants of a semi-continuous lateritic belt along the Konkan–Kanara lowlands have been interpreted as evidence of widespread Cenozoic lateritization in western India (Widdowson and Gunnell, 1999; Schmidt et al., 1983; Brückner and Bruhn, 1992). This geomorphic setting provided favourable conditions for prolonged chemical weathering and the development of deeply weathered lateritic profiles (Tardy et al., 1991).

The Southern Midland Zone is characterized by rolling and undulating lateritic terrain with pronounced short-distance variations in slope, elevation, drainage and degree of weathering. These landscape contrasts provide a suitable natural setting for investigating soil-forming processes under humid tropical conditions. The region experiences intense seasonal rainfall and prolonged chemical weathering, resulting in strong leaching of base cations and silica and relative enrichment of Fe and Al in the soil profiles. The juxtaposition of lateritic uplands, hill slopes and interhill valleys also results in substantial variation in soil moisture regimes and drainage conditions, which may influence profile development, clay translocation, rubification and elemental redistribution.

Natural vegetation in the region varies from tropical wet evergreen to moist deciduous forests and grasslands (Varghese and Menon, 1999; Rugmini and Balagopalan, 2006). Interhill valleys, locally referred to as *shola*, may contain peat and organic-rich deposits that preserve information on Holocene climatic and ecological conditions (Sukumar et al., 1993). However, these ecosystems have undergone degradation due to natural and anthropogenic disturbances and changing climatic conditions (Sajinkumar and Rani, 2015). The lateritic uplands support diverse vegetation communities, including evergreen and deciduous tree species, shrubs and ephemeral herbs, whereas cultivated areas are dominated by plantation and horticultural crops. Rubber (*Hevea brasiliensis*) is an important plantation crop in the Southern Midland Zone and is commonly cultivated on undulating and terraced lateritic slopes. The combination of highly weathered parent materials, intense monsoonal leaching,

varied topography and long-term agricultural use makes the region particularly suitable for investigating the relationships among soil colour, physicochemical properties, elemental composition, weathering intensity and metal accumulation.

2.2. Field studies

A semi-detailed soil survey of the rubber-growing regions of Kerala was conducted at a scale of 1:50,000. Five representative laterite-associated soil series occurring in the midland region, generally below 300 m mean sea level, were selected for detailed geochemical characterization (Fig. 1). The selected series have distinct variations in parent material, geomorphic position, slope, drainage, profile development and degree of laterization. The geographical coordinates and major morphological characteristics of the selected profiles are presented below.

P1. Madgaon series. The Madgaon series occurs at 11°35′32.0″ N and 75°50′48.7″ E and is characterized by an isohyperthermic soil temperature regime. The soils are associated with iron-rich lateritic profiles developed from Precambrian metasedimentary and crystalline rocks, including charnockites and khondalite, with extensive development of secondary laterite. The profile is characterized by a dark brown matrix (7.5YR 3/4, moist), clayey texture and approximately 28% coarse gravel. Common medium-sized pores and fine to very fine roots occur throughout the profile.

P2. Darbandora series. The Darbandora series is located at 11°20′24.6″ N and 76°00′34.2″ E. The soils occur on steep hills developed over quartzite and schistose parent materials. They are moderately deep and somewhat excessively drained, with a brown to dark reddish-brown matrix. The surface horizon has a dark brown matrix (7.5YR 3/2, moist), sandy clay loam texture and approximately 4% coarse gravel. The soil exhibits weak medium subangular blocky structure, slightly sticky and slightly plastic consistency, and a clear smooth horizon boundary.

P3. Kinalur series. The Kinalur series occurs in Kozhikode district at 11°02′08″ N and 75°05′00″ E. It belongs to the clayey, kaolinitic family of Ustic Kanhaplohumults. The soils are deep and well drained and occur mainly on uplands and mounds. The surface horizon is dark red and gravelly sandy clay loam, whereas the subsurface horizons are red to reddish brown with gravelly sandy clay, have well-developed argillic horizon. The profile

morphology indicates substantial clay accumulation and advanced pedogenic development under the prevailing humid tropical environment.

P4. Kanjirapalli series. The Kanjirapalli series occurs in Kottayam district at 9°44′00″ N and 76°51′48″ E and represents a benchmark lateritic soil of the Thodupuzha–Kanjirappally belt of the Madurai Granulite Block. The area is underlain predominantly by Precambrian crystalline rocks, including charnockites, granites and gneisses. The series is classified at the family level as loamy-skeletal, kaolinitic, Typic Kandihumults. The soils are deep and well drained, with dark red surface horizons and red argillic (Bt) horizons having a sandy clay loam texture. They generally occur on midland landscapes with slopes exceeding 15%.

P5. Athirampuzha series. The Athirampuzha series occurs at 9°39′34″ N and 76°31′35″ E. The soils have developed on hard lateritic materials derived from Precambrian high-grade metamorphic rocks, particularly charnockites and gneisses. The series is classified at the family level as clayey-skeletal, kaolinitic, Ustic Kanhaplohumults. The soils are deep and well drained and occur on uplands, mounds and hills, commonly on slopes exceeding 30%. The surface horizon is yellowish-red and gravelly clay, whereas the subsurface horizons are red to yellowish-red and gravelly argillic clay.

2.3. Laboratory analysis

Horizon-wise soil samples representing each soil series were air-dried, gently crushed, and passed through a 2-mm sieve. The resulting fine-earth fraction was used for laboratory analyses. Particle-size distribution was determined by the international pipette method. Soil pH was measured in 1:2.5 soil-to-water suspensions, while organic carbon was determined by the Walkley–Black method. Cation exchange capacity (CEC) and exchangeable bases were determined using the ammonium acetate method. Base saturation was calculated as the percentage ratio of the sum of exchangeable bases to CEC. Effective cation exchange capacity (ECEC) was calculated as the sum of exchangeable bases and exchangeable Al. Exchangeable Al was determined by extraction with 1 M KCl followed by titration. Apparent CEC and apparent ECEC were expressed on a clay basis as CEC/clay × 100 and ECEC/clay × 100, respectively (Jackson, 1973; Sarma et al., 1987).

For elemental analysis, soil samples were digested using a tri-acid mixture of nitric acid (HNO_3), perchloric acid ($HClO_4$), and hydrofluoric acid (HF), following the procedure

described by Page et al. (1982). Briefly, 2 g of soil passed through a 1-mm sieve was transferred to a 50-mL Teflon beaker, moistened with a small quantity of distilled water, and treated with 2 mL of 37% H_2O_2. The samples were gently heated to evaporate the excess moisture. Subsequently, 1 mL of 65% HNO_3, 1 mL of 65% $HClO_4$, and 6 mL of 45% HF were added, and the samples were heated for approximately 30 min until dense white fumes appeared. The beakers were then removed from the hot plate, cooled, and rinsed with a small quantity of distilled water. Thereafter, 4 mL of 37% HCl and 0.4 mL of 0.1 M H_3BO_3 were added, and the samples were heated again until the volume was reduced to approximately 1–2 mL. The digests were quantitatively transferred to 10-mL plastic tubes and diluted to volume with distilled water.

The concentrations of the major and trace elements were determined using inductively coupled plasma–atomic emission spectroscopy (ICP–AES; Prodigy, Teledyne Leeman Labs, USA) at the Division of Soil Resource Studies, ICAR–National Bureau of Soil Survey and Land Use Planning, Nagpur. Total sodium (Na) was determined separately following aqua-regia digestion using atomic absorption spectrophotometry, as described by Güven and Akinci (2011).

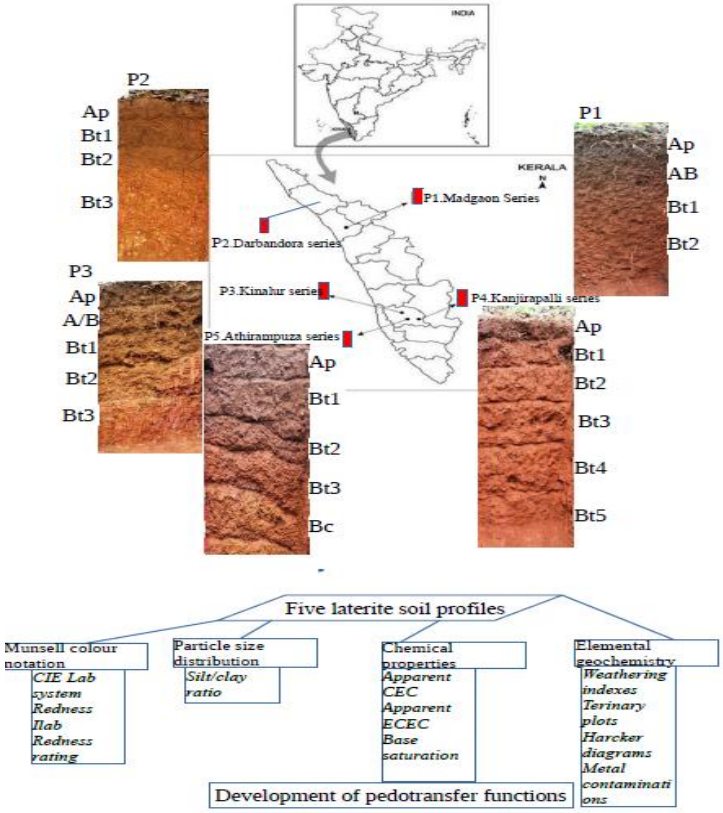


Fig.1. Location map of five laterite associated soil profiles and flow chart of methodology used in the study

2.4. Calculation of indices

Various indices were calculated to characterize soil redness, weathering intensity, lateritization, and metal enrichment in the studied lateritic soil profiles. Soil redness and the relative proportion of hematite to hematite + goethite were evaluated using Munsell colour notation and the CIE-L*a*b* colour system. Weathering and alteration indices were calculated from the major oxide composition of the soil samples. Metal enrichment and contamination indices were calculated by comparing the concentrations of selected trace elements in the studied soils with their respective background concentrations in the Upper Continental Crust (UCC). The indices, their corresponding equations, and references used for their calculation are presented in Table 1.

Table 1. Indices Used for the Characterization of Lateritic Soil Profiles of Kerala

Index	Formula	Reference
Colour indices		
Transformed Munsell notation to CIE-L*a*b* system	Munsell colour notation was transformed into CIE-L*a*b* colour coordinates	Vodyanitskii and Kirillova (2016)
$a^*_1(a/b)$	$a^* \times (a/b)$	Vodyanitskii and Kirillova (2016)
$b^*_1(b/a)$	$b^* \times (b/a)$	Vodyanitskii and Kirillova (2016)
Redness index	$a^*/(a^* + b^*)$	Vodyanitskii and Kirillova (2016)
Redness rating	$(0.51 - \text{Red})/(0.51 - 0.16)$	—
Redness index	$(10 - H) \times C/V$, where H is the numerical hue rating: 7.5R = 12.5, 10R = 10, 2.5YR = 7.5, 5YR = 5, 7.5YR = 2.5 and 10YR = 0	Torrent et al. (1983)
Weathering and alteration indices		
Chemical Index of Alteration (CIA)	$CIA = [Al_2O_3/(Al_2O_3 + CaO^* + Na_2O + K_2O)] \times 100$, where CaO* represents silicate-derived CaO	Nesbitt and Young (1982/1989)
Weathering Index of Parker (WIP)	$WIP = [(2Na_2O/0.35) + (MgO/0.90) + (2K_2O/0.25) + (CaO/0.70)]$	Parker (1970)
Si/Al ratio	SiO_2/Al_2O_3	Birkeland (1999)
Bases/Alumina ratio	$(CaO + MgO + Na_2O + K_2O)/Al_2O_3$	—
Bases/R_2O_3 ratio	$(CaO + MgO + Na_2O + K_2O)/(Al_2O_3 + Fe_2O_3)$	—
Reiche Product Index (RPI)	$RPI = 100 \times [SiO_2/(SiO_2 + R_2O_3)]$, where $R_2O_3 = Al_2O_3 + Fe_2O_3$	Reiche (1943)
Vogt ratio	$(Al_2O_3 + K_2O)/(MgO + CaO + Na_2O)$	Vogt (1927)
Ignition loss index	H_2O^*	Jayawardena (1994a)
Weathering Ratio (WR)	$(CaO + MgO + Na_2O)/TiO_2$	Chittleborough (1991)
Weathering Index-1 (WI-1)	$(CaO + SiO_2)/(Fe_2O_3 + TiO_2)$	Darmody (2005)
Weathering Index-	$(CaO + SiO_2)/(Al_2O_3 + Fe_2O_3 + TiO_2)$	Darmody (2005)

2 (WI-2)		
Index of Lateritisation (IOL)	$[(Al_2O_3 + Fe_2O_3)/(SiO_2 + Al_2O_3 + Fe_2O_3)] \times 100$	Schellmann (1981)
MIA(O)	$Al_2O_3/[Al_2O_3 + Fe_2O_3 + MgO + CaO^* + Na_2O] \times 100$	Babechuk et al. (2014)
MIA(R)	$(Al_2O_3 + Fe_2O_3)/[Al_2O_3 + Fe_2O_3 + MgO + CaO^* + Na_2O] \times 100$	Babechuk et al. (2014)
Metal pollution indices		
Enrichment Ratio (ER)	$$ER = \frac{(C_n/C_{ref})_{\text{sample}}}{(C_n/C_{ref})_{\text{background}}}$$ Where C_n is the concentration of the element of interest and C_{ref} is the concentration of the selected reference element. Titanium (Ti) is commonly used as the reference element because of its relatively conservative behaviour in soils. Back ground values of UCC was used from Taylor, and McLennan,1983. ER 1-2 -slightly contaminated ; 2-5-moderately contaminated, 5-20-severely contaminated, 20-40-highly contaminated	Birch and Olmos (2008)
Geo-accumulation Index (Igeo)	**$Igeo = \log_2[C_n/(1.5 \times B_n)]$**, where C_n is the measured concentration and B_n is the geochemical background concentration. The degree of contamination based on **Igeo values** can be stated in text form as follows: **Igeo ≤ 0:** Practically uncontaminated **0 < Igeo ≤ 1:** Uncontaminated to moderately contaminated **1 < Igeo ≤ 2:** Moderately contaminated **2 < Igeo ≤ 3:** Moderately to heavily contaminated **3 < Igeo ≤ 4:** Heavily contaminated **4 < Igeo ≤ 5:** Heavily to extremely contaminated **Igeo > 5:** Extremely contaminated	Bhuiyan et al. (2010)
Contamination Factor (Cf)	**$Cf = C_n(sample)/C_n(background)$** classes of Cf : <1=low; 1-3-moderate, 3 - 6—considerable, > 6 high	Zhao et al. (2012)
Pollution Load Index (PLI)	**$PLI = (CF_1 \times CF_2 \times CF_3 \times \ldots \times CF_n)^{1/n}$** PLI =<1 indicates baseline level of pollutants , above 1 indicates ongoing degradation	Tomlinson et al. (1980)
Potential Ecological Risk Factor (Er)	**$Er = Tr \times Cf$**, where Tr is the toxic-response factor and Cf is the contamination factor. The degree of potential ecological risk based on **Er values** is classified as follows: **Er < 40:** Low ecological risk **40 ≤ Er < 80:** Moderate ecological risk **80 ≤ Er < 160:** Considerable ecological risk **160 ≤ Er < 320:** High ecological risk **Er ≥ 320:** Very high ecological risk Based on the standardized toxic response factor suggested by Håkanson (1980), the toxic response factors for Cr, Cu, Ni, , and Zn are , 2, 5, 5, and 1, respectively.	Hakanson (1980)
Potential Ecological Risk Index (RI)	$$RI = \sum_{i=1}^{n} E_r^i = \sum_{i=1}^{n} (T_r^i \times C_f^i)$$ where **RI** is the overall potential ecological risk index, E_r^i is the potential ecological risk factor of the *i*th metal, T_r^i is its toxic-response factor, and C_f^i is its contamination factor. The potential ecological risk was classified based on RI values as	Hakanson (1980)

	follows: **RI < 150:** Low ecological risk **150 ≤ RI < 300:** Moderate ecological risk **300 ≤ RI < 600:** Considerable ecological risk **RI ≥ 600:** Very high ecological risk	
Modified Degree of Contamination (mCd)	$mC_d = \frac{\sum_{i=1}^{n} C_{fi}}{n}$ where C_{fi} is the contamination factor of the ith element and n is the total number of elements considered in the assessment. The Modified Degree of Contamination (mCd) is classified as follows: mCd < 1.5 indicates a nil to very low degree of contamination; 1.5 ≤ mCd < 2 indicates a low degree of contamination; 2 ≤ mCd < 4 indicates a moderate degree of contamination; 4 ≤ mCd < 8 indicates a high degree of contamination; 8 ≤ mCd < 16 indicates a very high degree of contamination; 16 ≤ mCd < 32 indicates an extremely high degree of contamination; and mCd ≥ 32 indicates an ultra-high degree of contamination.	Abrahim and Parker (2008)

2.5. Statistical analysis

Descriptive statistics and correlation analyses were performed using LibreOffice Calc. Multiple linear regression and K-means cluster analyses were conducted using the StatKingdom and StatBlue online statistical platforms. The coefficient of variation (CV) was used to assess the variability of soil properties across the study area following Harka (2021), variability was classified as low (CV < 20%), moderate (20–30%), high (30–50%), and very high (CV > 50%).

The strength of correlation coefficients ((r)) was interpreted as weak (0.10–0.39), moderate (0.40–0.69), strong (0.70–0.89), and very strong (0.90–1.00), following Schober et al. (2018). Triplots and biplots were generated using Triplot.com and StatKingdom, while depth-function graphs were prepared using LibreOffice Calc. The profile-weighted mean for each soil property was calculated by multiplying the value of the property in each horizon by the corresponding horizon thickness, summing the products across all horizons, and dividing by the total thickness of the soil profile.

3. Results

3.1. Munsell colour system

Five lateritic soil profiles comprised of 24 horizons (Table 2), including five Ap horizons, 17 Bt horizons, and one each of BC and AB horizons. Based on profile depth, the soils were

classified as moderately deep (P2 and P3), deep (P1 and P5), and very deep (P4), following the criteria of Sehgal et al. (1989).

According to the Munsell colour notation, two horizons had a hue of 7.5YR, 13 horizons had a hue of 5YR, and nine horizons had a hue of 2.5YR. The matrix colours ranged from very dark brown to dark red with increasing soil depth. In profile P1, the Ap/AB horizons were dark reddish brown (5YR 3/3 and 5YR 3/4), changing to red in the Bt1 horizon and subsequently to yellowish red (5YR 5/6) in the deeper Bt horizons. In the Darbandora series (P2), the Ap horizon had a very dark brown matrix (7.5YR 3/3), which changed to dark reddish brown in the underlying horizons (5YR 3/3, 5YR 3/4, and 2.5YR 3/4).

The Ap horizon of P3 exhibited a dark reddish brown (7.5YR 3/4), followed by dark reddish brown (5YR 3/4) to reddish brown (5YR 4/4) in the Bt horizons. Below 60 cm depth, the Bt horizon became red (2.5YR 4/6). In P4, the Ap horizon was dark reddish brown, whereas P5 exhibited a reddish-brown Ap horizon; in both profiles, the colour changed progressively to dark red and red in the underlying Bt horizons.

The redness rating exhibited irregular trends with depth, with a minimum value of 3.33 recorded for the 2.5YR 3/4 horizon in P2 and a maximum value of 10.0 recorded for the 7.5YR 3/4 horizon in P3. Based on profile-weighted mean redness ratings, the five profiles were arranged in ascending order as P4 (4.40) < P1 (5.09) < P2 (5.32) < P5 (5.80) < P3 (7.26).

3.2. CIELab system

The CIELab colour parameters exhibited distinct variations with soil depth across the studied profiles (Table 2). The L* value, representing lightness, showed an increasing trend with depth in profiles P3, P1 and P4, whereas relatively uniform values in P4 and P5. The L* values ranged from 30.8 in P2, P3, and P4 to a maximum of 61.7 in the Bt1 horizon of P1. The profile-weighted mean L* values ranged from 30.80 in P2 to 49.68 in P1.

The a* value, representing the red–green colour component, generally showed a gradual increase with depth. The profile-weighted mean a* values ranged from 13.41 in P2 to 18.52 in P5. The b* value, representing the yellow–blue colour component, exhibited a similar depth-wise trend, with profile-weighted mean values ranging from 18.16 to 28.06, the latter being recorded in P5.

The transformed colour indices also showed appreciable variation among the profiles. The a^*_1 values ranged from 0.45 in P3 to 0.91 in P2, with the maximum value recorded in the Bt3 horizon corresponding to the 2.5YR 3/4. The b^*_1 values ranged from 1.10 in the Bt3 horizon of P2 to 2.22 in the Ap horizon of the Kinalur series (P3). The Red and ILab indices generally followed patterns similar to those observed for the CIELab colour parameters, with variations occurring along the soil profiles (Table 2).

Table 2. Munsell color notation , CIELab values and redness rating indices of lateritic profiles, Kerala

Depth(cm)	Horizon	Matrix colour (moist	CIELab L	a	b	a*1(a/b)	b*1(b/a)	Redness rating (RR)*	Red a*/a+b	Ilab
P1.Madgaon series										
0-18	Ap	5YR3/4	41.2	9.7	15.5	0.63	1.60	6.67	0.38	0.64
18-46	A/B	5YR4/4	41.2	12.5	20.8	0.60	1.66	5.00	0.38	0.62
46-73	Bt1	2.5YR5/6	61.7	16.2	21.5	0.75	1.33	3.00	0.43	0.77
73-107	Bt2	5YR5/6	51.6	16.8	31.1	0.54	1.85	6.00	0.35	0.54
w̄			49.68	14.33	23.36	0.62	1.63	5.09	0.38	0.64
_P2-Darbandora series										
0-8	A	7.5YR3/3	30.8	7.8	16.4	0.48	2.10	7.50	0.32	0.46
8-19	Bt1	5YR3/4	30.8	12.7	19.6	0.65	1.54	6.67	0.39	0.67
19-51	Bt2	5YR3/4	30.8	12.7	19.6	0.65	1.54	6.67	0.39	0.67
51-89	Bt3	2.5YR3/4	30.8	15.4	16.9	0.91	1.10	3.33	0.48	0.91
w̄			30.80	13.41	18.16	0.74	1.40	5.32	0.42	0.75
P3.Kinalur series										
0-10	Ap	7.5YR 3/4	30.8	9.9	22	0.45	2.22	10.00	0.31	0.43
10-36	AB	5 YR 3/4	30.8	12.7	19.6	0.65	1.54	6.67	0.39	0.67
36-48	Bt1	5 YR 4/4	41.2	12.5	20.8	0.60	1.66	5.00	0.38	0.62
48-66	Bt2	5 YR 4/4	41.2	12.5	20.8	0.60	1.66	5.00	0.38	0.62
66-80	Bt3	2.5YR 4/6	41.2	21.2	26.3	0.81	1.24	11.25	0.45	0.82
w̄			36.52	13.76	21.52	0.63	1.62	7.26	0.39	0.64
P4. Kanjirapalli series										
0-13	Ap	5YR 3/3	30.8	9.9	14.6	0.68	1.47	5.00	0.40	0.70
13-32	Bt1	5 YR 3/4	30.8	12.7	19.6	0.65	1.54	6.67	0.39	0.67
32-56	Bt2	2.5 YR 3/6	30.8	22.2	26	0.85	1.17	5.00	0.46	0.86
56-83	Bt3	2.5 YR 3/6	30.8	22.2	26	0.85	1.17	5.00	0.46	0.86
83-112	Bt4	2.5YR 4/6	41.2	21.2	26.3	0.81	1.24	3.75	0.45	0.82
122-150	Bt5	2.5YR 4/6	41.2	21.2	26.3	0.81	1.24	3.75	0.45	0.82
w̄			32.70	18.07	22.58	0.74	1.19	4.40	0.41	0.75
P5.Athirampuza series										
0-16	Ap	5 YR 4/4 M	41.2	12.5	20.8	0.60	1.66	5.00	0.38	0.62
16-42	Bt1	5 YR 4/6 M	41.2	17.5	30.7	0.57	1.75	7.50	0.36	0.58
42-66	Bt2	5 YR 4/6	41.2	17.5	30.7	0.57	1.75	7.50	0.36	0.58
66-89	Bt3	2.5 YR 4/6 M	41.2	21.2	26.3	0.81	1.24	3.75	0.45	0.82
89-105	BC	2.5 YR 4/6 M	41.2	21.2	26.3	0.81	1.24	3.75	0.45	0.82
w̄			41.98	18.52	28.06	0.68	1.57	5.80	0.40	0.69

Note:w̄ =Profile weighted mean, redness rating (Torrent et al.(1983), Ilab= index of based on reference Red of hematite and goethite Vodyanitskii(2016), L=lightness, a=redness, b=yellowness

3.3. Soil Texture of Lateritic Soils

The textural characteristics of the red and lateritic soils of Kerala revealed considerable variation among the studied soil series (Table 3). In the Madgaon series (P1), the Ap/AB horizons had a sandy loam texture, with sand content ranging from 77.0 to 78.2% and clay from 11.0 to 11.6%. A distinct increase in clay content was observed in the underlying Bt horizons, where it increased to 27.7–43.6%. The silt-to-clay ratio ranged from 0.91 in the Ap

horizon to 1.13 in the Bt1 horizon, while the clay content increased by approximately 1.2 times from the surface horizon to the clay-enriched Bt horizons.

Profile P2 was predominantly clayey, with clay content ranging from 46.2 to 65.2%. The silt-to-clay ratio decreased from 0.72 in the Ap horizon to 0.40 in the Bt3 horizon. Sand content showed a progressive decrease with depth, from 20.7 to 7.0%, whereas the distribution of silt and clay exhibited irregular variations among the horizons.

In the Kinalur series (P3), sand, silt, and clay contents showed relatively slight inflictions with depth, and the profile was predominantly sandy clay loam. The profile-weighted mean of sand, silt, and clay were 48.47, 19.37, and 32.16%, respectively. The Kanjirapalli series (P4) also exhibited a sandy clay loam throughout the profile. Its profile-weighted mean for sand, silt, and clay contents were 56.75, 13.40, and 24.00%, respectively. The weighted mean for silt-to-clay ratio was 0.41.

The Athirampuzha series (P5) was predominantly clayey, particularly in the Bt horizons, where clay content exceeded 50%. The silt-to-clay ratio was less than 0.20 in the Bt horizons, with a profile-weighted mean of 0.20. The weighted mean contents of silt and sand were 10.26 and 37.52%, respectively. Sand content showed irregular variation, accompanied by an increasing trend in clay content in the Bt horizons.

Table 3. Textural and chemical characteristics

Depth			Particle size distribution(%)					OC	Exchangeable cations(cmol/kg)					CEC	ECEC	CEC/C	ECEC/	BS(%) NH4O
(cm)	Horizon	Texture	sand	silt	clay	silt/clay	pH	g/kg	Ca	Mg	Na	K	Al	cmol(p^+)kg^{-1}		*100	C*100	Ac
P1.Madgaon series Fine loamy, kaolinitic kanhaplic Haplustaffs																		
0-18	Ap	Sl	78.2	10.5	11.6	0.91	5.1	18.7	1.86	0.63	0.44	0.08	0.19	6.42	3.2	55.34	27.58	46.68
18-46	A/B	Sl	77	11.5	11.5	1.00	5.5	8.4	1.93	0.68	0.44	0.06	0.08	9.73	3.19	84.6	27.73	31.96
46-73	Bt1	SCl	41	31.3	27.7	1.13	5.5	7.9	2.9	0.82	0.36	0.09	0	6.31	4.17	22.77	15.05	66.07
73-107	Bt2	C	14.4	42	43.6	0.96	5.4	2.5	3.45	1.31	0.44	0.08	0.02	6.64	5.3	15.22	12.15	79.2
w̄			**48.23**	**26.02**	**25.80**	**1.01**	**5.40**	**8.13**	**2.65**	**0.91**	**0.42**	**0.08**	**0.06**	**7.33**	**4.11**	**42.03**	**19.55**	**58.05**
P2-Darbandora,,Goa, Very fine, Kaolinitic, family of Typic Kanhaplustalfs (Archean schists and ferruginous quartzite)																		
0-8	A	C	20.7	33.1	46.2	0.72	5.4	50.4	4.56	1.67	0.57	0.8	0.5	18.99	7.65	41.1	16.55	40.02
8-19	Bt1	C	9.1	28.7	62.2	0.46	5.3	25.2	3.94	1.65	0.63	0.23	0.37	19.65	6.82	31.59	10.96	40.95
19-51	Bt2	C	7	35.7	57.2	0.62	5.2	20.1	3.59	1.83	0.57	0.23	0.41	18.03	6.63	31.52	11.59	38.45
51-89	Bt3	C	8.8	26	65.2	0.40	5.2	14.7	3.51	2.13	0.66	0.23	0.38	16.46	6.91	25.24	10.59	45.57
w̄			**9.26**	**30.46**	**60.24**	**0.52**	**5.23**	**21.15**	**3.69**	**1.92**	**0.62**	**0.28**	**0.40**	**17.65**	**6.86**	**29.71**	**11.53**	**41.94**
P3-Kinalur series, Kozhikode, Kerala: Fine loamy, isohyperthermic family of Kaolinitic, Kanhaplic Haplustults (Granite Gneiss)																		
0-10	Ap1	SCl	47.2	21.2	31.6	0.67	4.5	31.9	0.46	0.24	0.05	0.17	1.42	7.4	2.3	23.41	7.27	12.5
10-36	AB	SCl	48.7	18.7	32.6	0.57	5.1	22.2	0.15	0.12	0.04	0.17	1.28	5.4	1.8	16.56	5.52	9
36-48	Bt1	SCl	48.5	19.3	32.2	0.60	5.3	14.8	0.22	0.14	0.06	0.14	1.06	6.1	1.6	18.94	4.96	9.2
48-66	Bt2	SCl	47.1	19.5	33.4	0.58	5.2	12	0.23	0.15	0.06	0.14	0.85	5.4	1.4	16.16	4.19	10.8
66-80	Bt3	SCl	50.7	19.2	30.1	0.64	5.1	6.1	0.32	0.19	0.04	0.14	0.86	5.1	1.6	16.94	5.31	13.7
w̄			**48.47**	**19.37**	**32.16**	**1.38**	**5.25**	**16.18**	**0.22**	**0.13**	**0.07**	**0.28**	**1.84**	**5.09**	**4.39**	**15.71**	**6.79**	**10.70**
P4-Kanjirapally series, Kottayam, Kerala: Loamy skeletal, Kaolinitic, family of Ustic Kandihumults (Charnokite)																		
0-13	Ap	SCl	69.9	9	21.2	0.42	4.8	23.5	0.58	0.13	0.12	0.15	0.57	4.5	1.6	21.22	7.54	21.7
13-32	Bt1	SCl	56.1	12.5	31.3	0.40	4.4	18.6	0.22	0.08	0.13	0.17	0.45	3.5	1.1	11.18	3.51	17.1
32-56	Bt2	SCl	59.9	11.1	28.9	0.38	4.5	15	0.23	0.07	0.14	0.08	0.32	3.7	0.8	12.8	2.76	14
56-83	Bt3	SCl	62.8	11.4	25.7	0.44	4.5	9	0.28	0.07	0.12	0.07	0.12	4.1	0.7	15.95	2.72	13.2
83-112	Bt4	SCl	57.1	11.3	28.5	0.40	4.4	11.1	0.24	0.08	0.12	0.07	0.07	3.9	0.6	13.68	2.1	13.2
122-150	Bt5	SCl	62.6	13.4	24	0.56	4.7	12.2	0.34	0.1	0.12	0.11	0.04	4	0.7	16.66	2.91	16.8
			56.78	**13.40**	**24.00**	**0.41**	**4.23**	**12.84**	**0.28**	**0.08**	**0.12**	**0.09**	**0.20**	**3.66**	**0.78**	**13.93**	**2.98**	**14.35**
P5.Athirampuza series, Ernakulam, Kerala:clayey skeletal, Kaolinitic, family of Ustic Kandihumults (Laterite)																		

0-16	Ap	SC	51.7	11	37.3	0.29	4	23.6	0.28	0.09	0.03	0.16	2	9	2.6	24.12	6.97	6.3
16-42	Bt1	C	39.7	8	52.3	0.15	3.8	12.6	0.23	0.05	0.03	0.15	2.68	8.1	3.4	15.48	6.5	5.7
42-66	Bt2	C	33.3	6.7	60	0.11	4.1	9.9	0.19	0.04	0.03	0.11	2.92	7.3	3.3	12.16	5.5	5.1
66-89	Bt3	C	34.6	11.8	53.6	0.22	4.3	6.7	0.23	0.05	0.04	0.11	2.63	6.4	3.1	11.94	5.78	6.7
89-105	BC	C	30.3	16.3	53.4	0.31	4.1	6.3	0.77	0.12	0.02	0.09	1.42	7	2.4	13.1	4.49	14
w̄			**37.52**	**10.26**	**52.23**	**0.20**	**4.05**	**11.41**	**0.31**	**0.06**	**0.03**	**0.12**	**2.43**	**7.51**	**3.04**	**14.90**	**5.88**	**7.14**

3.4. Soil chemical characteristics of Lateritic Soils

The Madgaon series (P1) was strongly acidic in the Ap horizon (pH 5.1) and moderately acidic in the AB/Bt horizons (pH 5.5). Organic carbon (OC) content was highest in the Ap horizon (16.7 g kg^{-1}) and decreased progressively with depth, from 8.4 to 2.5 g kg^{-1}, with a profile-weighted mean of 8.13 g kg^{-1}. Calcium (Ca) was the dominant exchangeable base and increased with depth from 1.86 to 3.45 cmol(+) kg^{-1}, followed by magnesium (Mg), which increased from 0.69 to 1.61 cmol(+) kg^{-1}. Exchangeable Na varied from 0.36 to 0.44 cmol(+) kg^{-1}, with only slight depth inflictions, whereas exchangeable K was very low (0.06–0.09 cmol(+) kg^{-1}). Exchangeable Al occurred only in trace amounts in the Ap/AB horizons (0.19–0.08 cmol(+) kg^{-1}). The profile-weighted mean CEC was 7.33 cmol(+) kg^{-1}, with horizon-wise values ranging from 9.75 cmol(+) kg^{-1} in the AB horizon to 6.31 cmol(+) kg^{-1} in the Bt1 horizon. ECEC increased with depth from 3.2 cmol(+) kg^{-1} in the Ap horizon to 5.3 cmol(+) kg^{-1} in the Bt2 horizon, with a profile-weighted mean of 4.11 cmol(+) kg^{-1}. The Bt horizons had apparent CEC values below 24 cmol(+) kg^{-1} clay and apparent ECEC values below 16 cmol(+) kg^{-1} clay, while base saturation exceeded 60%. Apparent CEC and ECEC generally decreased with depth, whereas base saturation showed an increasing trend (Table 3).

The Darbandora series (P2) was strongly acidic with pH values ranging from 5.2 to 5.4. The profile-weighted mean OC content was 21.15 g kg^{-1} and decreased markedly with depth, from 50.4 g kg^{-1} in the Ap horizon to 14.7 g kg^{-1} in the Bt3 horizon. Calcium dominated the exchange complex, although its concentration decreased with depth from 4.56 to 3.51 cmol(+) kg^{-1}. In contrast, exchangeable Mg increased from 1.67 to 2.13 cmol(+) kg^{-1}. The profile-weighted mean of exchangeable Na and K were 0.62 and 0.28 cmol(+) kg^{-1}, respectively. Exchangeable Na exhibited an irregular depth distribution (0.63–0.53–0.66 cmol(+) kg^{-1}), whereas its concentration was relatively uniform in the Bt horizons (approximately 0.23 cmol(+) kg^{-1}). CEC values ranged from 16.46 to 19.05 cmol(+) kg^{-1} in the Bt horizons, while ECEC ranged from 6.63 to 6.91 cmol(+) kg^{-1}. The Ap horizon had a CEC of 18.99 cmol(+) kg^{-1} and an ECEC of 7.65 cmol(+) kg^{-1}. Base saturation had a profile-weighted mean of 41.94% and showed only minor variation with depth. The apparent CEC

and ECEC showed decreasing trends with depth, with profile-weighted means of 27.91 and 11.53 cmol(+) kg^{-1} clay, respectively.

The Kinalur series (P3) was very strongly acidic in the Ap horizon and strongly acidic in the kandic B horizons. Clay content exceeded 30% in the subsurface horizons. Organic carbon decreased progressively from 31.9 g kg^{-1} in the Ap horizon to 6.1 g kg^{-1} in the Bt3 horizon. Base saturation remained below 35% throughout the profile. The subsurface horizons satisfied the criteria for a kandic horizon, with apparent CEC values below 16 cmol(+) kg^{-1} clay and apparent ECEC values below 12 cmol(+) kg^{-1} clay within 100 cm depth.

The Kanjirapalli (P4) and Athirampuzha (P5) series were very strongly acidic and contained more than 0.9% organic carbon throughout the profiles. Their profile-weighted mean OC contents were 12.84 g kg^{-1} in P4 and 11.41 g kg^{-1} in P5, respectively. The kandic horizons had very low base saturation, with values of 14.35% in P4 and 7.14% in P5. The apparent CEC and ECEC values were comparable to those reported for kandic horizons in other parts of India (Bhaskar et al., 2005; Bhattacharyya et al., 2006).

The occurrence of kandic genetic horizons in ferruginous soils of rubber-growing areas of Kerala and Tamil Nadu was previously reported by Krishnan et al. (1996). Similar chemical characteristics of ferruginous soils occurring in the Western Ghats and coastal regions of North Karnataka were reported by Patil and Dasog (1999).

3.5. Elemental composition

Table 4 presents the elemental composition of five laterite-associated soil profiles from Kerala. SiO_2 was the most abundant major oxide and exhibited variable depth distributions among the studied profiles. The Madgaon series (P1) had a weighted mean SiO_2 content of 49.34%, with a decreasing trend from 53.5% in the Ap horizon to 44.9% in the Bt1 horizon. In contrast, the Darbandora series (P2) had a weighted mean of 45.38% and showed an increasing trend, from 37.7% in the A horizon to 47.2% in the Bt2 horizon. The Kanjirapalli series (P4) had a reported weighted mean SiO_2 content of 37.42%, with SiO_2 decreasing from 45.4% in the Ap horizon to 33.0% in the Bt5 horizon. The Kinalur series (P3) had a weighted mean SiO_2 content of 54.77%, with slightly higher concentrations in the Bt1 and Bt2 horizons than in the surface horizons. The Athirampuzha series (P5) had a reported weighted mean SiO_2 content of 40.30%, with decrease in the Bt horizons.

The weighted mean Al_2O_3 content was 28.98% in P4, 28.03% in P5, 20.73% in P2, 18.60% in P1, and 17.12% in P3. In P1, Al_2O_3 increased markedly with depth, from 12.0% in the Ap horizon to 24.6% in the Bt2 horizon. In P3, Al_2O_3 varied from 17.4% in the Ap horizon to 17.8% in the Bt3 horizon, with weighted mean of 17.12%. In P4 and P5, Al_2O_3 showed higher concentrations in the subsurface horizons than in the surface horizons.

Fe_2O_3 exhibited a pronounced decrease with depth in the Madgaon series (P1), whereas an increasing trend was observed in the Athirampuzha series (P5); the other profiles showed irregular depth distributions. The Fe_2O_3 concentration in the surface horizon was 1.2% in P3, whereas it exceeded 15% in both P1 (15.7%) and P2 (15.9%). Based on the reported weighted mean Fe_2O_3 contents, the profiles were arranged in descending order as P4 (12.96%) > P1 (11.90%) > P2 (9.42%) > P5 (8.96%) > P3 (6.53%).

The TiO_2 content in the Ap horizon of P1 was 2.20% and decreased to 1.66% in the Bt1 horizon. In P2, TiO_2 concentrations were relatively uniform, ranging from 1.64 to 1.66% in the Bt horizons. The Kinalur series (P3) generally contained less than 1% TiO_2 throughout the profile, although the concentration reached 1.0% in the Bt1 horizon.

In most horizons, the concentrations of the alkali and alkaline-earth oxides were below 1%. An exception was P2, where the reported weighted mean concentrations of Na_2O (2.45%), CaO (1.63%), and K_2O (1.04%) exceeded 1%, while MgO was approximately 1.00%. In contrast, P5 showed relatively low reported weighted mean concentrations of CaO (0.38%), MgO (0.40%), Na_2O (0.18%), and K_2O (0.66%). Overall, the elemental composition revealed substantial variation among the soil series in the abundance and vertical distribution of SiO_2, Al_2O_3, Fe_2O_3, TiO_2, and the major base-forming oxides.

Table 4. Elemental composition of Lateritic soils of Kerala

Depth (cm)	Horizon	Elemental composition SiO_2	Al_2O_3	Fe_2O_3	TiO_2	CaO	MgO	Na_2O	K_2O	Cu	Zn	Mn	Ni	Cr	Cd	Zr	Ba	Sr	LOI (%)
		(%)								µg/g									
P1-Madgaon series																			
0-18	Ap	53.5	12	15.7	2.2	0.86	0.76	0.87	0.5	70	158	780	44	281	9	28	94	64	12.6
18-46	A/B	55	14.5	14.2	1.74	0.82	0.73	0.78	0.55	131	297	756	50	237	8	30	58	61	10.7
46-73	Bt1	44.9	19.7	13.9	1.66	0.77	0.56	0.61	0.83	133	157	331	59	198	8	21	46	51	16
73-107	Bt2	46	24.6	6.4	1.71	0.78	0.52	0.35	0.64	60	127	117	75	220	5	17	46	53	17.4
w̄		49.34	18.60	11.90	1.79	0.80	0.63	0.62	0.64	98.68	184.27	449.75	59.21	229.16	7.21	23.26	57.24	56.44	14.49
_P2-Darbandora series																			
0-8	A	37.7	16.5	15.9	1.46	0.96	1.1	0.61	1.34	74	195	1539	112	198	12	39	44	63	23.4
8-19	AB	45.8	21.7	6.8	1.62	0.48	1.02	0.68	1.55	71	188	1571	138	173	8	46	46	60	19.3
19-51	Bt1	45	19.6	11.1	1.64	0.43	0.93	0.66	1.63	72	201	1499	167	206	6	45	37	58	17.5
51-89	Bt2	47.2	22.3	7.4	1.66	0.45	1.03	0.6	1.7	147	256	1355	172	194	6	44	36	64	16.7
w̄		**45.38**	**20.73**	**9.42**	**1.63**	**0.49**	**1.00**	**0.63**	**1.62**	**104.1**	**222.34**	**1,450.**	**160.61**	**196.08**	**6.79**	**44.16**	**38.31**	**61.26**	**17.91**
P3-Kinalur series																			
0-10	Ap1	55.8	17.4	1.2	0.8	1.59	0.68	1.97	1.08	304	142	324	60	48	8	14	33	40	16.91
10-36	Ap2	54.4	16.4	8.1	0.7	2.13	0.71	2.46	1	47	156	311	56	82	9	13	68	34	14.02
36-48	Bt1	56.3	17.8	3.7	1	1.59	1.15	3.09	1.17	43	234	359	33	89	8	15	54	36	14.17
48-66	Bt2	57.2	17	3.9	0.8	1.39	0.65	2.74	0.98	42	204	275	49	94	9	15	40	33	13.26
66-80	Bt3	50.3	17.8	13.2	0.7	1.05	0.77	1.87	1.05	43	327	250	49	72	8	13	60	31	13.05

w̄		**54.77**	**17.12**	**6.53**	**0.78**	**1.63**	**0.77**	**2.45**	**1.04**	**76.70**	**206.68**	**301.05**	**50.25**	**79.75**	**8.55**	**13.88**	**53.83**	**34.30**	**14.06**
P4-Kanjirapally series																			
0-13	Ap	45.4	26.1	6.4	1.1	0.74	0.54	0.2	0.52	17	151	535	624	127	0	371	38.64	17.27	18.18
13--32	Bt1	37.9	27.3	12.7	1.1	0.46	0.49	0.17	0.51	34	140	707	384	99	0	350	36.21	15.79	19.59
32-56	Bt2	37.3	30.9	11.6	1	0.54	0.67	0.17	0.53	20	126	784	990	167	26	261	30.45	14.08	18.93
56-83	Bt3	36.1	27.6	14.9	1.1	0.57	0.48	0.19	0.63	251	137	484	416	121	67	513	32.3	13.88	18.52
83-112	Bt4	33.7	30	14.9	1.2	0.52	0.31	0.13	0.65	59	117	299	175	62	0	221	52.4	11.2	18.96
112-150	Bt5	33	31.3	12.7	1.2	0.42	0.29	0.15	0.5	316	109	357	507	69	0	256	19.74	11.94	20.39
	w̄	**37.42**	**28.98**	**12.96**	**1.12**	**0.56**	**0.49**	**0.17**	**0.59**	**90.63**	**132.57**	**547.32**	**499.84**	**113.16**	**21.72**	**341.54**	**38.68**	**14.05**	**19.05**
P5.Athirampuza series																			
0-16	Ap	46.8	24.6	8.3	1.9	0.44	0.43	0.22	0.79	15	185	360	296	116	0	220	25.91	20.8	16.56
16-42	Bt1	43.7	29.2	8.1	1.5	0.33	0.43	0.17	0.62	9	164	268	233	81	0	360	24.5	24.68	16.22
42-66	Bt2	39.2	30.4	12.5	1.4	0.55	0.41	0.17	0.69	162	148	169	156	91	65	473	42.81	24.78	15.12
66-89	Bt3	40.7	30.6	10.2	1.4	0.36	0.41	0.2	0.69	18	200	182	286	104	13	376	31.91	21.62	15.94
89-105	BC	41.6	31.8	7.8	1.4	0.33	0.45	0.17	0.71	18	145	188	415	67	13	269	26.67	21.69	15.41
	w̄	**40.30**	**28.03**	**8.96**	**1.43**	**0.38**	**0.40**	**0.18**	**0.66**	**40.51**	**161.49**	**220.31**	**256.91**	**87.19**	**16.59**	**331.61**	**28.82**	**21.81**	**15.12**

3.6. Trace elements

The presence of nine trace elements below 1000 mg/kg or 0.1% in lateritic profiles is primarily influenced by the weathering of bedrocks (Rollinson, 1993). The concentrations and depth-wise distribution of nine trace elements (Cu, Zn, Mn, Ni, Cr, Cd, Zr, Ba and Sr) in the studied lateritic soil profiles are presented in Table 4. Their distribution varied considerably among the profiles and horizons, reflecting differences in parent material, weathering intensity, leaching, organic matter, and possible association with Fe- and Mn-bearing phases under the humid climatic conditions of Kerala. Copper concentrations ranged from 9 μg g^{-1} in P5-Bt1 to 316 μg g^{-1} in P4-Bt5, while Zn ranged from 109 μg g^{-1} in P4-Bt5 to 327 μg g^{-1} in P3-Bt3. Manganese showed the widest concentration range, from 117 μg g^{-1} in P1-Bt2 to 1571 μg g^{-1} in P2-AB. Chromium ranged from 48 μg g^{-1} in P3-Ap1 to 281 μg g^{-1} in P1-Ap, whereas Ni ranged from 33 μg g^{-1} in P3-Bt1 to 990 μg g^{-1} in P4-Bt2. The concentrations of Zr ranged from 13 to 513 μg g^{-1}, with the maximum recorded in P4-Bt3. Ba ranged from 19.74 to 94 μg g^{-1}, while Sr showed comparatively lower concentrations across the profiles. Cadmium concentrations were generally low, ranging from 0 to 67 μg g^{-1}.

Copper exhibited contrasting depth distributions among the profiles. In P3, Cu decreased markedly from 304 μg g^{-1} in Ap1 to 47 μg g^{-1} in Ap2 and remained relatively low in the underlying Bt horizons (42–43 μg g^{-1}). In P4, Cu increased substantially from 17 μg g^{-1} in the Ap horizon to 251 μg g^{-1} in Bt3 and reached 316 μg g^{-1} in Bt5. In P5, Cu increased from 15 μg g^{-1} in the Ap horizon to 162 μg g^{-1} in Bt2, followed by lower concentrations in the deeper horizons. The reported profile-weighted mean Cu concentrations varied among the soil series, with P5 showing the lowest value (40.51 μg g^{-1}) and P2 a relatively high value (104.10 μg g^{-1}).

Zinc concentrations were generally higher in the subsurface horizons of P2 and P3. In P2, Zn increased from 195 μg g^{-1} in the A horizon to 256 μg g^{-1} in Bt2, while in P3 the concentration reached 234, 204 and 327 μg g^{-1} in Bt1, Bt2 and Bt3, respectively. These concentrations are substantially higher than the reported world average soil Zn concentration of 90 mg kg^{-1} (Bowen, 1979), although the magnitude of enrichment varied among the profiles.

Manganese exhibited considerable variability both among profiles and with depth. The highest concentration (1571 μg g^{-1}) occurred in the AB horizon of P2, followed by 1539, 1499 and 1355 μg g^{-1} in the A–Bt horizons of the same profile. In P1, Mn decreased markedly from 780 μg g^{-1} in the Ap horizon to 117 μg g^{-1} in Bt2, whereas P3, P4 and P5 showed variable depth distributions. The contrasting Mn patterns indicate that its vertical distribution was not uniform across the studied profiles.

Nickel concentrations showed particularly pronounced differences among the soil series. P1 and P3 generally had relatively low Ni concentrations, with profile-weighted means of 59.21 and 50.25 μg g^{-1}, respectively. In contrast, P4 showed markedly elevated Ni concentrations, reaching 990 μg g^{-1} in Bt2, while P5 recorded 415 μg g^{-1} in the BC horizon. The displayed horizon-wise data indicate substantially higher profile-weighted Ni concentrations in P4 and P5 than in P1 and P3. The occurrence of Ni concentrations exceeding 200 μg g^{-1} in several horizons, particularly in P4 and P5, indicates localized enrichment and warrants comparison with the adopted soil-quality or contamination guidelines.

4. Discussion

4.1. Elemental geochemistry in relation to colour, textural and chemical properties

The soil colours ranged from red and dark red to dark reddish brown, consistent with the formation and accumulation of secondary iron oxides during prolonged weathering and soil development (Hausenbuiller, 1978). The predominance of red hues in the subsurface horizons indicates the important role of iron-bearing minerals and their transformation during pedogenesis. In contrast, the relatively dark reddish-brown surface horizon of the P2 may be associated with the accumulation of organic matter, which can modify the expression of the underlying red colour. The progressive development of red to dark-red colours in the subsurface horizons suggests a comparatively stronger expression of pedogenic iron oxides, where the influence of surface organic matter is diminished.

The studied lateritic soils were predominantly acidic, although the magnitude of acidity and the associated chemical characteristics varied among the profiles. Such variation was reflected in differences in exchangeable bases, cation-exchange characteristics, base saturation and the distribution of major elemental oxides. The elemental composition further indicated substantial variation in SiO_2, Al_2O_3 and Fe_2O_3 among the soil series, demonstrating differences in the degree of weathering and relative accumulation or depletion of major soil-forming elements. In several profiles, Al_2O_3 constituted a prominent component of the sesquioxide fraction, indicating substantial alumina accumulation associated with advanced weathering and clay-mineral transformations.

The relationship between elemental composition and the degree of lateritization was further examined using the SiO_2–sesquioxide proportions in the triplot diagram. This approach helped to characterize the studied materials in relation to their silica and sesquioxide composition and provided a geochemical basis for interpreting their lateritic nature. The observed variations in SiO_2, Al_2O_3 and Fe_2O_3 among the profiles were consistent with differential removal of mobile constituents and relative concentration of less mobile elements during weathering under the humid to perhumid environmental conditions of Kerala.

The distribution of trace elements also varied markedly both among the soil series and with depth. Their distribution was influenced by the nature and degree of weathering of the parent material, redistribution through the soil profile, leaching, organic-matter interactions and possible association with Fe- and Mn-bearing phases. The occurrence of elevated concentrations of selected trace elements in particular horizons indicated that their behaviour cannot be interpreted solely from total concentration, but should be considered in relation to soil colour, clay content, organic carbon, acidity and the abundance of Fe- and Mn-bearing constituents.

4.2. CIELab system

The mean L*, a* and b* values were 38.05 ± 7.71, 15.41 ± 4.31 and 22.50 ± 4.52, respectively. The corresponding coefficients of variation (CV) were 20.27, 27.94 and 20.09%, indicating relatively greater variability in the red component (a*) than in lightness (L*) and yellowness (b*). The L* values ranged from 30.80 to 61.70, while a* and b* ranged from 7.80 to 22.20 and 14.60 to 31.10, respectively. The 99% confidence intervals for L*, a* and b* were 34.07–42.23, 13.59–17.23 and 19.91–25.09, respectively (Table 5).

The derived colour parameters a*1 and b*1 showed mean values of 0.68 ± 0.12 and 1.51 ± 0.28, with CVs of 17.49 and 18.57%, respectively. Their ranges were 0.45–0.91 and 1.10–2.22, respectively. The redness rating (RR), calculated following Torrent et al. (1983), varied from 3.00 to 11.25, with a mean value of 5.77 ± 1.92 and a CV of 33.34%, indicating comparatively greater variability in redness among the studied soil horizons. The 99% confidence interval for RR was 4.67–6.87.

The a*/(a+b) ratio showed a mean value of 0.40 ± 0.04, with a relatively low CV of 10.51%, and ranged from 0.31 to 0.48. Its 99% confidence interval was 0.38–0.42. The comparatively low variability of this ratio suggests that the relative contribution of the red component to the combined chromatic response remained relatively consistent across the studied soil horizons, despite the wider variation in the individual CIELab colour coordinates.

The correlation analysis (Table 6) revealed several significant relationships among the colour variables. L* showed a moderate positive correlation with b* (r = 0.41, significant at the 5% level), indicating that variation in lightness was associated with changes in the yellow component. A strong positive correlation was observed between a* and b* (r = 0.75, significant at the 1% level), suggesting that the red and yellow components varied in a closely associated manner across the studied horizons. The correlation between L* and a* was weak and non-significant (r = 0.21), indicating that variation in redness was not strongly related to overall lightness.

The a* parameter showed a strong positive correlation with *a*1 (r = 0.72, significant at the 1% level) and a/(a+b) (r = 0.71, significant at the 1% level). In contrast, a* showed a strong negative correlation with b1 (r = −0.70, significant at the 1% level). These relationships indicate that the derived colour indices were closely related to the red component of the CIELab colour space. The correlation between a1 and b*1 was very strong and negative (r = −0.97, significant at the 1% level), indicating an inverse relationship between these two derived colour parameters.

Redness rating showed a significant moderate positive correlation with b* (r = 0.55, significant at the 1% level) and a significant moderate negative correlation with a1 (r = −0.51, significant at the 5% level). However, its correlations with L (r = −0.25), a* (r = −0.28) and b1 (r = 0.06) were not significant. The a/(a+b) ratio showed a strong negative correlation with b1 (r = −0.98, significant at the 1% level) and a moderate negative correlation with RR (r =

−0.52, significant at the 1% level). It also showed a strong positive correlation with a (r = 0.71, significant at the 1% level).

Overall, the correlation analysis showed that the CIELab colour coordinates and derived indices are strongly interrelated and provide complementary quantitative measures of soil colour variation. The close relationships among a*, a1 and a/(a+b), together with the strong inverse relationships involving b*1, indicate that changes in the red component were important in differentiating the colour characteristics of the studied laterite-associated soils. The variation in RR further reflectd differences in soil redness among horizons, which can be interpreted in conjunction with Fe-bearing constituents, soil organic matter and other pedogenic properties. Thus, the CIELab system provides a quantitative complement to conventional Munsell colour assessment for characterizing colour variability in these laterite-associated soils.

Table 5. Descriptive statistics of soil colour using CIE Lab values and redness rating

Statistical summary	L	CIE a	b	a*1	b*1	RR	a*/a+b
Mean	38.05	15.41	22.50	0.68	1.51	5.77	0.40
Sd	7.71	4.31	4.52	0.12	0.28	1.92	0.04
CV(%)	20.27	27.94	20.09	17.49	18.57	33.34	10.51
Mini	30.80	7.80	14.60	0.45	1.10	3.00	0.31
Max	61.70	22.20	31.10	0.91	2.22	11.25	0.48
EF(%)	23.46	52.85	47.91	49.93	37.06	33.55	54.59
Confidence interval (99%level)							
Lower limit	34.07	13.59	19.91	0.61	0.65	4.67	0.38
Upper limit	42.23	17.23	25.09	0.75	2.38	6.87	0.42

Table 6. Correlation analysis between soil colour values

	CIE system						
Colour variables	L	a	b	a*1	b*1	RR	a*/a+b
L	1.00						
a	0.21	1.00					
b	0.41**	0.75*	1.00				
a*1	-0.06	0.72*	0.11	1.00			
b*1	0.02	-0.70*	-0.10	-0.97*	1.00		
RR	-0.25	-0.28	0.06	-0.51**	0.55*	1.00	
a/a+b	-0.03	0.71*	0.11	1.00	-0.98*	-0.52*	1.00

*significant at 1%level, **significant at 5%level, two tailed, degree of freedom (n-2) =22

4.3. Textural and chemical characteristics

The descriptive statistics of the textural and chemical properties of the studied soils (Table 7) showed considerable variability among the five laterite-associated soil series. The mean clay content was 37.55 ± 15.46%, with a high coefficient of variation (CV = 41.17%), and ranged from 11.50% to 65.20%. Sand and silt also exhibited high variability, with CV values of 47.44 and 53.10%, respectively. The mean silt/clay ratio was 0.54 ± 0.27, with a relatively high variability (CV = 49.15%). The observed variation in particle-size distribution reflects

differences in parent material, weathering intensity and pedogenic processes among the soil series. Sand and clay showed relatively low skewness, whereas silt/clay exhibited moderate positive skewness. Several chemical properties, particularly pH, exchangeable Al, Mg, Na and K, showed departures from normality based on the skewness/standard-error criterion (Hair et al., 2010; Hatem Georges et al., 2022). The distribution of organic carbon, exchangeable K, apparent CEC and ECEC was platykurtic, whereas several other properties exhibited leptokurtic distributions (Groeneveld and Meeden, 1984).

The depth distribution of clay and silt was an important feature of the studied pedons, with enrichment of clay in several subsurface Bt horizons relative to the surface horizons. In P1, the Ap horizon contained only 11.6% clay, whereas the argillic horizons showed a marked increase in clay content. This increase, together with the textural differentiation between surface and subsurface horizons, provides evidence for clay accumulation within the subsurface horizons and is consistent with the development of an argillic horizon. Similar clay enrichment in subsurface horizons has been reported for tropical soils by Patil and Dasog (1999) and Dubey et al. (2017).

Table 7. Descriptive statistics of textural and chemical properties of soils

Statistical	Sand	silt	clay			OC			Exchangeable bases (cmol/kg)			CEC	ECEC	Apparent	Apparent	Base saturation
parameters	----------%----------			silt/clay	pH	g/kg	Ca	Mg	Na	K	Al		cmol/kg	CEC	ECEC	(%)
Mean	44.02	18.30	37.55	0.54	4.81	15.98	1.28	0.52	0.22	0.16	0.86	8.05	3.04	23.65	8.76	24.08
Standard Error	4.26	1.98	3.16	0.05	0.11	2.10	0.31	0.14	0.05	0.03	0.18	1.02	0.44	3.39	1.43	4.11
Standard Deviation	20.88	9.72	15.46	0.27	0.53	10.31	1.50	0.67	0.22	0.15	0.90	4.97	2.16	16.59	7.00	20.12
Kurtosis	-0.65	0.08	-0.86	-0.06	-1.24	4.34	-0.48	0.41	-0.84	17.66	0.37	1.12	-0.23	7.76	2.87	1.27
Skewness	-0.34	1.00	0.26	0.58	-0.34	1.73	1.08	1.37	0.90	3.96	1.19	1.53	0.92	2.63	1.77	1.36
Minimum	7.00	6.70	11.50	0.11	3.80	2.50	0.15	0.04	0.02	0.06	0.00	3.50	0.60	11.18	2.10	5.10
Maximum	78.20	42.00	65.20	1.13	5.50	50.40	4.56	2.13	0.66	0.80	2.92	19.65	7.65	84.60	27.73	79.20
cv(%)	**47.44**	**53.10**	**41.17**	**49.15**	**10.99**	**64.54**	**117.13**	**129.89**	**102.10**	**91.34**	**104.36**	**61.80**	**71.15**	**70.14**	**79.95**	**83.56**
skewness/SE	**-0.08**	**0.50**	**0.08**	**10.67**	**-3.14**	**0.82**	**3.54**	**9.94**	**19.74**	**133.15**	**6.50**	**1.50**	**2.09**	**0.78**	**1.24**	**0.33**
Kutosis/SE	**-0.15**	**0.04**	**-0.27**	**-1.12**	**-11.51**	**2.06**	**-1.55**	**3.01**	**-18.41**	**593.67**	**2.04**	**1.11**	**-0.53**	**2.29**	**2.00**	**0.31**

In contrast, P3 contained 31.6% clay in the Ap horizon and showed only a small relative increase in clay content in the subsurface horizons (approximately 1.03–1.05 times the surface value). The subsurface horizons nevertheless exhibited low base saturation and low apparent CEC and ECEC, characteristics associated with strongly weathered, low-activity clay horizons. The combination of these properties should therefore be interpreted together with the complete morphological and chemical criteria used for soil classification rather than from clay enrichment alone.

The P4 and P5 series contained more than 30% clay in their subsurface horizons and showed approximately 1.2-fold enrichment relative to the surface horizons. Their low base saturation and low apparent CEC and ECEC indicate strongly weathered soil conditions and support the

recognition of low-activity clay characteristics. The appreciable exchangeable Al observed in these soils is also consistent with their strongly acidic and advanced weathering under the high-rainfall environment of Kerala. In comparison, P1 had relatively low exchangeable Al and a somewhat higher soil pH, suggesting differences in the intensity of weathering and base-status conditions among the profiles (Thomas, 1961).

The CEC values were generally higher than ECEC, reflecting the contribution of pH-dependent negative charges to the soil exchange complex. The difference between CEC and ECEC was particularly evident in the strongly weathered subsurface horizons of P4 and P5. Their apparent CEC values below 16 cmolc kg^{-1} clay and ECEC values below 12 cmolc kg^{-1} clay indicate low charge characteristics of the clay fraction. Such properties are commonly associated with highly weathered tropical soils dominated by low-activity clay minerals and Fe/Al oxides.

The silt/clay ratio provided additional evidence of the degree of weathering and textural differentiation. In P4, the ratio varied approximately from 0.38 to 0.56, whereas in the Bt horizons of P5 it ranged from 0.11 to 0.31 and generally declined with depth. The low silt/clay ratios in the subsurface horizons, particularly in P5, are indicative of advanced weathering and substantial relative clay accumulation. However, a low silt/clay ratio should be interpreted as supporting evidence rather than as an independent criterion for identifying a particular diagnostic horizon or soil order.

The sand/clay ratio has also been used as an indicator of laterization, with Buringh (1970) suggesting a value below 0.25 as a critical level. P5 satisfies this criterion in the relevant subsurface horizons. However, the usefulness of this ratio as a universal indicator of laterization is limited in highly weathered tropical soils. The relatively high silt contents observed in some of the studied soils may be related to the formation and persistence of stable microaggregates associated with Fe oxides, which can influence the measured particle-size distribution (Schmidt-Lorenz, 1979). Similar limitations of the sand/clay ratio for characterizing tropical soils have been reported by Ngongo and Langohr (1992), who suggested that a value of ≤0.5 may provide a more useful criterion under certain tropical soil conditions.

4.4. Correlations between textural and chemical properties

The correlation matrix (Table 8) revealed several significant relationships among the textural and chemical properties of the studied soils. A strong negative correlation was observed between sand and clay content ($r = -0.90$, $p < 0.05$), reflecting the contrasting contribution of these two particle-size fractions to the soil matrix. Sand also showed significant negative correlations with CEC ($r = -0.71$, $p < 0.05$) and ECEC ($r = -0.78$, $p < 0.05$), whereas clay showed positive correlations with CEC ($r = 0.57$, $p < 0.01$) and ECEC ($r = 0.71$, $p < 0.01$).

The silt/clay ratio was positively correlated with silt ($r = 0.55$, $p < 0.05$) and negatively correlated with clay ($r = -0.50$). These relationships are consistent with the mathematical dependence of the ratio on its component fractions and should therefore be interpreted primarily as textural relationships rather than as independent evidence of pedogenic processes. The pH of the soils was positively correlated with silt ($r = 0.80$, $p < 0.01$) and negatively correlated with exchangeable Al ($r = -0.66$, $p < 0.05$). The inverse relationship between pH and exchangeable Al is particularly relevant to the strongly acidic nature of these soils, because increasing soil acidity is generally associated with greater solubility and exchangeable forms of Al.

Exchangeable bases exhibited several significant positive relationships with one another and with the soil exchange complex. Exchangeable Ca showed positive correlations with Mg ($r = 0.80$, $p < 0.01$), Na ($r = 0.65$, $p < 0.01$), CEC ($r = 0.82$, $p < 0.01$) and base saturation ($r = 0.84$, $p < 0.01$). Exchangeable Mg was strongly correlated with Na ($r = 0.96$, $p < 0.01$), CEC ($r = 0.86$, $p < 0.01$) and ECEC ($r = 0.92$, $p < 0.01$). Similarly, exchangeable Na showed strong positive relationships with CEC ($r = 0.95$, $p < 0.01$) and ECEC ($r = 0.95$, $p < 0.01$). These relationships indicate that variation in exchangeable base status was closely associated with the overall cation-exchange characteristics of the soils.

Exchangeable K also showed significant positive relationships with CEC ($r = 0.82$, $p < 0.01$) and ECEC ($r = 0.54$, $p < 0.05$), although its relationship with the other exchangeable bases was comparatively weaker. The strong positive relationships between exchangeable bases and CEC/ECEC suggest that differences in the quantity and retention of exchangeable cations contributed substantially to variation in the effective and total exchange capacity of these soils.

The strong negative relationship between exchangeable Al and pH ($r = -0.66$, $p < 0.05$) and the significant negative relationships of exchangeable Al with several exchangeable bases

and exchange-capacity parameters showed the importance of soil acidity in controlling the chemical environment of these highly weathered soils. The soils under rubber plantations generally showed low CEC values, particularly in profiles other than P2, whereas P2 exhibited comparatively higher CEC. The relatively low CEC in the studied soils have limited nutrient-retention capacity in several of the profiles, despite the presence of substantial clay in some horizons. The observed chemical characteristics are broadly consistent with the low nutrient-retention capacity reported for highly weathered tropical soils (McKenzie et al., 2004; Hazelton and Murphy, 2007).

The role of exchangeable Al in highly weathered soils is particularly important because Al can interact with organic matter and mineral surfaces, whereas Fe is commonly associated with relatively insoluble oxide phases. Organic ligands can form complexes with metal ions, and the strength and nature of these interactions vary among cations and soil constituents (Sposito, 2008; Rowley et al., 2018). Such interactions may contribute to the observed variation in exchangeable Al and base cations among the studied profiles.

Table 8. Correlation matrix of textural and chemical properties

Correlations	sand	silt	clay	silt/clay	pH	OC g/kg	EXCa	ExMg	ExNa	ExK	ExAl	CEC	ECEC	apparent CEC	apparent ECEC	Base saturation
sand	1															
silt	**-0.72**	1.00														
clay	**-0.90****	0.35	1.00													
silt/clay	0.12	0.55**	-0.50	1.00												
pH	-0.17	**0.67****	-0.19	0.80**	1.00											
OC	-0.13	0.20	0.06	0.02	0.13	1.00										
ExCa	**-0.63****	**0.80****	0.36	0.49*	**0.65****	0.34	1.00									
ExMg	**-0.70****	**0.78****	0.46*	0.37	**0.62****	0.31	**0.96****	1.00								
ExNa	-0.47*	**0.65****	0.24	0.48*	**0.67****	0.28	**0.95****	**0.95****	1.00							
ExK	-0.42*	0.42*	0.31	0.05	0.26	0.82**	0.54**	0.51*	0.42*	1.00						
ExAl	-0.15	-0.40	0.46*	**-0.66****	**-0.65****	-0.03	-0.44*	-0.41*	-0.55**	-0.03	1.00					
CEC	**-0.71****	**0.57****	**0.61****	0.07	0.37	0.52**	**0.82**	**0.86****	**0.78****	**0.65****	-0.06	1.00				
ECEC	**-0.78****	**0.71****	**0.62****	0.22	0.44*	0.37	**0.92****	**0.92**	**0.83****	**0.59****	-0.06	**0.91****	1.00			
apparent CEC	0.23	0.06	-0.34	0.56**	0.49*	0.23	0.45*	0.38	**0.57****	0.17	-0.33	0.40	0.35	1.00		
apparent ECEC	0.08	0.24	-0.25	**0.68****	0.55**	0.17	0.60**	0.50*	**0.66****	0.17	-0.31	0.40	0.51*	**0.90****	1.00	
Base saturation	-0.37	**0.75****	0.04	**0.72****	**0.68****	0.00	**0.84****	**0.75****	**0.80****	0.15	**-0.60****	0.39	**0.64****	0.35	**0.62****	1.00

* Significant at $p < 0.05$; ** Significant at $p < 0.01$; two-tailed test; df = 22. Critical r values are 0.404 at the 5% level and 0.515 at the 1% level.

4.5. Pedotransfer functions

a) Prediction of CEC from the CIE **a** *value*

Simple linear regression analysis showed that the CIE *a* value was a significant predictor of CEC. The fitted regression equation was:

$$\mathbf{CEC = 15.74 - 0.51}a$$

The model explained 21% of the variability in CEC (R^2 = 0.21; adjusted R^2 = 0.17). The overall regression was statistically significant, $F(1, 22) = 5.72$, $p = 0.026$, indicating a significant linear relationship between the CIE *a* value and CEC. Thus, the CIE *a* value alone provided a modest predictive estimate of CEC in the studied soils. The relationship between observed and predicted CEC values is presented in Fig. 2, while the corresponding ANOVA and regression coefficient statistics are given in Supplementary Tables 1 and 2.

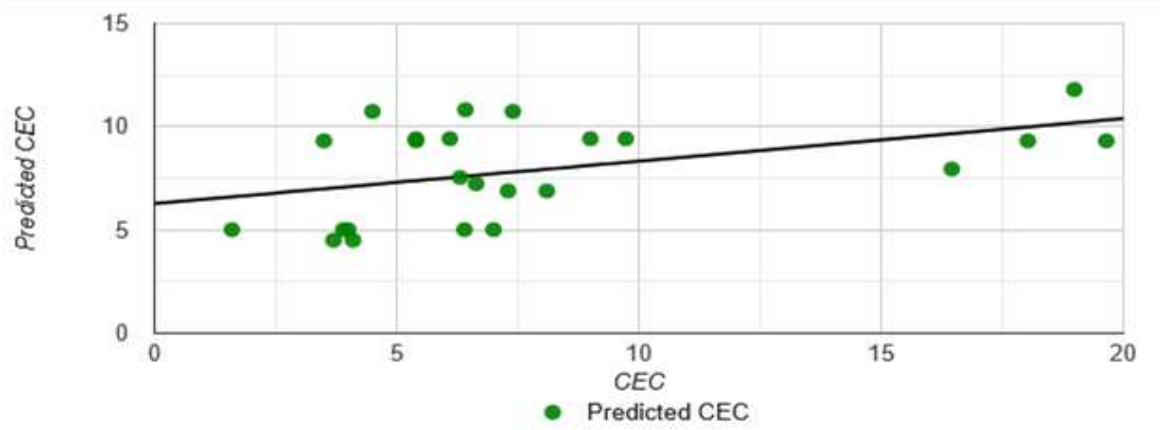


Fig. 2. Relationship between observed and predicted CEC of the studied soils.

b) Prediction of base saturation from the CIE L *value*

The simple linear regression between the CIE *L* value and base saturation was expressed as:

Base saturation = −12.01 + 0.95*L*

The regression model explained only 13% of the variation in base saturation (R^2 = 0.13; adjusted R^2 = 0.09). The overall regression was not statistically significant, $F(1, 22) = 3.38$, $p = 0.079$. Therefore, the CIE *L* value alone did not provide a statistically reliable prediction of base saturation in the present dataset.

c) Prediction of organic carbon from CIE Lab colour parameters

Multiple linear regressions were used to evaluate the combined predictive ability of CIE Lab colour parameters for soil organic carbon (OC). The resulting equation was:

OC = −25.94 − 0.39*L* + 3.29*a* − 3.14*b* + 50.48a_1*

The model showed a strong and statistically significant relationship between the colour parameters and OC, explaining 82% of the observed variation in OC (R^2 = 0.82; adjusted R^2 = 0.78). The overall regression was highly significant, $F(4, 19) = 21.18$, $p < 0.001$. All four predictors contributed significantly to the model: L ($t = -2.544$, $p = 0.020$), a ($t = 2.614$, $p = 0.017$), b ($t = -3.529$, $p = 0.002$), and a_1* ($t = 3.946$, $p < 0.001$). Thus, the combined CIE Lab colour parameters provided a substantially better prediction of OC than the individual colour variables considered separately (Supplementary Table 3, 4, 5 and Supplementary Fig. 1).

The use of soil colour parameters as a rapid and cost-effective approach for estimating soil organic matter or organic carbon has also been reported in previous studies (e.g., **Chen et al., 2018**). The redness rating (a_1*) provides an additional measure of relative soil redness. According to Vodyanitskii and Savichev (2017), soils may be categorized as having high redness when a_1* > 0.45, moderate redness at 0.25–0.45, and low redness when a_1* < 0.25.

d) Prediction of CEC from texture and organic carbon

Multiple linear regressions were also performed to estimate CEC using clay, silt and OC as predictor variables. The resulting pedotransfer function was:

CEC (cmol kg^{-1}) = −3.9 + 0.2 clay (%) + 0.2 silt (%) + 0.2 OC (g kg^{-1})

The model explained 69% of the variation in CEC (R^2 = 0.69) and was highly significant overall (F = 15.10, $p < 0.001$). All three predictors made significant contributions to the model. Clay (t = 3.569, p = 0.002) and OC (t = 3.363, p = 0.003) were significant at the 1% level, whereas silt (t = 2.391, p = 0.027) was significant at the 5% level. The variance inflation factor (VIF) values were less than 2, indicating no serious multicollinearity among the predictor variables. The relationship between observed and predicted CEC values is presented in the corresponding figure, and the ANOVA and regression coefficient statistics are provided in Supplementary Tables 6 and 7.

e) Prediction of ECEC from soil texture

A multiple linear regression model was developed to estimate ECEC from clay and silt contents:

ECEC (cmol kg^{-1}) = −1.477434 + 0.0599251 clay (%) + 0.123675 silt (%)

The model was statistically significant, $F(2, 21) = 20.48$, $p < 0.001$, and explained 66% of the variation in ECEC ($R^2 = 0.66$; adjusted $R^2 = 0.63$). The coefficient of multiple correlation (R) was 0.81, indicating a strong association between the observed and model-estimated ECEC values. Both predictor variables contributed significantly to the model: clay ($t = 3.161$, $p = 0.005$) and silt ($t = 4.10$, $p < 0.001$).

The intercept was not statistically significant ($t = -1.89$, $p = 0.07$); however, it was retained in the model because the regression equation should not be forced through the origin solely on the basis of a non-significant intercept. The model therefore indicates that the combined contribution of clay and silt content can explain a substantial proportion of the variability in ECEC of the studied soils.

4.6. Elemental geochemistry

The statistical summary of the major and trace elemental composition of the studied soils is presented in Table 9. SiO_2 was the dominant major oxide, with a mean concentration of 45.19 ± 7.43% and a coefficient of variation (CV) of 16.45%, ranging from 33.00 to 57.20%. Al_2O_3 had a mean concentration of 23.21 ± 6.21% (CV = 26.76%), whereas Fe_2O_3 averaged 10.07 ± 4.14% (CV = 41.17%). TiO_2 showed a relatively narrow range of 0.70–2.20%, with a mean of 1.33 ± 0.40% and moderate variability (CV = 29.76%). Among the alkaline and alkaline-earth oxides, CaO and Na_2O exhibited high to very high variability, with CV values of 60.85 and 113.18%, respectively. MgO (CV = 38.67%) and K_2O (CV = 42.98%) showed moderate variability. The relatively high variability of CaO and Na_2O indicates considerable heterogeneity in the abundance and distribution of these elements among the soil profiles.

The trace elements exhibited generally high to very high variability. Based on their mean concentrations, the principal trace elements occurred in the following descending order: Mn (575.00 μg g^{-1}) > Ni (231.08 μg g^{-1}) > Zn (177.67 μg g^{-1}) > Zr (167.08 μg g^{-1}) > Cr (133.17 μg g^{-1}) > Cu (89.83 μg g^{-1}) > Ba (42.65 μg g^{-1}) > Sr (35.24 μg g^{-1}) > Cd (12.00 μg g^{-1}). Mn showed the highest mean concentration, whereas Cd had the lowest. The high coefficients of variation observed for several trace elements, particularly Cd, Zr, Ni, Mn and Cu, showed substantial variability in their distribution within the studied soils. The mean LOI was 16.62 ± 2.85%, with a relatively low CV of 17.17%, indicating comparatively limited variability in the loss-on-ignition component.

Table 9. Descriptive statistics for elemental geochemistry

Statistical parameters	SiO_2	Al_2O_3	Fe_2O_3	TiO_2	**CaO**	**MgO**	Na_2O	K_2O	**Cu**	**Zn**	**Mn**	**Ni**	**Cr**	**Cd**	**Zr**	**Ba**	Sr	LOI
Mean	45.19	23.21	10.07	1.33	0.77	0.65	0.80	0.87	89.83	177.67	575.00	231.08	133.17	12.00	167.08	42.65	35.24	16.62
Standard Error	1.52	1.27	0.85	0.08	0.10	0.05	0.19	0.08	18.18	11.27	94.28	47.23	13.32	3.60	34.64	3.32	3.89	0.58
First Quartile	38.88	17.70	7.25	1.08	0.45	0.45	0.17	0.60	30.50	141.50	273.25	58.25	81.75	3.75	20.00	32.20	19.92	14.88
Third Quartile	51.10	29.40	13.38	1.65	0.89	0.76	0.80	1.06	131.50	200.25	762.00	318.00	195.00	9.75	289.25	47.60	54.25	18.62
Standard Deviation	7.43	6.21	4.14	0.40	0.47	0.25	0.91	0.37	89.06	55.23	461.88	231.40	65.27	17.62	169.69	16.25	19.06	2.85
Kurtosis	-1.05	-1.41	-0.78	-0.53	1.88	-0.59	1.08	0.03	1.63	1.47	0.44	3.93	-0.68	6.65	-1.06	3.15	-1.45	0.31
Skewness	0.12	-0.09	-0.37	0.12	1.52	0.62	1.52	1.05	1.56	1.31	1.30	1.84	0.67	2.66	0.65	1.44	0.37	0.11
Range	24.20	19.80	14.70	1.50	1.80	0.86	2.96	1.20	307.00	218.00	1,454.0 0	957.00	233.00	67.00	500.00	74.26	52.80	12.70
Minimum	33.00	12.00	1.20	0.70	0.33	0.29	0.13	0.50	9.00	109.00	117.00	33.00	48.00	0.00	13.00	19.74	11.20	10.70
Maximum	57.20	31.80	15.90	2.20	2.13	1.15	3.09	1.70	316.00	327.00	1,571.0 0	990.00	281.00	67.00	513.00	94.00	64.00	23.40
cv(%)	16.45	**26.76**	**41.17**	**29.76**	**60.85**	**38.67**	**113.18**	**42.98**	**99.14**	**31.09**	**80.33**	**100.14**	**49.01**	**146.83**	**101.56**	**38.09**	**54.09**	17.17

Table 10. Coefficient of individual predictors of Al_2O_3(%) (adjusted R-squared = 0.672)

	Coeff	**SE**	**t-stat**	**lower t0.025(20)**	**upper t0.975(20)**	**Stand Coeff**	**p-value**	**VIF**
b	23.05	5.21	4.42	12.18	33.93	0	0.00026	
L	-0.38	0.11	-3.47	-0.61	-0.15	-0.48	0.0024	1.33
b	1.08	0.17	6.32	0.72	1.44	0.84	0.0000036	1.23
redness rating	-1.69	0.39	-4.36	-2.49	-0.88	-0.55	0.00031	1.13

a) ***Al_2O_3(%) = 23.05 - 0.38 L + 1.08 b - 1.69 redness rating***

Multiple regression analysis revealed a strong and statistically significant relationship between Al_2O_3 and the CIE Lab colour parameters, with the model explaining 71% of the variation in Al_2O_3 (R^2 = 0.71; adjusted R^2 = 0.67; $F(3,20) = 16.72$, $p < 0.001$). All three predictors were statistically significant. L showed a negative relationship with Al_2O_3 ($t = -3.47$, $p = 0.0024$), whereas *b* showed a positive relationship ($t = 6.32$, $p < 0.001$) (Table 10). Redness rating was negatively related to Al_2O_3 ($t = -4.36$, $p < 0.001$). The VIF values (1.13–1.33) indicate that multicollinearity among the predictors was not a concern.

b) ***Mn = 1804.27 − 32.22L***

Simple linear regression indicated a significant relationship between Mn concentration and the CIE *L* value. The model explained approximately 29% of the variation in Mn concentration (R^2 = 0.29), and the regression was statistically significant, $F(1,22) \approx 9.1$, p = 0.006. The negative regression coefficient indicates that Mn concentration decreased with increasing *L* value.

The correlation analysis revealed several significant associations among the major and trace elements (Table 11). SiO_2 showed strong negative correlations with Al_2O_3 ($r = -0.79$, $p < 0.01$) and Fe_2O_3 ($r = -0.54$, $p < 0.01$), while significant positive correlations were observed with CaO ($r = 0.70$, $p < 0.01$) and Na_2O ($r = 0.79$, $p < 0.01$). The strong negative association

between SiO_2 and Al_2O_3 suggests contrasting behaviour of silica-rich and Al-rich phases during weathering and pedogenesis. Al_2O_3 was negatively correlated with CaO, MgO and Na_2O, but positively correlated with Ni (r = 0.68, p < 0.01) and Zr (r = 0.81, p < 0.01), indicating an association of these elements with Al-rich secondary phases (Al Chalabi, 2004).

Ni exhibited a significant negative correlation with SiO_2 (r = −0.59, p < 0.01) and significant positive correlation with Al_2O_3 (r = 0.68, p < 0.01), suggesting that its distribution was associated more closely with Al-rich phases than with silica-rich components. Ni also showed negative correlations with Na_2O (r = −0.53, p < 0.01) and Zr showed a strong positive correlation with Al_2O_3 (r = 0.81, p < 0.01), together with negative correlations with CaO, MgO, Na_2O and K_2O. These relationships indicate differential mobility and retention of the elements during soil weathering.

Chromium (Cr) showed a strong positive correlation with TiO_2 (r = 0.72, p < 0.01) and moderate positive correlations with MgO and Mn, suggesting an association with Ti- and Mn-bearing phases. Sr exhibited significant positive correlations with MgO (r = 0.72, p < 0.01), K_2O (r = 0.59, p < 0.01), Mn (r = 0.61, p < 0.01) and Cr (r = 0.76, p < 0.01), whereas it was negatively correlated with Al_2O_3 (r = −0.74, p < 0.01) and Zr (r = −0.74, p < 0.01). Ba showed significant positive correlations with CaO (r = 0.49, p < 0.05) and negative correlations with Al_2O_3 (r = −0.69, p < 0.01) and Ni (r = −0.53, p < 0.01).

The strong negative relationship of LOI with SiO_2 (r = −0.74, p < 0.01), together with its positive relationship with Al_2O_3 (r = 0.43, p < 0.05), indicates that the LOI component was relatively enriched in the more weathered, Al-bearing soil fractions.

Table 11. Correlation matrix for elemental composition

	SiO_2	Al_2O_3	Fe_2O_3	TiO_2	CaO	MgO	Na_2O	K_2O	Cu	Zn	Mn	Ni	Cr	Cd	Zr	Ba	Sr	LOI
SiO_2	1.00																	
Al_2O_3	**-0.79**	1.00																
Fe_2O_3	**-0.54**	0.07	1.00															
TiO_2	-0.06	-0.08	0.30	1.00														
CaO	**0.70**	**-0.66**	-0.38	**-0.53**	1.00													
MgO	**0.47**	**-0.68**	-0.17	0.05	0.38	1.00												
Na_2O	**0.79**	**-0.67**	**-0.49**	**-0.51**	**0.89**	**0.51**	1.00											
K_2O	0.28	**-0.42**	-0.30	0.01	0.19	**0.78**	0.37	1.00										
Cu	-0.12	-0.02	0.07	-0.10	0.07	-0.11	-0.02	0.02	1.00									
Zn	**0.52**	-0.53	-0.01	0.01	0.17	**0.56**	**0.41**	**0.45**	-0.19	1.00								
Mn	-0.06	-0.32	0.18	0.34	-0.19	**0.70**	-0.13	**0.65**	-0.01	0.24	1.00							
Ni	**-0.59**	**0.68**	0.10	-0.17	**-0.46**	-0.36	**-0.53**	**-0.42**	-0.07	**-0.44**	0.00	1.00						
Cr	0.15	**-0.45**	0.34	0.72	-0.16	**0.43**	-0.21	0.15	-0.09	0.19	**0.57**	-0.14	1.00					
Cd	-0.27	0.24	0.27	-0.11	-0.08	-0.13	-0.15	-0.13	0.34	-0.15	-0.11	0.15	-0.05	1.00				
Zr	**-0.67**	**0.81**	0.23	-0.08	**-0.56**	**-0.66**	**-0.62**	**-0.55**	0.04	**-0.45**	-0.30	**0.62**	-0.39	**0.51**	1.00			
Ba	**0.50**	**-0.69**	0.27	0.15	**0.49**	0.37	**0.41**	0.02	-0.18	0.28	0.08	**-0.53**	**0.43**	-0.06	-0.51	1.00		
Sr	**0.49**	**-0.74**	0.00	**0.52**	0.19	0.72	0.22	**0.59**	0.03	**0.44**	**0.61**	**-0.62**	**0.76**	-0.20	**-0.74**	**0.48**	1.00	
LOI	**-0.74**	**0.43**	0.16	-0.04	-0.37	-0.04	**-0.49**	0.12	0.16	**-0.52**	0.39	**0.45**	-0.07	-0.01	0.29	**-0.50**	-0.19	1.00

Note: Table value of r = 0.40*(p=0.05), 0.52**(p=0.01) two tailed, degree of freedom n-2=22

4.7. Harker Diagrams

Harker variation diagrams were used to examine the relationships among major-element oxides and to assess systematic changes in soil geochemistry associated with weathering and pedogenesis. The Harker diagrams showed relative enrichment of Al and Fe during pedogenesis, consistent with the preferential retention and accumulation of less mobile elements during progressive weathering (Schaetzl and Anderson 2015). In contrast, the alkali and alkaline-earth elements, particularly Na, K, Ca and Mg (Σbases), are generally more mobile and may be progressively depleted through the weathering of primary minerals such as feldspars. The regression analyses further demonstrate several significant relationships among the major oxides (Fig. 3).

The relationship between Al_2O_3 and SiO_2 is negative and highly significant ($p < 0.001$), indicating a progressive decrease in SiO_2 with increasing Al_2O_3. The relationship can be expressed as Al_2O_3 (%) = 52.92 − 0.66 SiO_2 (%), with $R^2 = 0.62$, $F(1,22) = 35.74$, $p < 0.001$ and 95% CI [42.48, 63.36]. Thus, SiO_2 accounts for approximately 62% of the observed variation in Al_2O_3, suggesting a strong inverse association between silica and alumina in the studied soils.

The relationship between Fe_2O_3 and SiO_2 is moderately negative and statistically significant, described by Fe_2O_3 (%) = 23.6 − 0.30 SiO_2 (%) ($R^2 = 0.29$, $F(1,22) = 8.85$, $p = 0.007$). This relationship indicates that Fe_2O_3 tends to increase as SiO_2 decreases, consistent with the relative enrichment of Fe under conditions of progressive weathering and the concomitant loss of more mobile silica-bearing components.

A positive relationship was observed between Fe_2O_3 and TiO_2, expressed as Fe_2O_3 (%) = 5.9 + 3.1 TiO_2 (%); however, the relationship was not statistically significant ($R^2 = 0.091$, $F(1,22) = 2.19$, $p = 0.153$). The low coefficient of determination indicates that TiO_2 explains only a small proportion of the variability in Fe_2O_3, and therefore no strong linear association between these two oxides can be established for the studied soils.

The relationship between Al_2O_3 and K_2O is negative and statistically significant at the 5% level, represented by Al_2O_3 (%) = 29.3 − 7.0 K_2O (%) ($R^2 = 0.18$, $F(1,22) = 4.79$, $p = 0.040$; $N = 24$). The inverse relationship suggests that increasing Al_2O_3 is associated with decreasing

K_2O, which may reflect the weathering of K-bearing primary minerals and the relative accumulation of Al-bearing secondary phases during pedogenesis.

Similarly, TiO_2 shows a weak but statistically significant negative relationship with Σbases, expressed as TiO_2 (%) = 1.6 − 0.10 Σbases (%) (R^2 = 0.18, F(1,22) = 4.70, p = 0.041). This relationship indicates that TiO_2 tends to increase as the concentration of exchangeable or total base-forming elements decreases. Although statistically significant, the relatively low R^2 indicates that Σbases explains only about 18% of the variability in TiO_2; therefore, this relationship should be interpreted as an association rather than evidence of a direct causal relationship.

Overall, the Harker relationships demonstrate systematic geochemical variation among SiO_2, Al_2O_3, Fe_2O_3, TiO_2, K_2O and Σbases. The significant inverse relationships involving SiO_2 and the base-forming elements, together with the relative enrichment of Al and Fe, indicate the influence of mineral weathering, element mobility and secondary mineral formation on the geochemical evolution of the studied soils.

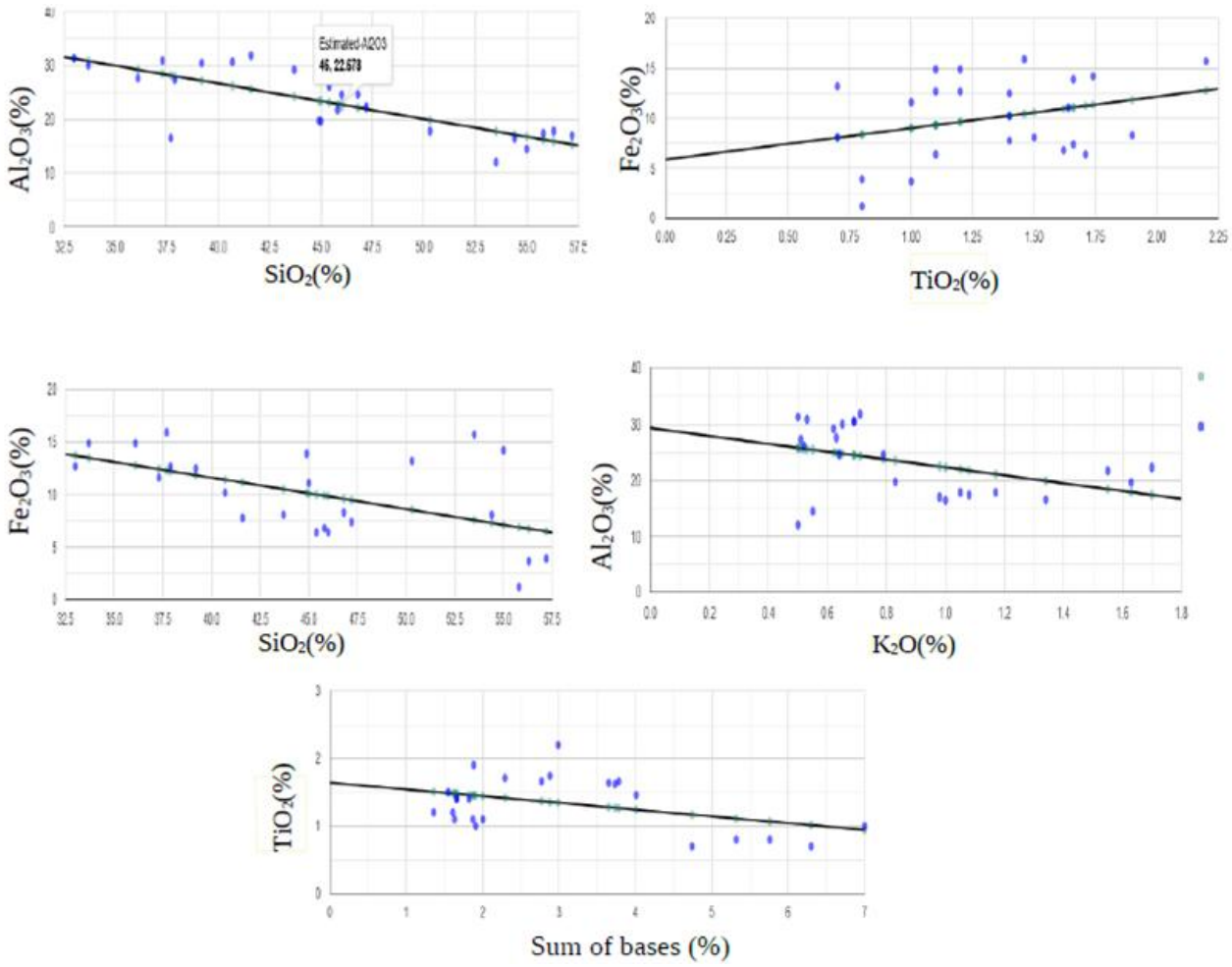


Fig.3. Elemental plots based on geochemistry: (A) Al_2O_3 vs. SiO_2 [wt %]; (B).Fe_2O_3 vs TiO_2 [wt %] (C) SiO_2 vs Fe_2O_3 [wt %]; (D) Al_2O_3 vs K_2O [wt %] and TiO_2 vs Σbases

4.8. Weathering Indices

Sixteen chemical weathering indices were used to assess the degree and intensity of weathering in the five lateritic soil profiles of Kerala (Table 12). These indices provide an integrated indication of the relative mobilization and retention of major elements during pedogenesis. In general, a progressive decrease in the ratios of relatively mobile elements, such as SiO_2, CaO, MgO and Na_2O, to relatively immobile elements, including Al_2O_3, Fe_2O_3 and TiO_2, reflects increasing leaching and chemical weathering intensity (Souri et al., 2006). The results indicate substantial weathering and differential element mobility among the studied profiles.

In the Kanjirapalli series (P4), the molar Si/Al ratio (Ruxton, 1968) is <2 in the kandic horizons, indicating advanced desilication and relative enrichment of Al. Such low Si/Al values are consistent with the dominance of highly weathered clay minerals, particularly

kaolinite, and possibly Al-rich secondary phases. In contrast, Si/Al ratios >3 in P1, P2 and P3 indicate relatively greater silica retention and suggest the persistence of quartz and other Si-bearing primary minerals, including muscovite. The values between 2 and 3 observed in P5 indicate an intermediate degree of weathering.

The SiO_2/R_2O_3 ratio (Gidigasu, 1976) further supports the differentiation of the studied soils according to their degree of weathering. Values ranging from 1.33 to 2.0 in the kandic horizons of P4 and P5 fall within the range generally associated with lateritic soils (Raychaudhuri, 1980), whereas values >2 in the other profiles indicate relatively lower degrees of desilication and are characteristic of non-lateritic tropical soils. Thus, the combined Si/Al and SiO_2/R_2O_3 ratios indicate that P4 and P5 have undergone stronger desilication and chemical weathering than P1–P3.

The occurrence of rubification and argilluviation/argillation in the subsurface horizons of the studied profiles revealed additional evidence of prolonged pedogenic alteration and intensive weathering. Under strongly weathered conditions, poorly crystalline Fe phases such as ferrihydrite may form through precipitation from supersaturated soil solutions (Chadwick et al., 2003). These processes contribute to the development of low SiO_2/R_2O_3 ratios and low base status in highly weathered profiles.

The weathering intensity was further supported by base saturation, with highly weathered soils generally characterized by low base saturation due to prolonged leaching of Ca, Mg, K and Na. Following the classification of Kalpage (1974) and Ranger (2002), soils with base saturation <35% represent strongly leached conditions. Collectively, the weathering indices, major-element relationships, low silica-to-sesquioxide ratios and low base saturation indicate that the studied Kerala lateritic soils have experienced prolonged chemical weathering, intense desilication and substantial depletion of mobile bases, with P4 and P5 showing comparatively stronger weathering characteristics.

The weighted mean Vogt residual index ranges from 1.61 in P1 to 1.30 in P3, indicating only moderate variation among the profiles, with additional changes occurring with depth. In most kandic horizons, the index remains below 1.4, except in P1, suggesting a relatively advanced degree of weathering. The observed values are broadly comparable with those reported for humid tropical soils of Cameroon (Che et al., 2012). The chemical index of alteration (CIA), chemical index of weathering (CIW) and plagioclase index of alteration (PIA) exceed 90 in

P4 and P5, indicating intense alteration of primary silicate minerals and pronounced removal of mobile base cations. These values are consistent with those reported for highly weathered lateritic profiles of Kerala (Sajinkumar et al., 2011).

The Parker index (WPI) also shows a marked decrease with increasing weathering intensity. Values <15 in P4 and P5 indicate substantially greater chemical weathering than in P1 and P2, where values exceed 40. Similar decreases in the Parker index with increasing weathering intensity and depth have been reported for strongly weathered soils (Eswaran and Raghu Mohan, 1973). The very high CIA values (>90) in P4 and P5, together with the strongly acidic reaction of these soils (pH <4.5), indicate extensive leaching of Ca, Na and K. Such depletion of base-forming elements promotes the relative accumulation of Al- and Fe-bearing phases during prolonged pedogenesis. The comparatively greater retention of K relative to Na may be associated with the slower release of K from K-bearing minerals and its partial fixation within clay minerals, whereas Na is generally more readily leached under humid conditions (Yang et al., 2004; Reeder et al., 2006).

The base/Al and base/R_2O_3 molar ratios provide further evidence of intense desilication and base depletion. In most profiles, the base/Al ratio and base/R_2O_3 ratio remain below 0.50 throughout the soil depth, although their depth distributions are somewhat irregular. P3 is an exception, with base/Al and base/R_2O_3 ratios reaching >0.65 and approximately 0.51, respectively, indicating comparatively greater retention of base cations. The low ratios in the other profiles reflect extensive depletion of Ca, Mg, Na and K relative to the relatively immobile Al and Fe components during prolonged weathering.

The molar Al/Ti ratio does not exhibit a consistent relationship with depth, with weighted mean values of 31.50 and 27.83 for P4 and P5, respectively. Nevertheless, an increasing depth trend is evident in P1, P4 and P5, with values ranging from a minimum of 9.69 in the Ap horizon of P1 to a maximum of 34.74 in the Bt5 horizon of P5. This increase may reflect progressive enrichment or preferential retention of Al relative to Ti in the more strongly weathered subsurface horizons. However, because both elements can be influenced by parent material and mineralogical composition, the Al/Ti ratio should be interpreted together with the other weathering indices rather than as an independent measure of weathering intensity.

The WPI, Parker index (PI), Si/Al ratio, Vogt residual index (Wp) and modified weathering–product index (MWPI) showed decreasing depth trends in the more strongly weathered

profiles. The declining values showed progressive depletion of silica and mobile elements and increasing relative enrichment of less mobile components with advancing weathering, consistent with observations reported by Jayawardena and Izawa (1994b) and Gupta and Seshagiri-Rao (2001). The particularly pronounced decrease in these indices within the Bt horizons of the highly weathered granite-to-granite-saprolite profiles is consistent with field observations showing a distinct transition between weathered bedrock and underlying saprolite.

Overall, the combined evidence from the CIA, CIW, PIA, Parker index, Vogt residual index, base/Al and base/R_2O_3 ratios, Si/Al ratio and related weathering indices indicates pronounced chemical weathering, extensive leaching of mobile bases and silica, and relative enrichment of Al- and Fe-bearing components in the more strongly weathered profiles, particularly P4 and P5. The consistency among the independent indices and the observed field characteristics strengthens the interpretation of advanced weathering and lateritic pedogenesis in these Kerala soil profiles.

4.9. Pedogenic Characteristics and Thresholds of Ferruginous Soils

The principal pedogenic characteristics considered for identifying threshold conditions in the ferruginous soils of the study area were (i) the total Al/total Fe ratio, (ii) soil pH, (iii) base saturation, and (iv) chemical weathering indices, including CIA, CIW, PIA and the Vogt Residual (VR) index. The total Al/Fe ratio generally exceeds unity in several genetic horizons and is associated with pronounced depletion of exchangeable bases, particularly in the argillic B horizons where base saturation commonly falls below 20%. The depletion of base cations reflects prolonged leaching under acidic conditions and their replacement on the exchange complex by acidic cations, particularly H^+ and Al^{3+} and hydroxy-Al species.

The soils varied from very strongly acidic (pH <4.0) to strongly acidic (pH 4.0–5.0) and moderately acidic conditions (pH <5.5). Increasing acidity was accompanied by greater exchangeable acidity and a predominance of monomeric inorganic Al. In several horizons, exchangeable acidity constitutes more than 60% of the effective CEC, indicating a high degree of Al saturation (Thomas and Hargrove, 1984; Bhaskar et al., 2009). Within this relatively narrow pH range, the soil exchange complex shifts towards increasing dominance by Al, hydroxy-Al species and H^+, representing an important pedogenic threshold in strongly weathered tropical soils (Sparks, 1995).

It is important to distinguish between the degree of cumulative weathering and the current rate of weathering. Although the high CIA, CIW and PIA values indicate a strongly weathered state, present-day weathering rates may be comparatively slow because prolonged weathering has already depleted much of the readily weatherable primary mineral fraction (Stewart et al., 2001). Therefore, the high weathering-index values primarily represent the integrated effect of long-term pedogenesis rather than necessarily indicating rapid contemporary mineral weathering.

The topsoil characteristics of several profiles are also noteworthy. The surface horizons contain incompletely mineralized organic matter, presumably favoured by intensive rubber cultivation and regular incorporation of leaf litter, and generally have organic carbon contents >0.6%, dark brown to blackish-brown colours in the 5YR hue range, base saturation <10% and pH <5.0. These characteristics are consistent with the concept of modic surface horizons described in the FAO classification framework (FAO, 1998). The occurrence of modic topsoils in ferruginous soils of the Shillong Plateau has also been reported, with Bhaskar et al. (2009) suggesting their potential recognition at the subgroup level in Sombrihumults.

The identification of argillic horizons in these highly weathered soils can, however, be complicated by the difficulty of recognizing diagnostic clay skins. This limitation has been highlighted in reviews of the red and ferruginous soils of India, including the Kerala and northern Indian regions (Pal et al., 2014). The weak or poorly expressed clay skins in some profiles may consequently result in the placement of certain soils within Dystrudepts rather than more strongly developed Ultisol-related taxa, despite evidence of advanced weathering.

The total Al/Fe ratio varies considerably among the studied profiles, ranging from 10.97 in P1 to 0.94 in P2, with values commonly falling between 2 and 3 in several genetic horizons. The variation reflects differences in the relative accumulation and redistribution of Al and Fe during pedogenesis. However, the Al/Fe ratio should be interpreted together with redox morphology, drainage status, Fe mineralogy and other weathering indicators because the ratio alone does not provide unequivocal evidence of anaerobiosis or Fe reduction. Where associated with prolonged saturation and other redox features, a decline in Fe relative to Al may indicate enhanced Fe mobilization under reducing conditions (Thompson et al., 2006).

The high CIA and CIW values further indicate extensive alteration of primary silicate minerals and substantial depletion of mobile base-forming elements. In combination with the

stable geomorphic setting and the strongly weathered mineralogical characteristics, these indices support an interpretation of predominantly autochthonous soil development on a relatively stable terrain within the southern monsoonal zone (SMZ) of Kerala. The particularly high PIA values in P4 and P5 indicate extensive alteration of plagioclase feldspars, accompanied by depletion of primary plagioclase and relative enrichment of secondary Al-bearing clay minerals. These observations are consistent with the progressive transformation of primary silicate minerals into secondary aluminous phases during prolonged chemical weathering (Ray et al., 2008).

Overall, the combination of very low base saturation, strongly acidic pH, high Al saturation, elevated CIA/CIW/PIA values, variable Al/Fe ratios and the development of argillic and kandic horizons provides evidence for advanced pedogenesis and intense chemical weathering in the studied ferruginous soils. The observed thresholds represent the cumulative effects of prolonged leaching, desilication, base depletion, secondary clay formation and relative enrichment of Al and Fe under humid tropical conditions.

4.10. Weathering Ratios and Weathering Indices

According to Chittleborough (1991), the weighted mean weathering ratio (WR) is <2 in all profiles except P3, which records a markedly higher weighted mean of 9.04. In general, WR shows a decreasing trend with depth, indicating progressive alteration and redistribution of weathering products within the soil profile. In P5, the ratio remains consistently low, with values <1.15 throughout the profile, suggesting a highly weathered condition with strong depletion of mobile constituents relative to the less mobile components. The significance of this ratio lies in its sensitivity to the relative behaviour and redistribution of Al during weathering, which complements indices based primarily on the mobility of alkali and alkaline-earth elements (Price and Velbel, 2003).

The WR1 and WR2 indices, derived from the Chemical Index of Alteration (CIA) concept of Nesbitt and Young (1982), distinguish clear differences in the degree of weathering among the profiles. Based on the weighted mean CIA values, P3 (65.84%) is classified as slightly weathered, P1 (82.59%) and P2 (80.64%) as highly weathered, and P4 (92.84%) and P5 (92.68%) as extremely weathered. The very high CIA values in P4 and P5 indicate extensive alteration of primary silicate minerals and pronounced depletion of mobile base cations. The

contrasting value in P3 suggests substantially lower overall weathering intensity relative to the other profiles.

The Harnois Chemical Index of Weathering (CIW; Harnois, 1988), which excludes K_2O and therefore reduces the influence of K-bearing minerals such as K-feldspar (Fedo et al., 1995), exhibits depth patterns broadly comparable to those of CIA. The index varied from 64.75 in the AB horizon of P3 to 97.19 in the Bt5 horizon of P5, indicating a progression from comparatively weak to extremely intense chemical weathering. The similar depth behaviour of CIA and CIW across profiles developed from different parent materials suggests that prolonged pedogenesis and leaching have exerted a strong influence on the major-element composition of these soils.

The K-free Weathering Indices WI-1 and WI-2 of Darmody et al. show comparatively irregular depth distributions. Their weighted mean values range from 6.83 to 24.06 for WI-1 and from 1.61 to 4.37 for WI-2, with the reported extremes occurring among P4 and P3. These indices provide additional evidence for progressive redistribution of major elements during pedogenesis. The relative enrichment of Al and Fe is consistent with the preferential retention of these comparatively less mobile elements, whereas Ca and other mobile constituents are progressively depleted through the weathering of primary minerals, particularly plagioclase feldspars. Such geochemical behaviour is characteristic of progressive chemical weathering and has also been reported for soils of Karamaidan, Central Asia (Aquino et al., 2024).

The coefficient of variation (CV) further highlights differences in the stability of the weathering indices within the profiles. Following the variability classes proposed by Harka (2021), VR and CIA show low variability (CV <20%), indicating relatively consistent behaviour with depth. The Richie Index (RI) shows moderate variability, whereas WR, Parker Index, WI-1, WI-2, mSi/mAl and $mSiO_2/mR_2O_3$ exhibit high variability. The remaining indices show very high variability (Fig. 4), reflecting stronger vertical differentiation in elemental mobility and redistribution. Such variability may result from differences in parent material, mineralogical composition, drainage conditions, intensity of leaching and the degree of pedogenic development among the profiles.

Overall, the weathering indices consistently demonstrate a gradient of chemical weathering from P3 through P1/P2 to the highly weathered P4 and P5 profiles. The agreement among

CIA, CIW, WR, WI-1, WI-2 and the silica-to-aluminium and silica-to-sesquioxide ratios provides complementary evidence for progressive desilication, depletion of mobile bases and relative enrichment of Al- and Fe-bearing phases during prolonged tropical weathering.

Table 12. Weathering indices of lateritic soils of Kerala

Horizon	mSi/mAl	mSi/mR2O3 (RPI)	VR	CIA%	WIP RI*100(Rieche index)	WIP *100(ParkerIndex)	WR(Chittleborough)	WI-1 (Darmody)	WI-2 (Darmody)	mFe/mAl	B/mAl	B/R2O3	Harnois	mSI/mTI	PIA	mAl/mTI
P1-Madgaon series																
Ap	7.57	3.66	2.07	75.38	24.36	19.57	1.75	7.19	3.72	9.05	0.47	0.23	80.03	73.19	78.71	9.67
BW1	6.44	3.62	1.78	79.27	25.29	19.28	2.08	8.4	3.68	10.3	0.37	0.21	83.94	76.42	82.94	11.87
Bt1	3.87	2.48	1.56	83.34	30.1	21.18	1.8	7.06	2.53	8.59	0.25	0.16	89.13	73.2	88.31	18.92
Bt2	3.17	2.53	1.26	88.56	30.28	15.94	1.52	12.68	2.58	19.1	0.2	0.16	92.5	71.23	92.15	22.45
w̄	**4.94**	**2.99**	**1.61**	**82.59**	**27.93**	**18.75**	**1.78**	**9.22**	**3.05**	**12.45**	**0.30**	**0.18**	**87.31**	**73.41**	**86.51**	**16.64**
P2-Darbandora,,Goa, Very fine, Kaolinitic, family of Typic Kanhaplustalfs (Archean schists and ferruginous quartzite)																
A	3.88	2.24	1.73	75.94	28	30.56	2.97	5.47	2.31	6.3	0.49	0.29	85.72	72.95	83.67	18.81
A2	3.59	2.77	1.3	81.7	27.57	32.81	2.21	12.27	2.8	17.9	0.34	0.26	91.59	72.75	90.44	20.31
Bt1	3.9	2.65	1.47	80.05	28.23	33.41	2.02	8.4	2.68	10.78	0.36	0.26	91.3	73.34	89.88	18.82
Bt2	3.59	2.75	1.31	81.83	28.58	34.2	2.08	11.82	2.78	16.95	0.44	0.34	92.51	72.81	91.39	20.7
w̄	**3.73**	**2.67**	**1.40**	**80.64**	**28.28**	**33.42**	**2.15**	**10.08**	**2.70**	**13.89**	**0.40**	**0.30**	**91.35**	**73.01**	**90.04**	**19.81**
P3-Kinalur series, Kozhikode, Kerala: Fine loamy, isohyperthermic family of Kaolinitic, Kanhaplic Haplustults (Granite Gneiss)																
Ap1	5.44	4.94	1.11	68.15	18.82	39.77	7.69	54.59	5.09	123.6	0.61	0.56	73.94	80.48	71.52	14.79
Ap2	5.63	4.11	1.37	62.67	22.03	44.59	10.87	15.86	4.28	17.86	0.77	0.56	67.44	81.16	64.75	14.41
Bt1	5.37	4.46	1.2	63.71	21.03	52.7	8.53	27.05	4.59	40.44	0.7	0.59	69.06	79.49	66.24	14.81
Bt2	5.71	4.73	1.21	65.77	20.12	44.82	8.5	28.37	4.86	38.99	0.53	0.44	70.73	80.95	68.34	14.17
Bt3	4.8	3.15	1.52	71.98	26.6	37.28	7.76	9.37	3.22	10.13	0.57	0.38	78.12	79.45	76.08	16.57
w̄	**5.44**	**4.24**	**1.30**	**65.84**	**21.85**	**43.98**	**9.04**	**24.06**	**4.37**	**37.87**	**0.65**	**0.51**	**71.10**	**80.48**	**68.61**	**14.84**
P4-Kanjirapally series, Kottayam, Kerala: Loamy skeletal, Kaolinitic, family of Ustic Kandihumults (Charnokite)																
Ap	2.95	2.44	1.21	90.82	30.98	12.77	2.17	14.28	2.45	18.86	0.15	0.13	93.97	78.81	93.75	24.32
Bt1	2.36	1.75	1.35	92.98	36.11	11.49	1.68	6.85	1.77	7.93	0.12	0.09	96.07	67.76	95.94	28.76
Bt2	2.05	1.6	1.28	93.23	38.82	12.49	2.31	7.4	1.62	8.55	0.13	0.1	96.07	65.38	95.95	31.92
Bt3	2.22	1.6	1.4	91.65	37.78	13.67	1.83	5.71	1.62	6.44	0.13	0.09	95.35	66.61	95.14	30.01
Bt4	1.91	1.4	1.38	92.7	40.26	12.81	1.27	5.27	1.42	6.01	0.11	0.08	96.28	63.47	96.12	33.29
Bt5	1.79	1.37	1.31	94.18	40.15	10.51	1.14	5.89	1.39	6.91	0.09	0.07	96.87	62.19	96.78	34.76
w̄	**2.10**	**1.59**	**1.33**	**92.84**	**38.23**	**12.16**	**1.64**	**6.83**	**1.61**	**8.08**	**0.12**	**0.09**	**96.00**	**65.89**	**95.86**	**31.50**
P5.Athirampuza series, Ernakulam, Kerala:clayey skeletal, Kaolinitic, family of Ustic Kandihumults (Laterite)																
Ap	3.23	2.46	1.31	90.36	31.7	15.81	0.93	10.39	2.48	14.99	0.15	0.11	95.49	71.01	95.21	21.99
Bt1	2.54	2.04	1.24	93.51	35.59	12.6	1.03	10.55	2.06	14.34	0.11	0.09	97.08	68.53	96.95	26.98
Bt2	2.19	1.66	1.32	92.24	39.4	14.12	1.3	6.91	1.68	8.34	0.12	0.09	95.96	65.97	95.79	30.15
Bt3	2.26	1.78	1.27	93.12	38.15	13.91	1.13	8.4	1.79	10.61	0.11	0.08	96.88	66.6	96.75	29.51
BC	2.23	1.83	1.21	93.55	37.83	13.96	1.13	10.52	1.85	14.18	0.1	0.08	97.31	66.37	97.19	29.89
w̄	**2.47**	**1.94**	**1.27**	**92.68**	**36.64**	**13.92**	**1.10**	**9.33**	**1.96**	**12.42**	**0.12**	**0.09**	**96.60**	**67.65**	**96.44**	**27.83**
Mean	**3.70±**	**2.67±**	**1.38±**	**83.20±**	**30.74±**	**23.76±**	**3.15±**	**12.53±**	**2.72±**	**18.63±**	**0.31±**	**0.23±**	**88.47±**	**72.09±**	**87.50±**	**22.41±**
±SD	**1.61**	**1.07**	**0.22**	**10.65**	**6.82**	**12.95**	**2.98**	**10.76**	**1.11**	**24.09**	**0.22**	**0.17**	**9.90**	**5.86**	**10.80**	**7.38**
CV%	**43.67**	**40.24**	**15.27**	**12.81**	**22.18**	**54.52**	**94.43**	**85.83**	**41.00**	**129.28**	**69.70**	**74.27**	**11.19**	**8.13**	**12.33**	**32.91**

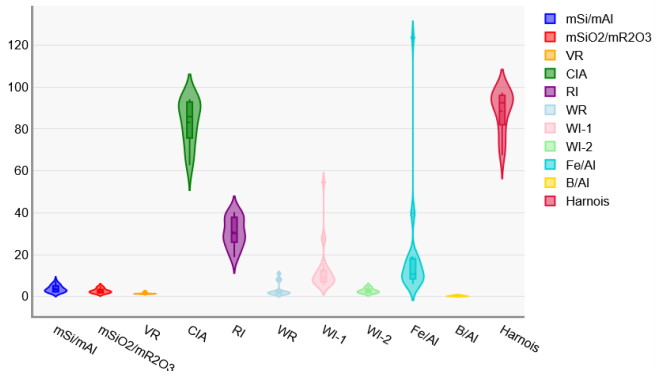


Fig. 4. Violin plot for weathering indices under study

Table 13.Correlation matrix of weathering indexes

Correlations	mSi/mAl	mSi/mR2O3 (RPI)	VR	CIA	RI*100 (Rieche index)	WIP *100(Parker Index)	WR (Chittleborough)	WI-1 (Darmoody)	WI-2 (Darmoody)	Fe/Al	B/Al	B/R2O3	Harnois	SI/TI	PIA	Al/TI
mSi/mAl	1.00															
mSi/mR2O3	0.88	1.00														
VR	0.51	0.05	1.00													
CIA	-0.85	-0.92	-0.18	1.00												
Riechie index	-0.89	-0.96	-0.17	0.93	1.00											
Parker index	0.65	0.82	-0.07	-0.93	-0.85	1.00										
Chittleborough	0.59	0.79	-0.16	-0.88	-0.73	0.85	1.00									
Darmoody-1	0.42	0.75	-0.44	-0.59	-0.65	0.60	0.64	1.00								
Darmoody-2	0.88	1.00	0.05	-0.92	-0.96	0.83	0.80	0.76	1.00							
Fe/Al	0.36	0.66	-0.40	-0.49	-0.56	0.49	0.52	0.98	0.66	1.00						
B/Al	0.82	0.87	0.19	-0.98	-0.90	0.93	0.86	0.54	0.88	0.46	1.00					
B/R2O3	0.72	0.89	-0.06	-0.96	-0.89	0.96	0.91	0.71	0.90	0.62	0.96	1.00				
Harnois	-0.84	-0.92	-0.14	0.97	0.89	-0.86	-0.92	-0.61	-0.93	-0.51	-0.94	-0.93	1.00			
Si/Ti	0.79	0.90	0.06	-0.87	-0.93	0.79	0.78	0.61	0.89	0.50	0.84	0.84	-0.85	1.00		
PIA	-0.84	-0.92	-0.14	0.98	0.89	-0.87	-0.92	-0.62	-0.93	-0.51	-0.95	-0.93	1.00	-0.85	1.00	
Al/Ti	-0.96	-0.88	-0.44	0.86	0.95	-0.72	-0.58	-0.43	-0.88	-0.36	-0.84	-0.75	0.81	-0.87	0.82	1.00

4.11. Correlation among Weathering Indices

Correlation analysis revealed strong and significant associations among most of the sixteen weathering indices used in the study (Table 13), indicating that many of these indices respond similarly to the progressive alteration and redistribution of major elements during pedogenesis. Most weathering indices showed close interrelationships and can therefore provide broadly comparable estimates of relative weathering intensity. The Vogt Residual (VR) index was an exception, showing only moderate positive correlations with mSi/mAl ($r = 0.51$), WI-1 ($r = 0.44$) and WI-2 ($r = 0.40$). This relatively weaker association suggests that VR may capture somewhat different aspects of elemental redistribution compared with indices primarily based on the depletion of mobile elements.

The strong intercorrelations among the weathering indices are consistent with previous studies showing that several commonly used indices can be used as alternative or complementary proxies for assessing the degree of chemical weathering (Marković et al., 2008; Buggle et al., 2011; Terhorst et al., 2014; Schaetzl and Anderson 2015). In the present study, the Chemical Index of Alteration (CIA), Parker index (PI) and Chemical Index of Weathering (CIW/Harnois) exhibited very strong correlations with one another ($r > 0.90$), indicating that these indices provide highly consistent estimates of the weathering gradient in the studied Kerala soils. Following the interpretation of correlation strength suggested by Schober et al. (2018), these relationships represent very strong associations.

Considering both the strength of inter-index correlations and their geochemical basis, CIA, Parker index and CIW appear to be particularly useful complementary indicators for characterizing the weathering gradient of the studied Kerala soils. However, because these

indices are not completely independent, their use should be considered complementary rather than as separate, independent measures of weathering intensity. The remaining indices, particularly VR, WI-1 and WI-2, may provide additional information on specific aspects of elemental redistribution and should therefore be retained where a more comprehensive assessment of pedogenic weathering is required.

4.12. Depth Function of MIA(O), MIA-R and IOL in Soils of Kerala

The depth distribution of the Index of Lateritization (IOL) shows distinct vertical variations among the studied soil profiles (Fig. 5). In P1, IOL values increase from 19.52 in the Ap horizon to 27.27 in the Bt horizons, producing a pronounced subsurface bulge. In P2, the index decreases progressively with depth, from 29.41 to 25.23. P3 records a relatively low IOL value of 16.10 in the Ap horizon, followed by a slight increase to 18.94 in the Bt horizons and a subsequent decline to 15.60 in the underlying horizons. In the highly weathered profiles P4 and P5, IOL generally increases towards the subsurface, with values reaching approximately 40.86 in the Bt horizons of P4 and increasing from 27.35 in the Ap horizon of P5. Despite these profile-specific variations, IOL generally shows higher values in the genetic B horizons, particularly the argillic and kandic horizons, indicating greater chemical alteration in the subsurface horizons.

The observed IOL distribution is consistent with the progressive alteration associated with laterization, during which prolonged weathering promotes the dissolution and redistribution of silica-bearing minerals and the relative concentration of Fe and Al sesquioxides in the weathering residue. This process is reflected morphologically by the development of dominant red to reddish-brown subsurface horizons characteristic of the midland soils of Kerala (Widdowson and Gunnell, 1999). The IOL was developed as a complementary index to the SiO_2–Al_2O_3–Fe_2O_3 (SAF) diagram and provides an additional quantitative measure of the degree of lateritic alteration (Hill et al., 2000). In the present study, most IOL values are <40, indicating moderate silica loss relative to Al_2O_3 and Fe_2O_3 and a weathering regime broadly consistent with kaolinitization rather than extreme ferrallitization. The use of IOL therefore provides useful information on the progressive alteration of the parent material and development of lateritic soil characteristics (Schellmann, 2003; Widdowson, 2007).

The depth functions of MIA(O) and MIA-R show broadly comparable patterns across the profiles, although MIA(O) consistently records lower values than MIA-R (Fig. 5). Both

indices generally increase towards the subsurface horizons, particularly in the more strongly weathered profiles. In P4 and P5, MIA(O) values exceed 70–80% in several horizons, whereas most horizons of P1, P2 and P3 show values between 44 and 70%. The corresponding MIA-R values exceed 90% in P4 and P5, while values generally range from 66 to 89% in P1–P3. The higher values in P4 and P5 are consistent with more advanced alteration and greater depletion of labile elements relative to the relatively immobile components.

The difference between the two MIA formulations is important for interpreting the weathering pathway. MIA(O) treats total Fe, together with Al, as a relatively immobile component, whereas MIA-R incorporates Fe differently to account for situations in which Fe may behave as a mobile element during weathering of mafic minerals. Consequently, the two indices can provide complementary information on the contribution of Fe mobility to the overall weathering signal. Increasing MIA values indicate progressive depletion of labile elements, particularly Ca, Na, K and Mg, with Fe potentially contributing to the mobile fraction depending on mineralogical and redox conditions.

The progressive increase in MIA(O) from less weathered to more strongly weathered materials is also consistent with the influence of parent-rock composition, with MIA(O) generally increasing from mafic towards felsic compositions as weathering removes readily mobilized elements. However, its magnitude is also affected by the initial Fe and Mg contents of the parent material. The particularly high MIA-R values in P4 and P5 indicate extensive alteration of primary igneous silicates and substantial depletion of labile constituents. Values approaching 100% are consistent with advanced breakdown of primary silicate minerals and the development of secondary weathering products, particularly kaolinite and halloysite, although intermediate clay minerals such as vermiculite, illite and smectite may occur depending on parent-rock composition, drainage conditions and the stage of weathering (Fedo and Babechuk, 2023).

Overall, the depth functions of IOL, MIA(O) and MIA-R reveal a coherent pattern of progressive subsurface weathering. The generally higher values in argillic and kandic horizons, together with the associated depletion of labile base-forming elements, indicate that the B horizons represent zones of intensified chemical alteration and secondary mineral formation. The particularly high MIA(O) and MIA-R values in P4 and P5, coupled with their high CIA, CIW and PIA values, reinforce the interpretation that these profiles have

undergone substantially more advanced chemical weathering and lateritic transformation than P1–P3.

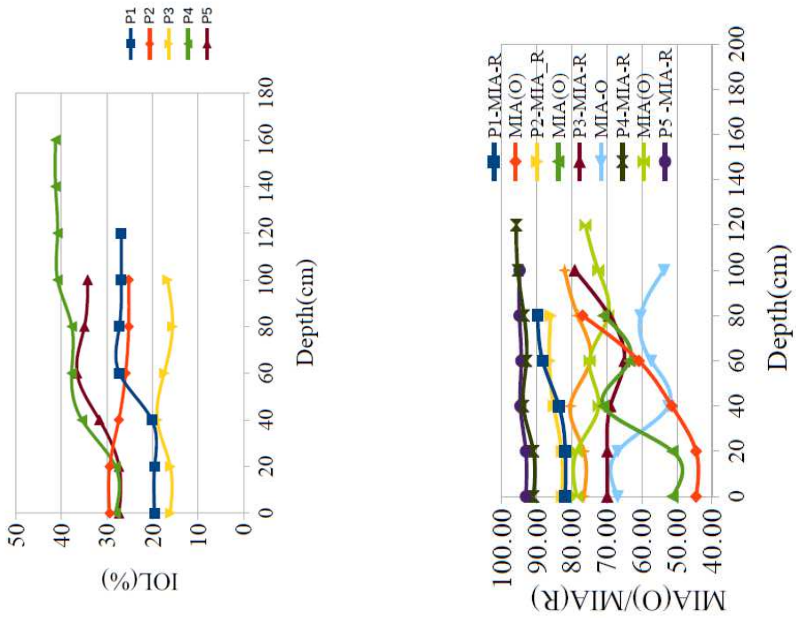


Fig. 5. Depth functions of IOL, MIA(O) and MIA-R in soils

4.13. Relationship of Weathering Indices with CIE L*a*b* Colour Parameters

Multiple regression analysis was performed to examine the relationship between the weathering indices and soil colour parameters expressed in the CIE L*a*b* system. The analysis revealed significant relationships between the weathering indices and selected colour attributes.

*1. IOL = 135.1 + 1.4 a + 233.4 a*1 - 1.6 rr - 692 a/a+b*

The model showed a strong and statistically significant overall relationship between IOL and the selected CIE L*a*b* colour parameters, with ($F(4,19)=8.19$), ($p<0.001$), ($R^2=0.63$), and adjusted ($R^2=0.56$). Thus, approximately 63% of the variation in IOL was explained collectively by the four colour variables included in the model. Examination of the individual regression coefficients showed that all four predictors made statistically significant contributions to the model: (a) ((t=3.911), (p<0.001)), (a_1^*) ((t=2.438), (p=0.025)), redness rating (RR) ((t=-2.323), (p=0.031)), and the (a/(a+b)) ratio ((t=-2.559), (p=0.019)). The significant association of IOL with these colour parameters indicates that variations in soil redness and related chromatic attributes are closely associated with the degree of lateritization.

2.MIA((O) = 68.7 - 0.6 L + 1.6 b - 2.6 rr

Multiple linear regression indicated a statistically significant collective relationship between MIA(O) and the three colour parameters (L), (b), and RR, with (F(3,20)=6.97), (p=0.002), (R^2=0.51), and adjusted (R^2=0.44). The model therefore explained approximately 51% of the observed variation in MIA(O), indicating a moderate-to-strong association between the alteration index and soil colour characteristics. The significant contribution of these colour parameters suggests that changes in soil lightness, yellowness, and redness are systematically related to variations in the degree of chemical alteration.

3.MIA((R) = 68.8 + 1.1 a

This regression model showed a statistically significant but moderate relationship between MIA(R) and the (a) colour parameter, with (F(1,22)=9.14), (p=0.006), (R^2=0.29), and adjusted (R^2=0.26). The model explained approximately 29% of the variation in MIA(R), indicating that the (a) value provides a significant, although comparatively limited, prediction of MIA(R). The positive regression coefficient suggests that increasing redness is associated with increasing MIA(R) values. The observed and predicted values for IOL, MIA(O), and MIA(R) are presented in Fig. 6.

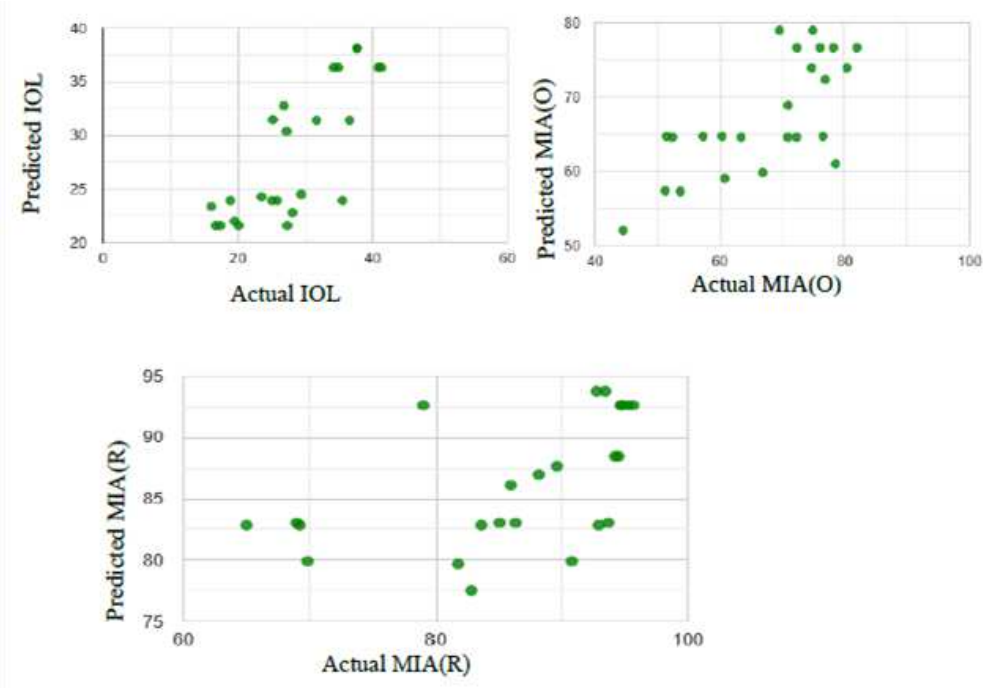


Fig. 6. Graph showing predicted vs actual IOL, MIA(O) and MIA®

4.14. Ternary Plots

a) S–A–F Diagram

The S–A–F ternary diagram proposed by Schellmann (1986b) was used for the chemical classification of the lateritic soils based on the relative proportions of SiO_2, Al_2O_3, and Fe_2O_3 (Fig. 7). The studied soils occur on relatively stable terrain in the midland region of Kerala and considered predominantly *in situ* soils. The distribution of the samples within the S–A–F diagram indicates progressive depletion of SiO_2 relative to Al_2O_3 and Fe_2O_3 with increasing intensity of chemical weathering, consistent with the general weathering trend reported by Hill et al. (2000) and Babechuk et al. (2014). The observed compositional trend suggests that weathering has resulted in substantial silica loss while Al-bearing phases remain relatively enriched, indicating the development of strongly weathered, Al-dominated soil materials. In contrast, the relatively limited displacement toward the Fe_2O_3 apex suggests that pronounced ferruginization or Fe accumulation is less developed than the Al-dominated weathering pathway. Thus, the S–A–F distribution indicates predominantly in-situ chemical weathering with progressive desilication and relative Al enrichment, accompanied by comparatively weak Fe accumulation during the earlier stages of lateritization.

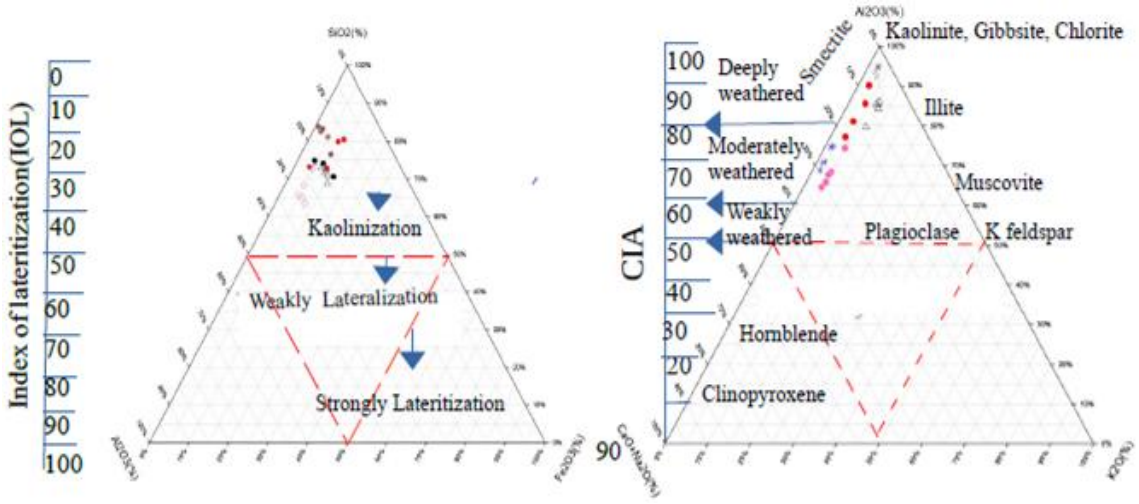


Fig.7 .S-A-F and A-CN-K diagram for soils of Kerala

b) A–CN–K Diagram

The A–CN–K ternary diagram (Fig. 7), based on the relative proportions of Al_2O_3, $CaO+Na_2O$, and K_2O, indicates that the studied soils have undergone moderate to intense

chemical weathering, accompanied by substantial depletion of the more mobile base-forming elements. The distribution of the samples toward the Al_2O_3 apex reflects progressive removal of Ca, Na, and K from primary minerals, particularly plagioclase and K-feldspar, relative to the parent material (Nesbitt and Young, 1982; Nesbitt and Wilson, 1992). The observed weathering trend broadly follows the A–CN direction, indicating progressive desilication and depletion of Ca and Na, followed by further loss of K with increasing weathering intensity. Samples approaching the Al_2O_3 apex therefore represent highly weathered materials in which Al-bearing secondary phases have become relatively enriched. This pattern is consistent with advanced alteration and kaolinization, although the A–CN–K diagram alone cannot distinguish individual secondary clay minerals such as kaolinite, illite, chlorite, or smectite. The greater degree of weathering observed in subsurface horizons, particularly those associated with kandic properties, compared with some surface horizons suggests progressive pedogenic alteration with depth. The variation in sample positions within the diagram may further reflect differences in parent material, topographic position, drainage, and climatic conditions, which collectively influence the intensity and pathway of soil weathering.

c) A–CNKM–F Diagram

The A–CNKM–F ternary diagram proposed by Nesbitt and Wilson (1992) was used to evaluate the development and relative enrichment of Al_2O_3 and Fe_2O_3 during weathering and to examine the relationship between the parent material and the studied soil horizons. In this diagram, the magnitude of elemental depletion during weathering can be inferred from the length of the vector extending from the CNKM–A line toward the A–F line (Babechuk et al., 2014). The distribution of the soil samples indicates progressive depletion of the more mobile elements (Ca, Na, K and Mg) relative to the comparatively immobile Al and Fe, resulting in their relative enrichment in the weathered soil material. The mobile elements are not completely removed, as indicated by the position of several samples toward the central portion of the diagram, suggesting varying degrees of elemental loss during pedogenesis. The overall sample distribution indicates a progressive weathering trend toward both the A and F apices, representing contrasting tendencies of Al enrichment (kaolinization) and Fe enrichment (ferruginization/lateritization), respectively. The relative position of individual horizons along these trends suggests that the studied soils have experienced variable degrees of chemical weathering, with Al-dominated alteration generally more prominent than pronounced Fe accumulation.

d) AF–CNK–M Diagram

The AF–CNK–M diagram (Fig. 8), following Babechuk et al. (2014), was used to evaluate the relative mobility of major elements during weathering, with the relatively immobile elements Al and Fe represented by the AF apex, Mg (representing mafic components) by the M apex, and Ca–Na–K (CNK), largely associated with feldspar minerals, by the CNK apex. Weathering involving preferential dissolution and removal of Ca, Na, and K from feldspar relative to Mg results in a shift of soil compositions away from the CNK and M apices and toward the AF field. The distribution of the studied soils indicates substantial depletion of the major base cations and progressive relative enrichment of Al and Fe, reflecting advanced chemical weathering.

The AF–CNK–M distribution, together with the MIA(O) values, provides evidence of progressive alteration and loss of mobile elements, particularly Mg, toward the AF field. The studied soil horizons exhibit MIA(O) values >80%, compared with values <65% in the parent material, indicating a marked increase in the degree of chemical alteration during pedogenesis. The relative enrichment of Fe_2O_3 in the highly weathered horizons further suggests retention and concentration of Fe during intense weathering. Under well-drained and oxidizing conditions, Fe is commonly retained as relatively insoluble Fe(III)-bearing oxides and oxyhydroxides, whereas under reducing conditions Fe(II) becomes more soluble and may be mobilized along with other mobile elements (Babechuk et al., 2014). However, the AF–CNK–M diagram and total Fe_2O_3 concentration alone cannot establish Fe valence or redox conditions; such interpretations require supporting mineralogical, morphological, or geochemical evidence. Overall, the AF–CNK–M diagram and elevated MIA(O) values indicate progressive depletion of mobile bases and Mg, accompanied by relative enrichment of Al and Fe, consistent with advanced chemical weathering of the studied soils.

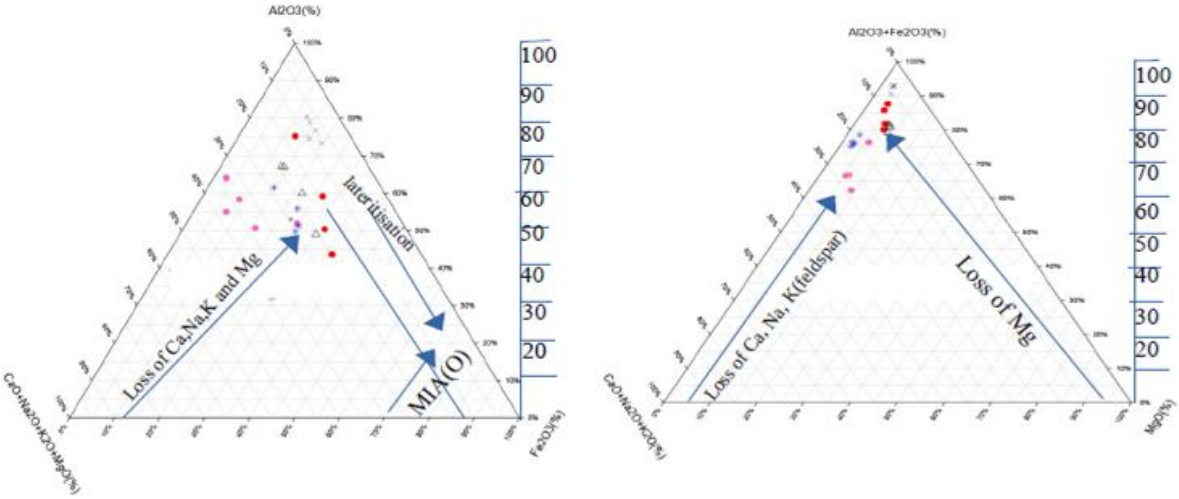


Fig.8. A-L-F and AF–CNK–M diagram for soils of Kerala

4.15. Major Element and Trace Metal Contamination

The degree of elemental enrichment and contamination in the studied soils was assessed using the enrichment ratio (ER), geo-accumulation index (I_{geo}), contamination factor (C_f), pollution load index (PLI), modified contamination factor (mC_f), and ecological risk index (E_{ir}) (Tables 6 and 7; Table 14). The ER and I_{geo} values were calculated using the elemental abundances of the Upper Continental Crust (UCC) reported by Taylor and McLennan (1995). For the major elements, most oxides exhibited ER values below 1, indicating relative depletion compared with the UCC and suggesting their preferential mobilization during weathering. In contrast, Fe exceeded an ER of 1 in the genetic horizons of all profiles, while Mn showed ER >1 particularly in P2, indicating relative enrichment of these elements within the soil profiles. The I_{geo} values for most major elements were negative, indicating an uncontaminated status. Fe was generally classified as uncontaminated to moderately contaminated, except in P3 (Kinalur series), where the values remained within the uncontaminated category. The C_f values for SiO_2, CaO, MgO, Na_2O, and K_2O were consistently <1, corresponding to low contamination, whereas Al_2O_3 and Mn generally showed C_f values between 1 and 3, indicating moderate contamination. Fe_2O_3 and TiO_2 exceeded a C_f value of 3 in some horizons of P1 and P2, indicating considerable enrichment relative to the reference background (Zhao et al., 2012). Nevertheless, the PLI values for the major elements remained <1, indicating an overall low level of contamination and a condition close to the baseline level (Mohiuddin et al., 2011).

Among the trace elements (Table 15), Cu showed considerable spatial and vertical variability, with a mean ER of 1.47 ± 1.79 and a high coefficient of variation. Particularly high ER values were observed in the Ap horizon of P3 (7.60), the Bt2 horizon of P4 (6.43), and P5 (2.31), suggesting localized enrichment of Cu and a possible anthropogenic contribution. In general, ER values <2 indicate little or no enrichment relative to the crustal background, whereas values substantially >2 indicate increasing enrichment and may warrant consideration of anthropogenic inputs. The enrichment of Cu may be influenced by its strong association with Fe and Al oxides and its retention through adsorption and complexation processes controlled by soil pH, organic carbon, and cation-exchange capacity (Hooda, 2010; Solly et al., 2020). Weathering and release of Fe and Mn from parent materials may also contribute to the redistribution and retention of Cu within soil profiles (Ko, 2014). Zn exhibited a mean ER of 1.08 ± 0.59 (CV = 54.28%), with most horizons showing ER values close to or below 1, indicating predominantly crustal control, although slight enrichment was evident in some horizons of P3. Similarly, Ni generally exhibited ER values <1, suggesting a predominantly lithogenic or crustal source, with slight enrichment in P3 and P5 where ER values ranged between 1 and 2.

Cadmium exhibited the most pronounced enrichment among the trace elements. The mean ER for Cd was 43.13 ± 44.89, with a very high CV of 104.08%, while its mean concentration was 12.00 ± 17.62 μg g^{-1} (CV = 148.60%), compared with a UCC value of only 0.098 μg g^{-1} (Taylor and McLennan, 1995). The exceptionally high ER values indicate substantial Cd enrichment relative to the crustal background. Such enrichment may be associated with agricultural inputs, including organic manures containing elevated concentrations of trace metals, phosphate fertilizers, pesticides, and other agrochemicals (Luo et al., 2009; Prasanth et al., 2013; Syamlal and Sayantan, 2024b). The use of Bordeaux mixture may also contribute particularly to Cu accumulation, although it is not considered a primary source of Cd. The I_{geo} values for Cd varied markedly with depth, from −3.90 in P1 to 7.89 in P5, with a mean of 4.81 ± 1.69 (CV = 35.15%), indicating a range from uncontaminated conditions in some horizons to heavy or extreme Cd accumulation in others. Cu showed moderate contamination according to I_{geo} in P3, whereas the remaining profiles were predominantly within the uncontaminated category.

The contamination-factor assessment further highlighted the contrasting behaviour of individual trace elements. The mean C_f values for Cu (3.31), Zn (2.71), Ni (2.44), and Cr

(1.55) corresponded to moderate to considerable contamination, whereas Cd exhibited an exceptionally high mean C_f of 111.3, indicating very high contamination relative to the reference background. In contrast, Ba and Sr had mean C_f values <1, indicating low contamination and predominantly lithogenic control. Despite the elevated C_f values of individual trace metals, the mean PLI was 0.73 ± 0.19 (CV = 25.93%), which remained below unity and therefore indicated an overall pollution load close to the baseline level. This apparent contrast between the PLI and individual C_f values reflects the mathematical behaviour of the PLI, which integrates the contamination factors of multiple elements; consequently, a very high enrichment of one element, particularly Cd, does not necessarily result in a PLI >1 when the remaining elements have relatively low contamination factors.

The modified contamination factor (mC_f) provided further evidence of substantial variability in the overall degree of elemental contamination. The mean mC_f was 10.63 ± 3.87, ranging from 6.54, classified as high contamination, to 22.52, corresponding to extremely high contamination. The ecological risk index (E_{ir}) for Cr, Ni, Zn, and Cu had a mean value of 36.66 ± 19.48, with a range of 17.74–97.61 and a CV of 53.12%, indicating considerable spatial variability but generally low ecological risk for these elements. In contrast, Cd contributed disproportionately to the ecological risk because of its very high enrichment and contamination factor. Overall, the results indicate that most major elements and several trace metals are predominantly controlled by parent material and pedogenic weathering, whereas localized enrichment of Cu and, particularly, Cd suggests potential anthropogenic inputs. The coexistence of low overall PLI values with very high Cd enrichment emphasizes the importance of evaluating individual contaminants alongside composite pollution indices when assessing the environmental quality of agricultural soils.

Table 14. Metal contamination of major elements in lateritic soils of Kerala

		Enrichment ratio								Igeo accumulation index								Cf									
Depth (cm)	Horizon	SiO_2	Al_2O_3	Fe_2O_3	**CaO**	**MgO**	Na_2O	K_2O	MnO	SiO_2	Al_2O_3	Fe_2O_3	TiO_2	**CaO**	**MgO**	Na_2O	K_2O	MnO	SiO_2	Al_2O_3	Fe_2O_3	TiO_2	**CaO**	**MgO**	Na_2O	K_2O	PLI	mcf
P1																												
0-18	Ap	0.41	0.40	1.78	0.10	0.17	0.11	0.07	0.72	-0.89	-0.92	1.22	1.55	-2.97	-2.12	-2.75	-6.11	-0.06	0.82	0.79	3.50	3.11	0.21	0.35	0.22	0.15	1.44	0.66
18-46	A/B	0.42	0.48	1.61	0.10	0.17	0.10	0.08	0.70	-0.85	-0.65	1.08	1.21	-3.04	-2.18	-2.90	-5.97	-0.11	0.84	0.96	3.16	2.43	0.20	0.33	0.20	0.16	1.39	0.64
46-73	Bt1	0.34	0.65	1.58	0.09	0.13	0.08	0.12	0.31	-1.14	-0.21	1.05	1.15	-3.13	-2.56	-3.26	-5.38	-1.30	0.69	1.30	3.10	2.29	0.18	0.25	0.16	0.24	0.61	0.58
73-107	Bt2	0.35	0.81	0.73	0.09	0.12	0.04	0.09	0.11	-1.10	0.11	-0.07	1.19	-3.11	-2.67	-4.06	-5.75	-2.80	0.71	1.62	1.43	2.38	0.19	0.24	0.09	0.19	0.22	0.44
P2																												
0-8	A	0.29	0.54	1.81	0.11	0.25	0.08	0.20	1.42	-1.39	-0.46	1.24	0.96	-2.81	-1.58	-3.26	-4.69	0.92	0.58	1.09	3.54	1.92	0.23	0.50	0.16	0.40	2.84	0.76
8-19	Bt1	0.35	0.72	0.77	0.06	0.23	0.09	0.23	1.45	-1.11	-0.07	0.01	1.11	-3.81	-1.69	-3.10	-4.48	0.95	0.70	1.43	1.51	2.22	0.11	0.46	0.17	0.46	2.90	0.70
19-51	Bt2	0.34	0.65	1.26	0.05	0.21	0.08	0.24	1.38	-1.14	-0.22	0.72	1.13	-3.97	-1.83	-3.14	-4.40	0.88	0.69	1.29	2.47	2.26	0.10	0.42	0.17	0.48	2.77	0.72
51-89	Bt3	0.36	0.74	0.84	0.05	0.23	0.08	0.25	1.25	-1.07	-0.03	0.14	1.15	-3.90	-1.68	-3.28	-4.34	0.74	0.73	1.47	1.65	2.29	0.11	0.47	0.15	0.50	2.50	0.70
P3																												
0-10	Ap1	0.42	0.57	0.14	0.19	0.15	0.25	0.16	0.30	-0.82	-0.39	-2.49	0.09	-2.08	-2.28	-1.57	-5.00	-1.33	0.86	1.15	0.27	0.19	0.38	0.31	0.51	0.32	0.60	0.43
10-36	AB	0.41	0.54	0.92	0.25	0.16	0.32	0.15	0.29	-0.86	-0.47	0.27	-0.10	-1.66	-2.22	-1.25	-5.11	-1.39	0.84	1.08	1.80	-0.20	0.51	0.32	0.63	0.29	0.57	
36-48	Bt1	0.43	0.59	0.42	0.19	0.26	0.40	0.17	0.33	-0.81	-0.35	-0.86	0.42	-2.08	-1.52	-0.92	-4.88	-1.18	0.86	1.17	0.82	0.83	0.38	0.52	0.79	0.35	0.66	0.66
48-66	Bt2	0.43	0.56	0.44	0.17	0.15	0.35	0.14	0.25	-0.79	-0.42	-0.79	0.09	-2.28	-2.34	-1.09	-5.14	-1.56	0.88	1.12	0.87	0.19	0.33	0.30	0.70	0.29	0.51	0.49
66-80	Bt3	0.38	0.59	1.50	0.13	0.18	0.24	0.15	0.23	-0.97	-0.35	0.97	-0.10	-2.68	-2.10	-1.64	-5.04	-1.70	0.77	1.17	2.94	-0.20	0.25	0.35	0.48	0.31	0.46	
P4																												
0-13	Ap	0.34	0.73	0.93	0.17	0.09	0.34	0.06	0.20	-1.13	-0.05	0.28	1.18	-2.21	-3.01	-1.13	-6.36	-1.88	0.69	1.45	1.83	2.36	0.35	0.19	0.69	0.12	0.41	0.60
13-32	Bt1	0.33	0.70	1.53	0.13	0.09	0.36	0.07	0.18	-1.18	-0.10	1.00	1.26	-2.61	-3.01	-1.06	-6.26	-2.08	0.67	1.40	3.01	2.53	0.26	0.19	0.72	0.13	0.35	0.61
32-56	Bt2	0.34	0.68	1.81	0.17	0.08	0.43	0.06	0.17	-1.16	-0.14	1.24	0.90	-2.24	-3.32	-0.81	-6.36	-2.18	0.68	1.36	3.54	1.80	0.34	0.15	0.86	0.12	0.33	0.60
56-83	Bt3	0.30	0.67	1.85	0.13	0.09	0.53	0.07	0.18	-1.30	-0.16	1.28	0.79	-2.68	-3.04	-0.50	-6.17	-2.03	0.62	1.34	3.63	1.59	0.25	0.18	1.06	0.14	0.37	0.61

83-112	Bt4	0.35	0.68	1.57	0.14	0.10	0.44	0.07	0.15	-1.12	-0.14	1.03	0.68	-2.50	-2.91	-0.76	-6.14	-2.35	0.70	1.36	3.07	1.36	0.28	0.20	0.88	0.14	0.30	0.59
122-150	Bt5	0.35	0.73	1.34	0.15	0.09	0.39	0.07	0.16	-1.08	-0.05	0.81	0.79	-2.45	-3.08	-0.94	-6.23	-2.24	0.72	1.45	2.63	1.59	0.29	0.18	0.78	0.14	0.32	0.58
P5																												
0-16	Ap	0.36	0.81	0.94	0.05	0.10	0.03	0.12	0.33	-1.08	0.11	0.30	1.34	-3.94	-2.94	-4.73	-5.45	-1.18	0.72	1.62	1.85	2.68	0.11	0.20	0.06	0.23	0.66	0.47
16-42	Bt1	0.33	0.96	0.92	0.04	0.10	0.02	0.09	0.25	-1.18	0.36	0.27	1.00	-4.35	-2.94	-5.10	-5.80	-1.60	0.67	1.92	1.80	2.00	0.08	0.20	0.04	0.18	0.49	0.40
42-66	Bt2	0.30	1.00	1.42	0.07	0.09	0.02	0.10	0.16	-1.33	0.42	0.89	0.90	-3.61	-3.01	-5.10	-5.64	-2.27	0.60	2.00	2.78	1.80	0.13	0.19	0.04	0.20	0.31	0.42
66-89	Bt3	0.31	1.01	1.16	0.04	0.09	0.03	0.10	0.17	-1.28	0.43	0.60	0.90	-4.23	-3.01	-4.87	-5.64	-2.16	0.63	2.02	2.27	1.80	0.09	0.19	0.05	0.20	0.34	0.40
89-105	BC	0.32	1.05	0.89	0.04	0.10	0.02	0.10	0.17	-1.25	0.48	0.21	0.90	-4.35	-2.87	-5.10	-5.60	-2.11	0.64	2.10	1.74	1.80	0.08	0.20	0.04	0.21	0.35	0.39

Table 15. Trace metal contamination in lateritic soils of Kerala

Depth					ER					Igeo accumulation index							Cf									
(cm)	**Cu**	**Zn**	**Mn**	**Ni**	**Cr**	**Cd**	**Zr**	**Ba**	**Sr**	**Cu**	**Zn**	**Ni**	**Cr**	**Cd**	**Ba**	**Sr**	**Cu**	**Zn**	**Ni**	**Cr**	**Cd**	**Ba**	**Sr**	PLI	mcdf	ERI
P1																										
0-18	0.64	0.51	0.25	0.23	0.75	20.87	0.03	0.04	0.04	-0.96	-1.98	-2.14	-0.41	4.38	-4.90	-4.69	2.80	2.23	1.00	3.31	91.84	0.17	0.18	0.93	9.69	27.84
18-46	1.51	1.22	0.31	0.33	0.80	23.46	0.05	0.03	0.05	0.29	-1.69	-1.61	-0.32	4.55	-4.46	-5.04	5.24	4.18	1.14	2.79	81.63	0.11	0.17	1.04	13.63	41.64
46-73	1.60	0.68	0.14	0.40	0.70	24.59	0.03	0.03	0.04	-0.57	-2.81	-1.31	-0.51	4.62	-4.91	-5.31	5.32	2.21	1.34	2.33	81.63	0.08	0.15	0.88	11.43	40.17
73-107	0.70	0.53	0.05	0.50	0.76	14.92	0.03	0.02	0.04	-0.91	-4.35	-1.00	-0.40	3.90	-5.26	-5.35	2.40	1.79	1.70	2.59	51.02	0.08	0.15	0.79	8.72	27.49
P2																										
0-8	1.01	0.95	0.75	0.87	0.80	41.93	0.07	0.03	0.06	-0.07	-0.41	-0.20	-0.33	5.39	-3.83	-5.19	2.96	2.75	2.55	2.33	122.45	0.08	0.18	0.94	10.84	34.93
8-19	0.88	0.83	0.69	0.97	0.63	25.20	0.07	0.03	0.05	-0.27	-0.53	-0.05	-0.67	4.66	-3.74	-5.28	2.84	2.65	3.14	2.04	81.63	0.08	0.17	0.94	10.91	36.60
19-51	0.88	0.88	0.65	1.16	0.74	18.67	0.07	0.02	0.05	-0.19	-0.62	0.21	-0.44	4.22	-3.79	-5.61	2.88	2.83	3.80	2.42	61.22	0.07	0.17	0.97	12.16	41.06
51-89	1.77	1.10	0.58	1.18	0.69	18.44	0.07	0.02	0.06	0.14	-0.78	0.24	-0.54	4.20	-3.84	-5.66	5.88	3.61	3.91	2.28	61.22	0.07	0.18	1.15	15.93	57.12
P3																										
0-10	7.60	1.27	0.29	0.85	0.35	51.02	0.05	0.04	0.07	0.34	-1.79	-0.23	-1.50	5.67	-4.44	-4.74	12.16	2.00	1.36	0.56	81.63	0.06	0.11	0.71	16.26	70.75
10-36	1.34	1.59	0.32	0.91	0.69	65.60	0.05	0.09	0.07	0.67	-1.66	-0.14	-0.54	6.04	-4.35	-3.50	1.88	2.20	1.27	0.96	91.84	0.12	0.10	0.63	6.54	19.89
36-48	0.86	1.67	0.26	0.38	0.52	40.82	0.04	0.05	0.05	0.74	-1.96	-1.42	-0.93	5.35	-4.66	-4.35	1.72	3.30	0.75	1.05	81.63	0.10	0.10	0.60	7.01	17.74
48-66	1.05	1.82	0.25	0.70	0.69	57.40	0.05	0.05	0.06	0.87	-2.03	-0.52	-0.53	5.84	-4.34	-4.46	1.68	2.87	1.11	1.11	91.84	0.07	0.09	0.59	6.94	19.05
66-80	1.23	3.34	0.26	0.80	0.61	58.31	0.05	0.08	0.06	1.74	-1.97	-0.33	-0.72	5.87	-4.35	-3.68	1.72	4.61	1.11	0.85	81.63	0.11	0.09	0.65	8.48	20.47
P4																										
0-13	0.75	0.72	0.09	0.25	0.36	30.01	0.03	0.05	0.02	-0.47	-3.43	-1.98	-1.46	4.91	-5.25	-4.38	2.56	2.42	0.86	1.24	102.04	0.16	0.08	0.67	7.33	22.01
13-32	0.74	1.09	0.08	0.11	0.24	31.18	0.02	0.04	0.02	0.12	-3.71	-3.14	-2.05	4.96	-5.42	-4.70	2.68	3.86	0.41	0.87	112.24	0.14	0.07	0.57	8.02	21.05
32-56	6.43	0.94	0.09	0.18	0.45	40.09	0.04	0.04	0.02	-0.09	-3.44	-2.49	-1.15	5.33	-4.81	-4.71	18.00	2.59	0.50	1.26	112.24	0.11	0.07	0.77	22.52	97.61
56-83	0.85	1.17	0.11	0.16	0.37	54.95	0.03	0.04	0.03	0.23	-3.19	-2.67	-1.45	5.78	-4.95	-4.48	2.20	3.00	0.41	0.95	142.86	0.12	0.07	0.52	6.75	17.95
83-112	1.17	0.90	0.10	0.25	0.54	46.77	0.04	0.05	0.03	-0.15	-3.39	-2.02	-0.89	5.55	-4.83	-4.26	2.80	2.13	0.59	1.29	112.24	0.13	0.07	0.59	7.01	21.67
122-150	1.14	0.80	0.09	0.04	0.55	39.25	0.03	0.05	0.03	-0.33	-3.40	-4.52	-0.86	5.29	-4.86	-4.20	2.96	2.04	0.11	1.44	102.04	0.14	0.07	0.47	6.76	20.28
P5																										
0-16	0.16	0.70	0.14	1.77	0.36	0.00	0.30	0.01	0.02	-0.52	-2.89	0.82	-1.48	0.00	-1.71	-6.33	0.60	2.61	6.73	1.36	0.00	0.05	0.06	0.59	11.40	41.97
16-42	0.12	0.78	0.13	1.77	0.32	0.00	0.63	0.01	0.02	-0.36	-2.97	0.82	-1.65	0.00	-0.66	-6.07	0.36	2.31	5.30	0.95	0.00	0.04	0.07	0.49	9.03	32.49
42-66	2.31	0.76	0.09	1.27	0.38	236.88	0.89	0.03	0.03	-0.41	-3.54	0.34	-1.39	7.89	-0.17	-5.17	6.48	2.08	3.55	1.07	663.27	0.08	0.07	0.81	13.33	54.35
66-89	0.26	1.02	0.09	2.32	0.44	47.38	0.71	0.02	0.02	0.03	-3.43	1.22	-1.19	5.57	-0.50	-5.59	0.72	2.82	6.50	1.22	132.65	0.06	0.06	0.62	11.38	41.36
89-105	0.26	0.74	0.10	3.37	0.28	47.38	0.51	0.02	0.02	-0.43	-3.38	1.75	-1.83	5.57	-0.98	-5.85	0.72	2.04	9.43	0.79	132.65	0.05	0.06	0.57	13.09	54.38
Mean	**1.47**	**1.08**	**0.25**	**0.87**	**0.54**	**43.13**	**0.16**	**0.04**	**0.04**	**-0.02**	**-2.47**	**-0.85**	**-0.97**	**4.81**	**-3.79**	**-4.94**	**3.73**	**2.71**	**2.44**	**1.54**	**111.39**	**0.10**	**0.11**	**0.73**	**10.63**	**36.66**
SD	**1.79**	**0.59**	**0.21**	**0.80**	**0.18**	**44.89**	**0.25**	**0.02**	**0.02**	**0.60**	**1.13**	**1.52**	**0.52**	**1.69**	**1.65**	**0.72**	**3.94**	**0.73**	**2.43**	**0.76**	**122.78**	**0.04**	**0.05**	**0.19**	**3.87**	**19.48**
minimum	0.12	0.51	0.05	0.04	0.24	0.00	0.02	0.01	0.02	-0.96	-4.35	-4.52	-2.05	0.00	-5.42	-6.33	0.36	1.79	0.11	0.56	0.00	0.04	0.06	0.47	6.54	17.74
maximum	7.60	3.34	0.75	3.37	0.80	236.88	0.89	0.09	0.07	1.74	-0.41	1.75	-0.32	7.89	-0.17	-3.50	18.00	4.61	9.43	3.31	663.27	0.17	0.18	1.15	22.52	97.61
CV(%)	**122.10**	**54.25**	**85.63**	**92.29**	**33.37**	**104.08**		**52.43**	**43.61**				**0.00**	**35.15**				**27.04**	**99.45**	**48.91**	**110.22**	**37.76**	**42.86**	**25.93**	**36.36**	**53.12**

5. Conclusions

This study investigated the elemental geochemistry, morphopedogenic characteristics, weathering behaviour, and trace-metal status of five laterite-associated soil series under rubber cultivation in the Southern Midland Zone of Kerala. The integration of soil morphology, texture, CIE L*a*b* colour parameters, major- and trace-element geochemistry, weathering indices, regression models, ternary diagrams, bivariate relationships, and contamination indices provided a comprehensive assessment of pedogenic development and elemental redistribution within the soil profiles. The studied soils ranged in texture from sandy loam in P1 to sandy clay loam in P3 and P4 and clay in P2, with a general increase in clay content with depth. They were characterized by relatively low ECEC/CEC, high organic carbon contents in the surface horizons, and low base saturation, reflecting strong leaching and advanced pedogenic development and supporting their classification within Ultisol- and Alfisol-related soil groups.

The CIE L*a*b* colour parameters effectively captured variations in soil redness and their relationship with pedogenic processes. The numerical redness rating derived from Munsell colour showed a significant relationship with the CIE colour coordinates, particularly the *a* and *b* parameters. The multiple regression model for organic carbon demonstrated a strong relationship with CIE L*a*b* variables ($R^2 = 0.82$, $p < 0.01$), indicating that colour parameters can provide useful quantitative information on organic-carbon-related variation in these soils. Similarly, Al_2O_3 exhibited a strong relationship with colour variables and redness rating ($R^2 = 0.71$, $p = 0.001$), suggesting that soil colour provides a useful indirect indicator of changes in the composition and distribution of Al-bearing soil constituents. However, colour should be regarded as a proxy for pedogenic and compositional variation rather than as a direct measure of individual mineral phases.

The major-element composition was dominated by SiO_2 (mean 41.49%), followed by Al_2O_3 (23.21%) and Fe_2O_3 (10.07%). Their vertical variation and negative relationships indicate progressive redistribution and relative enrichment of Al and Fe associated with the depletion of more mobile constituents during weathering. The suite of weathering indices consistently demonstrated substantial chemical alteration, particularly in the Kangirapalli (P4) and Athirampuzha (P5) series, which showed very high CIA, CIW, PIA, and MIA values and were characterized as extremely weathered. In comparison, the Kinalur series (P3) exhibited a comparatively lower degree of weathering. The A–CN–K, S–A–F, and AF–CNK–M ternary diagrams supported the interpretation of progressive depletion of mobile base cations and silica, accompanied by relative enrichment of Al and Fe. Collectively, these patterns indicate intensive in-situ chemical weathering under the humid tropical conditions of Kerala, although the degree and pathway of weathering vary among soil series and horizons.

The regression analyses further demonstrated a quantitative association between soil colour and weathering intensity. IOL showed a significant relationship with redness-related variables, including the a/a+b ratio and a_1, with the model explaining approximately 63% of the observed variation ($R^2 = 0.63$). MIA(O) also exhibited a significant relationship with the a coordinate and redness rating ($R^2 = 0.51$), whereas MIA(R) showed a comparatively weaker relationship with a ($R^2 = 0.29$). These relationships demonstrate the potential of CIE L*a*b colour measurements for estimating spatial and vertical variations in weathering-related properties, particularly in rubified horizons. Nevertheless, the regression models represent

statistical associations and should be independently validated before being applied for quantitative prediction across different soil-forming environments.

The contamination assessment revealed contrasting behaviour among the trace elements. Composite pollution indices indicated a generally low overall pollution load, with PLI values remaining below unity, and Cr, Ni, Cu, and Zn generally presenting low ecological risk. However, Cd exhibited exceptionally high enrichment and contamination relative to the UCC background, with localized Cu enrichment also evident in some horizons. The results therefore suggest that most elemental variation is associated with parent material and pedogenic weathering, whereas the pronounced Cd enrichment may reflect additional anthropogenic inputs associated with agricultural management practices. The occurrence of high contamination factors for individual elements despite a PLI below unity highlights the importance of interpreting composite indices together with element-specific enrichment and contamination measures.

Overall, the study demonstrates a close association between soil colour, elemental redistribution, and chemical weathering in laterite-associated soils of the rubber-growing region of Kerala. CIE L*a*b* colour parameters, when combined with conventional soil morphology and geochemical weathering indices, provide a useful approach for characterizing pedogenic differentiation, rubification, and the redistribution of Fe- and Al-bearing constituents. The findings also establish quantitative relationships that may support rapid assessment of weathering intensity where extensive laboratory characterization is impractical. Future investigations should incorporate high-resolution sampling along complete soil profiles, mineralogical characterization, and spatially distributed geochemical measurements to better resolve the evolution of laterite-derived soils. Long-term monitoring should also focus on establishing pedogenic thresholds and detecting changes in weathering processes, elemental mobility, and trace-metal accumulation associated with climatic variability and anthropogenic management of rubber plantations.

Acknowledgements

The authors gratefully acknowledge the technical staff of ICAR-NBSS&LUP for their valuable assistance during the fieldwork and laboratory investigations.

Author contributions

BPB (B. P. Bhaskar) conceived the study and developed the main research idea. PND (P. N. Dubey) and RPS (R. P. Sharma) conducted the field and laboratory investigations. BPB, PSB (P. S. Butte) and RPS performed the data analysis and prepared the first draft of the manuscript. BPB provided overall supervision and secured funding for the study. All authors reviewed and approved the final manuscript.

Funding

This study was funded by the Indian Council of Agricultural Research (ICAR), Department of Agricultural Research and Education (DARE), Ministry of Agriculture and Farmers Welfare, Government of India.

Data availability

The dataset generated and analysed during the current study is available from the corresponding author upon reasonable request.

Declarations

Ethics approval and consent to participate

Not applicable. This study did not involve human or animal participants.

Clinical Trial Registration

This study is not a clinical trial. It involved field-based and laboratory investigations of laterite-associated soils and did not involve human participants, patients, clinical interventions, or medical treatments. Therefore, clinical trial registration is not applicable.

Consent for publication

All authors have read and approved the final manuscript and consented to its publication.

Competing interests

The authors declare that they have no competing interests.

AI use disclosure

Grammarly was used to identify grammatical errors, punctuation issues, and awkward sentence constructions in the manuscript.

References

1. Abbaslou, H., Abtahi, A., Baghernejad, M. (2013). Effect of weathering and mineralogy on the distribution of major and trace elements (Hormozgan Province, Southern Iran). *International Journal of Forest, Soil and Erosion*, 3(1), 15–25.
2. Abrahim, G.M.S., Parker, R.J. (2008). Assessment of heavy metal enrichment factors and the degree of contamination of marine sediments from Tamaki Estuary, Auckland, New Zealand. *Environmental Monitoring and Assessment*, 136, 227–238. https://doi.org/10.1007/s10661-007-9678-2
3. Achyuthan, H. (1996). Geomorphic evolution and genesis of laterites around the east coast of Madras, Tamil Nadu, India. *Geomorphology*, 16, 71–76.
4. Al-Chalabi, S.N.A. (2004). *Mineralogy and origin of chromite in Qalander area, Northern Iraq*. MSc thesis, Salahaddin University-Erbil, Iraq, 104 p.
5. Aquino, A., Scardia, G., Prud'homme, C., Dave, A.K., Lezzerini, M., Johansson, A.E., Marquer, L., Safaraliev, N., Lauer, T., Fitzsimmons, K.E. (2024). Variability in geochemical weathering indices in loess over the last full glacial cycle at Karamaidan, Central Asia (Tajikistan). *Frontiers in Earth Science*, 12, 1347910. https://doi.org/10.3389/feart.2024.1347910
6. Babechuk, M.G., Widdowson, M., Kamber, B.S. (2014). Quantifying chemical weathering intensity from two contrasting basalt profiles, Deccan Traps, India. *Chemical Geology*, 363, 56–75. https://doi.org/10.1016/j.chemgeo.2013.10.027
7. Basavaraj, B., Sarma, V.A.K. (1993). Iron bearing clay mineralogy of some selected soils of Peninsular India. In: Sehgal, J., Sarma, V.A.K., Batta, R.K., Gajbhiye, K.S., Nagabhushana, S.R., Venugopal, K.R. (eds.) *Red and Lateritic Soils of India – Resource Appraisal and Management*. NBSS Publication 37, National Bureau of Soil Survey and Land Use Planning, Nagpur, India, pp. 143–152.
8. Beyala, V.K.K., Onana, V.L., Priso, E.N.E., Parisot, J.C., Ekodeck, G.E. (2009). Behaviour of REE and mass balance calculations in a lateritic profile over chlorite schists in South Cameroon. *Chemie der Erde – Geochemistry*, 69, 61–73. https://doi.org/10.1016/j.chemer.2008.08.003
9. Bhaskar, B.P. (2026). Assessment of weathering pattern in laterite associated soils of Nellore Schist Belt, Andhra Pradesh, India. *Indian Journal of Plant and Soil*, 13(1), 25–45. https://doi.org/10.21088/ijps.2348.9677.13126.3
10. Bhaskar, B.P., Gopal Tiwari. (2017). Geochemical interpretations of laterite associated soils of East Coast, Andhra Pradesh. *Chemical Science Review and Letters*, 6(21), 187–197. Article CS302048011.

11. Bhaskar, B.P., Raja, P., Srinivas, C.V. (1999). Genetic interpretation of pedological characteristics of laterite associated soils of Somasila Project, Andhra Pradesh. *Gondwana Geological Magazine*, 14(2), 39–47.
12. Bhaskar, B.P., Saxena, R.K., Vadivelu, S., Baruah, U., Butte, P.S., Dutta, D.P. (2005). Pedogenesis in high-altitude soils of Meghalaya Plateau. *Agropedology*, 14(1), 9–23.
13. Bhaskar, B.P., Saxena, R.K., Vadivelu, S., Baruah, U., Sarkar, D., Raja, P., Butte, P.S. (2009). Intricacy in classification of pine-growing soils in Shillong Plateau, Meghalaya, India. *Soil Survey Horizons*, 50(1), 11–16.
14. Bhaskar, B.P., Sharma, R.P., Baruah, U., et al. (2026). Pedological controls on soil erodibility in high-altitude Ultisols and associated soils of the Meghalaya Plateau, India. *Discover Soil*, 3, 113. https://doi.org/10.1007/s44378-026-00274-1
15. Bhattacharya, A.K., Kurien, T.K., Krishnanunni, K., et al. (1979). Geomorphic mapping in parts of Kerala State. *Journal of the Indian Society of Photo-Interpretation and Remote Sensing*, 7, 1–9. https://doi.org/10.1007/BF02991450
16. Bhattacharyya, T., Pal, D.K., Lal, S., Chandran, P., Ray, S.K. (2006). Formation and persistence of Mollisols on zeolitic Deccan basalt of humid tropical India. *Geoderma*, 136, 609–620.
17. Bhattacharyya, T., Sarkar, D., Sehgal, J.L., Velayutham, M., Gajbhiye, K.S., Nagar, A.P., Nimkhedkar, S.S. (2009). *Soil taxonomic database of India and the states (1:250,000 scale)*. NBSS Publication 143. National Bureau of Soil Survey and Land Use Planning, Nagpur.
18. Bhuiyan, M.A.H., Parvez, L., Islam, M.A., Dampare, S.B., Suzuki, S. (2010). Heavy metal pollution of coal mine-affected agricultural soils in the northern part of Bangladesh. *Journal of Hazardous Materials*, 173, 384–392. https://doi.org/10.1016/j.jhazmat.2009.08.085
19. Birch, G.F., Olmos, M.A. (2008). Sediment-bound heavy metals as indicators of human influence and biological risk in coastal water bodies. *ICES Journal of Marine Science*, 65, 1407–1413. https://doi.org/10.1093/icesjms/fsn139
20. Birkeland, P.W. (1999). *Soils and Geomorphology*. Oxford University Press, New York, 430 p.
21. Bourgeon, G. (1989). *Explanatory booklet on the reconnaissance soil map of forest area, Western Karnataka and Goa*. Institut Français de Pondichéry, Travaux de la Section Scientifique et Technique, Hors Série No. 20, 96 pp. + 2 annexes including 1 map.
22. Bowen, H.J.M. (1979). *Environmental Chemistry of the Elements*. Academic Press, London, UK, 333 p.
23. Bruckner, H. (1989). Küstennahe Tiefländer in Indien – ein Beitrag zur Geomorphologie der Tropen. *Düsseldorfer Geographische Schriften*, 28.
24. Brückner, H., Bruhn, N. (1992). Aspects of weathering and peneplanation in southern India. *Zeitschrift für Geomorphologie, Neue Folge, Supplementband*, 91, 43–66.
25. Bruhn, N. (1990). Substratgenese – Rumpfflächendynamik. Bodenbildung und Tiefenverwitterung in saprolitisch zersetzten granitischen Gneisen aus Südindien. *Kieler Geographische Schriften*, 74.
26. Buchanan, F. (1807). *A journey from Madras through the countries of Mysore, Canara and Malabar*. East India Company, London.
27. Buggle, B., Glaser, B., Hambach, U., Gerasimenko, N., Marković, S. (2011). An evaluation of geochemical weathering indices in loess–paleosol studies. *Quaternary International*, 240(1–2), 12–21.
28. Buringh, P. (1970). *Introduction to the Study of Soils in Tropical and Subtropical Regions*. Wageningen; Oxford/New Delhi.

29. Chadwick, O.A., Gavenda, R.T., Kelly, E.F., Ziegler, K., Olson, C.G., Elliott, W.C., Hendricks, D.M. (2003). The impact of climate on the biogeochemical functioning of volcanic soils. *Chemical Geology*, 202, 195–223.
30. Chandni, N.P., Subramanian, A., Baskar, S., et al. (2026). Trace metal and health risk analysis of water and soil of Periyar River basin, Kerala. *Water Science*, 40, 6. https://doi.org/10.1007/s44533-025-00009-1
31. Chandran, P., Ray, S., Bhattacharyya, T., Srivastava, P., Krishnan, P., Pal, D.K. (2005). Lateritic soils (Ultisols) of Kerala, India: Their genesis and taxonomy. *Australian Journal of Soil Research*, 43, 839–852. https://doi.org/10.1071/SR04128
32. Che, V.B., Fontijn, K., Ernst, G.G.J., Kervyn, M., Elburg, M., Van Ranst, E., Suh, C.E. (2012). Evaluating the degree of weathering in landslide-prone soils in the humid tropics: The case of Limbe, SW Cameroon. *Geoderma*, 170, 378–389.
33. Chittleborough, D.J. (1991). Indices of weathering for soils and palaeosols formed on silicate rocks. *Australian Journal of Earth Sciences*, 38(1), 115–120. https://doi.org/10.1080/08120099108727959
34. Collier, J.S., Sansom, V., Ishizuka, O., Taylor, R.N., Minshull, T.A., Whitmarsh, R.B. (2008). Age of Seychelles–India break-up. *Earth and Planetary Science Letters*, 272, 264–277.
35. Damodaran, A. (1954). *Progress report for the field season 1952–53: A note on the traverses in Malnad areas of parts of Malabar and Nilgiri districts*. Geological Survey of India, unpublished report.
36. Darmody, R.G., Thorn, C.E., Allen, C.E. (2005). Chemical weathering and boulder mantles, Kärkevagge, Swedish Lapland. *Geomorphology*, 67, 159–170.
37. Deepthy, R., Balakrishnan, S. (2005). Climatic control on clay mineral formation: Evidence from weathering profiles developed on either side of the Western Ghats. *Journal of Earth System Science*, 114, 545–556. https://doi.org/10.1007/BF02702030
38. Dubey, P.N., Bhaskar, B.P., Chandran, P., Singh, P.B., Mishra, B.K. (2016). Geochemistry of some ferruginous soils of Kerala, India. *Journal of Applied and Natural Science*, 8(1), 196–207. https://doi.org/10.31018/jans.v8i1.773
39. Dubey, P.N., Bhaskar, B.P., Chandran, P., Singh, P.B., Mishra, B.K. (2017). Major and trace element geochemistry in ferruginous soils developed under the hot humid Malabar region, India. In: *Sustainable Management of Land Resources*, 1st edn. Apple Academic Press, pp. 32.
40. Eswaran, H., Raghu Mohan, N.G. (1973). The microfabric of petroplinthite. *Soil Science Society of America Proceedings*, 37, 79–82.
41. FAO (1998). *World Reference Base for Soil Resources*. ISSS–ISRIC–FAO. World Soil Resources Reports No. 84. FAO, Rome, 88 p.
42. Fedo, C.M., Babechuk, M.G. (2023). Petrogenesis of siliciclastic sediments and sedimentary rocks explored in three-dimensional Al_2O_3–CaO*+Na_2O–K_2O–FeO+MgO (A–CN–K–FM) compositional space. *Canadian Journal of Earth Sciences*, 60, 818–838. https://doi.org/10.1139/cjes-2022-0051
43. Fedo, C.M., Nesbitt, H.W., Young, G.M. (1995). Unraveling the effects of potassium metasomatism in sedimentary rocks and paleosols, with implications for paleoweathering conditions and provenance. *Geology*, 23(10), 921–924. https://doi.org/10.1130/0091-7613(1995)023<0921>2.3.CO;2
44. George, A., Venugopal, A., Vashisht, A.K. (2023). Heavy metal contamination in soil and groundwater around industrial areas of Kollam District, Kerala, India. *Environmental Monitoring and Assessment*, 195, 265. https://doi.org/10.1007/s10661-022-10880-5
45. Gidigasu, M.D. (1976). *Laterite Soil Engineering: Development in Geotechnical Engineering*. Elsevier Scientific Publishing Company, Amsterdam.

46. Groeneveld, R.A., Meeden, G. (1984). Measuring skewness and kurtosis. *The Statistician*, 33(4), 391–399.
47. Gupta, A.S., Seshagiri Rao, K. (2001). Weathering indices and their applicability for crystalline rocks. *Bulletin of Engineering Geology and the Environment*, 60, 201–221.
48. Güven, D.E., Akıncı, G. (2011). Comparison of acid digestion techniques to determine heavy metals in sediment and soil samples. *Gazi University Journal of Science*, 24(1), 29–34.
49. Hair, J.F., Black, W.C., Babin, B.J., Anderson, R.E. (2010). *Multivariate Data Analysis*, 7th edn. Pearson Education International, Upper Saddle River, NJ.
50. Hakanson, L. (1980). An ecological risk index for aquatic pollution control: A sedimentological approach. *Water Research*, 14, 975–1001. https://doi.org/10.1016/0043-1354(80)90143-8
51. Harindranath, C.S., Venugopal, K.R., Raghu Mohan, N.G., Sehgal, J.L., Velayutham, M. (1999). *Soils of Goa for optimising land use*. NBSS Publication 74. National Bureau of Soil Survey and Land Use Planning, Nagpur, India, 131 p.
52. Harka, A.E., Jilo, N.B., Behulu, F. (2021). Spatial-temporal rainfall trend and variability assessment in the upper Wabe Shebelle River Basin, Ethiopia: Application of innovative trend analysis method. *Journal of Hydrology: Regional Studies*, 37, 100915.
53. Harnois, L. (1988). The CIW index: A new chemical index of weathering. *Sedimentary Geology*, 55(3–4), 319–322. https://doi.org/10.1016/0037-0738(88)90137-6
54. Hatem, G., Zeidan, J., Goossens, M., Moreira, C. (2022). Normality testing methods and the importance of skewness and kurtosis in statistical analysis. *BAU Journal – Science and Technology*, 3(2), Article 7. https://doi.org/10.54729/KTPE9512
55. Hausenbuiller, R.L. (1978). *Soil Science: Principles and Practices*. W.M.C. Brown Company Publishers, Iowa, USA.
56. Hazelton, P.A., Murphy, B.W. (2007). Interpreting soil test results: What do all the numbers mean? *CSIRO Publishing*, Collingwood, Australia.
57. Hill, I.G., Worden, R.H., Meighan, I.G. (2000). Geochemical evolution of a paleolaterite: The Interbasaltic Formation, Northern Ireland. *Chemical Geology*, 166, 65–84.
58. Hooda, P.S. (2010). *Trace Elements in Soils*. John Wiley & Sons Ltd., Chichester, UK.
59. Jackson, M.L. (1973). Soil chemical analysis—advanced course. 2nd ed. Department of Soil Science, University of Wisconsin, Madison, WI, USA.
60. Jayawardena, U. de S., Izawa, E. (1994a). A new chemical index of weathering for metamorphic silicate rocks in tropical regions: A study from Sri Lanka. *Engineering Geology*, 36(3–4), 303–310.
61. Jayawardena, U. de S., Izawa, E. (1994b). Application of present indices of chemical weathering for Precambrian metamorphic rocks in Sri Lanka. *Bulletin of the International Association of Engineering Geology*, 49, 55–61.
62. Kalpage, F.S.C.P. (1974). *Tropical Soils: Classification, Fertility and Management*. University of Malaya, Kuala Lumpur, 294 p.
63. Kamath, S.U. (1985). *Karnataka State Gazetteer: Uttara Kannada District*. Gazetteer of India, Government of Karnataka, Bangalore, India.
64. Karathanasis, A.D., Johnson, D.M.C., Matocha, C.J. (2005). Biosolid colloid-mediated transport of copper, zinc, and lead in waste-amended soils. *Journal of Environmental Quality*, 34(4), 1153–1164. https://doi.org/10.2134/jeq2004.0403
65. Ko, T.H. (2014). Nature and properties of lateritic soils derived from different parent materials in Taiwan. *The Scientific World Journal*, 2014, Article ID 247194, 4 p. https://doi.org/10.1155/2014/247194

66. Krishnan, P., Venugopal, K.R., Sehgal, J.L. (1996). *Soils of Kerala for optimising land use*. NBSS Publication 48b. National Bureau of Soil Survey and Land Use Planning, Nagpur, India, 54 p. (Soil Series of India, 10).
67. Luo, L., Ma, Y., Zhang, S., Wei, D., Zhu, Y.G. (2009). An inventory of trace element inputs to agricultural soils in China. *Journal of Environmental Management*, 90, 2524–2530. https://doi.org/10.1016/j.jenvman.2009.01.011
68. Mahoney, J.J. (1988). Deccan Traps. In: Macdougall, J.D. (ed.) *Continental Flood Basalts*. Kluwer, Dordrecht, pp. 151–194.
69. Manju, C.S., Narayanan Nair, V., Lalithambika, M. (2001). Mineralogy, geochemistry and utilization study of the Madayi Kaolin Deposit, North Kerala, India. *Clays and Clay Minerals*, 49, 355–369. https://doi.org/10.1346/CCMN.2001.0490409
70. Marković, S.B., Bokhorst, M.P., Vandenberghe, J., McCoy, W.D., Oches, E.A., Hambach, U., et al. (2008). Late Pleistocene loess–palaeosol sequences in the Vojvodina region, north Serbia. *Journal of Quaternary Science*, 23, 73–84. https://doi.org/10.1002/jqs.1124
71. McKenzie, N.J., Jacquier, D.J., Isbell, R.F., Brown, K.L. (2004). Australian soils and landscapes: An illustrated compendium. *CSIRO Publishing*, Collingwood, Australia. https://doi.org/10.1071/9780643100732
72. Mohiuddin, K.M., Ogawa, Y., Zakir, H.M., Otomo, K., Shikazono, N. (2011). Heavy metals contamination in water and sediments of an urban river in a developing country. *International Journal of Environmental Science and Technology*, 8, 723–736.
73. Nair, K.M., Mandal, C., Chaturvedi, A., Thayalan, S., Ramesh Kumar, S.C., Ramamurthy, V., Anil Kumar, K.S., Srinivas, S., Naidu, L.G.K., Sarkar, D. (2010). Agro-ecological units of Kerala. *Annual Report 2009–10*, pp. 148–154.
74. Nair, M.M. (1987). Coastal geomorphology of Kerala, India. *Journal of the Geological Society of India*, 29, 450–458.
75. Narayanaswamy. (1992). *Geochemistry and genesis of laterite in parts of Cannore District, North Kerala*. Ph.D. thesis, Cochin University of Science and Technology, Kochi, India.
76. Nesbitt, H.W., Wilson, R.E. (1992). Recent chemical weathering of basalts. *American Journal of Science*, 292(10), 740–777.
77. Nesbitt, H.W., Young, G.M. (1982). Early Proterozoic climates and plate motion inferred from major element chemistry of lutites. *Nature*, 299, 715–717.
78. Nesbitt, H.W., Young, G.M. (1989). Formation and diagenesis of weathering profiles. *Journal of Geology*, 97, 129–147.
79. Ngongo, L., Langohr, R. (1992). Classifying strongly weathered soils from the Zairian Basin into the revised international soil classification systems (Soil Taxonomy 1990; FAO–UNESCO legend, 1986). *Pedologie*, XLII-2, 99–117.
80. Omana, P.K., Santhosh, M. (1995). Gold in laterites: A challenging prospect in Gondwana terranes. In: Yoshida, M. et al. (eds.) *Gondwana Research Group, Memoir No. 2*, pp. 159–166.
81. Page, A.L. (ed.) (1982). *Methods of Soil Analysis, Part 2: Chemical and Mineralogical Properties*, 2nd edn. Agronomy Monograph 9. American Society of Agronomy, Madison, WI, USA.
82. Pal, D.K., Wani, S.P., Sahrawat, K.L., Srivastava, P. (2014). Red ferruginous soils of tropical Indian environments: A review of the pedogenic processes and their implications for edaphology. *Catena*, 121, 260–278.
83. Parker, A. (1970). An index of weathering for silicate rocks. *Geological Magazine*, 107, 501–504.

84. Patil, P.L., Dasog, G.S. (1999). Genesis and classification of ferruginous soils in Western Ghat and Coastal region of North Karnataka. *Agropedology*, 9, 1–15.
85. Prasanth, K.M., Sreekala, P.P., Sandeep, S., Kripa, P.K., Sreejesh, K. (2013). Heavy metals and their fractions in soils of Koratty region, Kerala. *Research Journal of Recent Sciences*, 2 (ISC-2012), 171–176.
86. Price, J.R., Velbel, M.A. (2003). Chemical weathering indices applied to weathering profiles developed on heterogeneous felsic metamorphic parent rocks. *Chemical Geology*, 202, 397–416. https://doi.org/10.1016/S0009-2541(02)00342-3
87. Ramahashay, B.C., Rao, K.S., Mehta, V.K., Bhavana, P.R. (1987). Mineralogy and geochemistry of lateritic soil profiles in Kerala, India. *Chemical Geology*, 60(1–4), 327–330. https://doi.org/10.1016/0009-2541(87)90139-2
88. Ramasamy, S.M., Gunasekaran, S., Saravanavel, J., Melwyn Joshua, R., Rajaperumal, R., Kathiravan, R., Palanivel, K., Muthukumar, M. (2020). Geomorphology and landslide proneness of Kerala, India: A geospatial study. *Landslides*. https://doi.org/10.1007/s10346-020-01562-9
89. Ranger, J., Allie, S., Gelhaye, D., Pollier, B., Turpault, M.P., Granier, A. (2002). Nutrient budgets for a rotation of a Douglas-fir plantation in the Beaujolais (France) based on a chronosequence study. *Forest Ecology and Management*, 171, 3–16.
90. Ray, P.D., Caballero, M., Lozano, R., Smykatz-Kloss, W. (2008). Geochemistry of late Quaternary sediments from Tecocomulco Lake, Central Mexico: Implications to chemical weathering and provenance. *Chemie der Erde – Geochemistry*, 68(4), 383–393.
91. Raychaudhuri, S.P. (1980). The occurrence, distribution, classification and management of laterite and lateritic soils. *O.R.S.T.O.M. Série Pédologie*, 18(3–4), 249–252.
92. Reeder, S., Taylor, H., Shaw, R.A., Demetriades, A. (2006). Introduction to the chemistry and geochemistry of the elements. In: Tarvainen, T., de Vos, W. (eds.) *Geochemical Atlas of Europe, Part 2: Interpretation of Geochemical Maps, Additional Tables, Figures, Maps, and Related Publications*. Geological Survey of Finland, Espoo, pp. 48–429.
93. Reiche, P. (1943). Graphic representation of chemical weathering. *Journal of Sedimentary Petrology*, 13, 53–68.
94. Rollinson, H.R. (1993). *Using Geochemical Data: Evaluation, Presentation, Interpretation*. Pearson Education Limited, Harlow, UK, 352 p.
95. Rowley, M.C., Grand, S., Verrecchia, É.P. (2018). Calcium-mediated stabilisation of soil organic carbon. *Biogeochemistry*, 137, 27–49. https://doi.org/10.1007/s10533-017-0410-1.
96. Rugmini, P., Balagopalan, M. (2006). Evaluation of factor patterns of soils in different plantations and natural forests in the Western Ghats, Kerala. *Indian Journal of Forestry*, 29(3), 271–275. https://doi.org/10.54207/bsmps1000-2006-Z9J8L1
97. Ruxton, B.P. (1968). Measures of the degree of chemical weathering of rocks. *Journal of Geology*, 76, 518–527.
98. Sahasrabudhe, Y.S., Deshmukh, S.S. (1981). The laterites of the Maharashtra State. In: *Proceedings of the International Seminar on Lateritisation Processes*, Trivandrum, India, 11–14 December 1979, pp. 209–220.
99. Sajinkumar, K.S., Anbazhagan, S., Pradeepkumar, A.P., Rani, V.R. (2011). Weathering and landslide occurrences in parts of Western Ghats, Kerala. *Journal of the Geological Society of India*, 78, 249–257.
100. Sajinkumar, K.S., Rani, V.R. (2015). Contrasting anthropogenically influenced landslides in two different terrain conditions in the southwestern part of Peninsular India. In: Lollino, G. et al. (eds.) *Engineering Geology for Society and Territory*, Vol. 2, pp. 1005–1010.

101. Sarma, V.A.K., Krishnan, P., Budhihal, S.L. (1987). *Laboratory Methods*. NBSS Publication, Technical Bulletin 14. National Bureau of Soil Survey and Land Use Planning, Nagpur.
102. Satyanarayana, K.V.S., Thomas, P.K. (1962). Studies on laterite associated soils. II. Chemical composition of lateritic profiles. *Journal of the Indian Society of Soil Science*, 10, 213–222.
103. Saunders, A.D., Jones, S.M., Morgan, L.A., Pierce, K.L., Widdowson, M., Xu, Y. (2007). Regional uplift associated with continental large igneous provinces: The roles of mantle plumes and the lithosphere. *Chemical Geology*, 241, 282–318.
104. Sawarakar, A.R. (1980). Geological and geomorphological features in part of Nilambur Valley, Kozhikkode District, Kerala State, with special reference to the alluvial gold deposits in the area. *Geological Survey of India, Special Publication*, 5, 29–37.
105. Schaetzl, R.J., Anderson, S. (2015). *Soils: Genesis and Geomorphology*, 2nd edn. Cambridge University Press, Cambridge, 795 p.
106. Schellmann, W. (1981). Considerations on the definition and classification of laterites. In: *Proceedings of the International Seminar on Lateritisation Processes*, IGCP 129 and IAGC, Trivandrum, India, pp. 1–10. Oxford and IBH Publishing Company, New Delhi.
107. Schellmann, W. (1986a). A new definition of laterite. *Geological Survey of India Memoir*, 120, 1–7.
108. Schellmann, W. (1986b). On the geochemistry of laterites. *Chemie der Erde*, 45, 39–52.
109. Schellmann, W. (2003). Discussion of "A critique of the Schellmann definition and classification of laterite" by R.P. Bourman and C.D. Ollier. *Catena*, 52, 77–79.
110. Schmidt, P.W., Prasad, V., Ramam, P.K. (1983). Magnetic ages of some Indian laterites. *Palaeogeography, Palaeoclimatology, Palaeoecology*, 44, 185–192.
111. Schmidt-Lorenz, R. (1979). Laterization alias plinthization, a main process of soil formation. In: *Proceedings of the International Seminar on Laterization*, UNESCO-IUGS, Trivandrum, India.
112. Schober, P., Boer, C., Schwarte, L.A. (2018). Correlation coefficients: Appropriate use and interpretation. *Anesthesia & Analgesia*, 126(5), 1763–1768.
113. Sehgal, J. (1998). Red and lateritic soils: An overview. In: Sehgal, J., Blum, W.E., Gajbhiye, K.S. (eds.) *Red and Lateritic Soils: Managing Red and Lateritic Soils for Sustainable Agriculture*, Vol. 1. Oxford & IBH Publishing Co. Pvt. Ltd., New Delhi, pp. 3–11.
114. Sehgal, J., Saxena, K.K., Vadivelu, S. (1989). *Field Manual: Soil Resource Mapping of Different States*, 2nd edn. Bulletin No. 13. National Bureau of Soil Survey and Land Use Planning, Nagpur.
115. Sheldon, N.D., Retallack, G.J., Tanaka, S. (2002). Geochemical climofunctions from North American soils and application to paleosols across the Eocene–Oligocene boundary in Oregon. *The Journal of Geology*, 110(6), 687–696. https://doi.org/10.1086/342865
116. Sivaranjasingham, S., Alexander, L.T., Cady, J.G., Cline, M.G. (1962). Laterite. *Advances in Agronomy*, 14, 1–60.
117. Soil Survey Staff (2022). *Keys to Soil Taxonomy*, 13th edn. United States Department of Agriculture, Natural Resources Conservation Service, Soil Survey Staff, Washington, DC.
118. Solly, E.F., Weber, V., Zimmermann, S., Walthert, L., Hagedorn, F., Schmidt, M.W.I. (2020). A critical evaluation of the relationship between the effective cation exchange capacity and soil organic carbon content in Swiss forest soils. *Frontiers in Forests and Global Change*, 3, 98. https://doi.org/10.3389/ffgc.2020.00098

119. Souri, B., Watanabe, M., Sakagami, K. (2006). Contribution of Parker and product indexes to evaluate weathering condition of yellow-brown forest soils in Japan. *Geoderma*, 130, 346–355. https://doi.org/10.1016/j.geoderma.2005.02.007
120. Sparks, D.L. (1995). *Environmental Soil Chemistry*. Academic Press, San Diego, CA.
121. Sposito, G. (2008). The chemistry of soils. 2nd ed. Oxford University Press, New York, NY, USA.
122. Stewart, B.W., Capo, R.C., Chadwick, O.A. (2001). Effects of rainfall on weathering rate, base cation provenance and Sr isotope composition of Hawaiian soils. *Geochimica et Cosmochimica Acta*, 65, 1087–1099.
123. Sukumar, R., Ramesh, R., Pant, R.K., et al. (1993). A $\delta^{13}C$ record of late Quaternary climate change from tropical peats in southern India. *Nature*, 364, 703–706. https://doi.org/10.1038/364703a0
124. Syamlal, C.A., Sayantan, D. (2024a). Accumulation of heavy metals (Cr, Cu, As, Cd, Pb, Zn, Fe, Ni, Co) in the water, soil and plants collected from Edayar region, Ernakulam, Kerala, India. *Plant Science Today*, 11(4), 907–923. https://doi.org/10.14719/pst.3385
125. Syamlal, C.A., Sayantan, D. (2024b). Harnessing nature's power to cleanse water bodies through phytoremediation of aquatic plants. *Asian Journal of Advances in Agricultural Research*, 24(7), 119–132. https://doi.org/10.9734/ajaar/2024/v24i7528
126. Tardy, Y., Kobilsek, B., Paquet, H. (1991). Mineralogical composition and geographical distribution of African and Brazilian periatlantic laterites: The influence of continental drift and tropical paleoclimates during the past 150 million years and implications for India and Australia. *Journal of African Earth Sciences*, 12, 283–295.
127. Taylor, S.R., McLennan, S.M. (1995). The geochemical evolution of the continental crust. *Reviews of Geophysics*, 33, 241–265.
128. Terhorst, B., Kühn, P., Damm, B., Hambach, U., Meyer-Heintze, S., Sedov, S. (2014). Paleoenvironmental fluctuations as recorded in the loess–paleosol sequence of the Upper Paleolithic site Krems-Wachtberg. *Quaternary International*, 351, 67–82. https://doi.org/10.1016/j.quaint.2013.03.045
129. Thomas, G.W. (1961). Forms of aluminium in cation exchangers. In: *Transactions of the 7th International Congress of Soil Science*, Madison, Wisconsin, Vol. 2, pp. 364–369.
130. Thomas, G.W., Hargrove, W.L. (1984). The chemistry of soil acidity. In: Adams, F. (ed.) *Soil Acidity and Liming*. American Society of Agronomy, Madison, WI.
131. Thompson, A., Chadwick, O.A., Rancourt, D.G., Chorover, J. (2006). Iron-oxide crystallinity increases during soil redox oscillations. *Geochimica et Cosmochimica Acta*, 70, 1710–1727.
132. Tomlinson, D.L., Wilson, J.G., Harris, C.R., Jeffrey, D.W. (1980). Problems in the assessment of heavy-metal levels in estuaries and the formation of a pollution index. *Helgoländer Meeresuntersuchungen*, 33, 566–575. https://doi.org/10.1007/BF02414780
133. Torrent, J., Barrón, V. (1993). Laboratory measurement of soil color: theory and practice. In: Bigham, J.M., Ciolkosz, E.J. (eds.) *Soil Color*. SSSA Special Publication 31, pp. 21–33. Soil Science Society of America, Madison, WI.
134. Torrent, J., Schwertmann, U., Fechter, H., Alférez, F. (1983). Quantitative relationships between soil color and hematite content. *Soil Science*, 136, 354–358. https://doi.org/10.1097/00010694-198312000-00004
135. Valeton, I. (1994). Element concentration and formation of ore deposits by weathering. In: Schwarcz, K., Germann, K. (eds.) *Lateritization Processes and Supergene Ore Formation*. *Catena*, 21(2–3), 99–129.
136. Varghese, A.O., Menon, A.R.R. (1999). Floristic composition, dynamics and diversity of Myristica swamp forests of southern Western Ghats, Kerala. *Indian Forester*, 125(8), 775–783. https://doi.org/10.36808/if/1999/v125i8/5597

137. Varghese, T., Byju, G. (1993). *Laterite Soils*. Technical Monograph No. 1. State Committee on Science, Technology and Environment, Kerala, India.
138. Vodyanitskii, Y.N., Kirillova, N.P. (2016). Conversion of Munsell color coordinates to CIE-L*a*b* system: Tables and calculation examples. *Moscow University Soil Science Bulletin*, 71(4–5), 139–146.
139. Vodyanitskii, Y.N., Savichev, A. (2017). The influence of organic matter on soil color using the regression equations of optical parameters in the CIE-L*a*b* system. *Annals of Agrarian Science*, 15, 380–385.
140. Vodyanitskii, Yu.N. (2016). Application of the CIELAB system to characterize soil color. *Eurasian Soil Science*, 49, 1259–1268.
141. Vodyanitskii, Yu.N. (2019). Determination of the ratio hematite/goethite by soil color. *Annals of Agrarian Science*, 17, 180–187.
142. Vogt, T. (1927). Sulitjelmefeltets geologi og petrografi. *Norsk Geologisk Tidsskrift*, 121, 1–560.
143. Widdowson, M. (2007). Laterite and ferricrete. In: Nash, D.J., McLaren, S.J. (eds.) *Geochemical Sediments and Landscapes*. Wiley-Blackwell, Oxford, UK, pp. 46–94.
144. Widdowson, M., Cox, K.G. (1996). Uplift and erosional history of the Deccan Traps, India: Evidence from laterites and drainage patterns of the Western Ghats and Konkan Coast. *Earth and Planetary Science Letters*, 137, 57–69.
145. Widdowson, M., Gunnell, Y. (1999). Lateritization, geomorphology and geodynamics of a passive continental margin: the Konkan and Kanara lowlands of western peninsular India. *Special Publications of the International Association of Sedimentologists*, 27, 245–274.
146. Yang, S.Y., Li, C.X., Yang, D.Y., Li, X.S. (2004). Chemical weathering of the loess deposits in the lower Changjiang Valley, China, and paleoclimatic implications. *Quaternary International*, 117, 27–34.
147. Yousefifard, M., Youbi, N., Jallalian, A., Khadun, H., Makkizadeh, M.A. (2014). Mass balance of major elements in relation to weathering in soils developed on igneous rocks in semi-arid region, northwestern Iran. *Journal of Mountain Science*, 9, 41–58. https://doi.org/10.1007/s11629-012-2208-x
148. Zhao, S., Feng, C., Yang, Y., Niu, J., Shen, Z. (2012). Risk assessment of sedimentary metals in the Yangtze Estuary: New evidence of the relationships between two typical index methods. *Journal of Hazardous Materials*, 241–242, 164–172.

Supplementary Files

This is a list of supplementary files associated with this preprint. Click to download.

- Supplementarydata.docx